Controlled release of an antimicrobial substance from polymeric matrices

By

Hanneke Diedericks

Thesis presented in fulfilment of the requirements for the degree of

Masters of Science (Polymer Science)

at

Stellenbosch University

Super visor: Prof. AJ van Reenen

Co-supervisor: Dr. L Cronje

Department of Chemistry and Polymer Science

Faculty of Science

March 2016

Declaration

By submitting this thesis/dissertation electronically, I declare that the entirety of the work contained therein is my own, original work, that I am the sole author thereof (save to the extent explicitly otherwise stated), that reproduction and publication thereof by Stellenbosch University will not infringe any third party rights and that I have not previously in its entirety or in part submitted it for obtaining any qualification.

Hanneke Diedericks March 2016

Abstract

The main goal of this study was to develop polymeric artifacts (nanofibers and films) infused with an antimicrobial agent, 2,3-dihydroxybenzoic acid and study the release of DHBA as a function of the structure and properties of selected polymers. The effect of hydrophilic and hydrophobic polymers on the release behavior was the main focus of this study.

Four different polymers, poly (vinyl alcohol) (PVA), chitosan, poly (ethylene-co-vinyl alcohol) (EVOH) and poly (styrene-co-maleic anhydride) (SMA); all different in their hydrophilic-hydrophobic nature were used. Controlling the release of DHBA from these polymers have however not been investigated to our knowledge. Various parameters can influence the release of an agent from a matrix, which includes the type of polymer used and interactions between the polymer and the agent.

To effectively study the release of DHBA from electrospun nanofibers, it was important for the different polymer nanofibers to have similar average fiber diameters. This was done by investigating the effect different electrospinning parameters has on the fiber diameter. Incorporation of DHBA into the polymer artifacts (films and nanofibers) was successful with minimum loss of the agent. Interaction between polymer and agent was confirmed using FTIR. The interaction can be ascribed to the size of the molecular structure of the polymers, the smaller molecules showed hydrogen bonding with the agent with the larger molecules, limited interaction was observed. Thermal analysis of the matrices was studied using techniques such as DSC and TGA. These results revealed changes in the stability of the DHBA-loaded matrices compared to the pure polymer matrix. These changes can be attributed to the interaction between the polymer and the agent.

The release of DHBA from the films and nanofibers was investigated using UV spectroscopy. A burst release was observed which is explained by the type of polymer used. Although the burst

release of this agent has been documented, the ability to control the release of DHBA has not been done. Controlling the release of DHBA from the films and nanofibers was done by a coating process. SEM and FTIR were used to confirm the successful coating of these nanofibers. These coated nanofibers showed retardation of the release of DHBA. The more hydrophilic polymer used showed the greatest effect on the release behavior. These results confirmed the effect the type of polymer used has on the release of DHBA.

Opsomming

Die hoofdoel van hierdie studie was die ontwikkeling van polimeriese artifakte (films and nanovesels) gekombineer met ‘n antimikrobiese agent, 2,3-dihidroksibenzoësuur (DHBA) en die vrystelling van DHBA as ‘n funksie van die struktuur en eienskappe van gekiesde polimere. Die effek van hidrofiliese and hidrofobiese polimere op die vrystelling gedrag was die hooffokus van hierdie studie.

Vier verskillende polimere, poliviniel alkohol (PVA), chitosan, poliëtileen (ko-viniel alkohol) (EVOH) en poli (stireen-ko-maleïen anhidried) (SMA), almal verskillend in hidrofiliese-hidrofobiese natuur is gebruik. Om die vrystelling van DHBA van die polimere te beheer was nog nie volgens ons kennis al gedoen nie. Verskeie parameters kan die vrystelling van die agent van ‘n matriks beïnvloed, dit sluit in die tipe polimeer en interaksies tussen die polimeer en die agent.

Om die vrystelling van DHBA van die elektro-gespinde vesels effektief te bestudeer, is dit belangrik vir die verskillende polimeer vesels om soortgelyke gemiddelde vesel diameters te hê. Dit is gedoen deur die effek van verskillende elektrospin parameters op die vesel diameter te ondersoek. Inkorporasie van DHBA binne-in die polimeer artefakte was suksesvol met minimale verlies van die agent. Die interaksie tussen die polimeer en die agent is bevestig met fourier-transform infrarooi spektroskopie (FTIR). Die interaksie kan toegeskryf word aan die grootte van die molekulêre struktuur van die polimeer. Die kleiner molekules was deur waterstofbindings in interaksie met die agent, waar die interaksie beperk was met die groter molekules. Termiese analise van die matrikse is uitgevoer d.m.v. tegnieke soos differensieëlskandeerkalorimetrie (DSC) and termiese-gravimetriese analise (TGA). Die resultate wat verkry is het bewys dat daar verandering in die stabiliteit van die DHBA-gelaaide matrikse was in vergelyking met die skoon polimeer matriks. Die verandering kan toegeskryf word aan die interaksie tusen die polimeer en die agent.

Die vrystelling van DHBA van die films en nanovesels is bestudeer d.m.v. ‘n UV spektroskoop. ‘n Gebarste vrystelling is opgemerk wat verduidelik is deur die tipe polimeer wat gebruik was. Alhoewel die gebarste vrystelling van hierdie agent al gedokumenteer is, is die vermoë om die vrystelling van DHBA te beheer nog nie gedoen nie. Die beheer van DHBA van die films en nanovesels is gedoen deur ‘n bedekking proses. Skandeerelektron spektroskopie (SEM) en FTIR is gebruik om die suksesvolle bedekking van die nanovesels te bevestig. Die bedekte nanovesels het retardasie van die vrystelling van DHBA getoon. Die meer hidrofiliese polimeer het die grootste effek op die vrystelling gedrag getoon. Hierdie resultate bevestig die effek wat die tipe polimeer op die vrystelling van DHBA het.

Acknowledgements

First of all, I give thanks to my promoter, Prof. AJ van Reenen for your support and guidance. I appreciate all your advice and it was an honor having you as my study leader.

Dr. Lizl Cronje, my co-supervisor, for her support and motivation during group meetings.

To all my friends for their support, without you it would not have been possible. Thank you for showing interest in my work and encouraging me.

I would also like to thank the following people:

- The Olefin Research group for their great advice and interesting conversations in the office.
- Administrative and technical staff at Polymer Science Institute.
- Divann Robertson for your assistance with DSC.
- Madeleine Frazenburg for your help and support of SEM analysis.
- Illana Bergh at Roediger agencies for the TGA analysis.
- I also want to thank the National Research Foundation (NRF) for the financial support, providing me with the opportunity to attain my MSc.degree.
- Last but definitely not the least, I would like to thank, my Mom (Ilse), Dad (Riaan), brothers and Berno for always trying to understand what my work is about and showing me I can do it. I appreciate all your sacrifices and the love you showed me.

Table of contents

List of figures

List of tables

List of abbreviations

Ag	Silver
ATR-FTIR	Attenuated total refluctance - Fourier transform infrared
BCNU	1,3-bis (2-chloroethyl)-1-nitrosourea
BSA	Bovine Serum Albumin
CipHCl	Ciprofloxacin
CS	Chitosan
DCM	Dichloromethane
DDS	Drug delivery system
DHBA	2,3-dihydroxybenzoic acid
DMAc	N,N-dimethylacetamide
DMF	N,N-dimethylformamide
DMSO	Dimethylsulfoxide
DSC	Differential scanning calorimetry
EVA	Ethylene-co-vinyl acetate
EVOH	poly (ethylene-co-vinyl alcohol)
FR	Flow rate
GA	Glutaraldehyde
Iso	Isopropanol
KET	Ketoprofen
MA	Maleic anhydride
NaCl	Sodium chloride
NPs	Nanoparticles
PBS	Phosphate buffered saline
PDLLA	Poly (D,L-lactide)
PEG	Poly (ethylene glycol)
PEO	Poly (ethylene oxide)

PEVA	Poly (ethylene-co-vinyl acetate)
PLA	Poly (lactic acid)
PLLA	Poly (L-lactic acid)
PLGA	Poly (lactic-co-glycolic acid)
PPX	Poly (p-xylylene)
PS	Polystyrene
PVA	Poly (vinyl alcohol)
PVB	Poly (vinyl butyral)
RK	Rasberry ketone
SD	Spinning distance
SEM	Scanning electron microscopy
SMA	Poly (styrene-co-maleic anhydride)
TA	Thermal analysis
TFA	Trifluoroacetic acid
TGA	Thermogravimetric analysis
UV	Ultraviolet

Chapter 1

Introduction and Objectives

This chapter offers a brief introduction about the study as well the objectives to be achieved. An overview on the different chapters will also be summarized.

1.1 Introduction

For many years, the major focus of antimicrobial related research has been on the synthesis or discovery of potent agents with specific biological activity. While this continues to be an important area of research, increasing attention is being devoted to the manner in which these agents are delivered[1]. Several studies have been carried out in order to design, characterize and develop controlled delivery of an agent. The introduction of the electrospinning technique to controlled release inspired a new era of investigation in which the incorporation of the agent into the electrospun fibers can serve as effective delivery system[2]. The release of agents from electrospun nanofibers can occur via various pathways namely diffusion, desorption and scaffold degradation. These are all determined by the type of polymer used as the carrier of the agent.

Electrospinning is a very simple method for producing nanofibers from polymers. Electrospun nanofibers have emerged as a novel delivery system within the last decade. This technique makes it possible to incorporate a variety of agents into the fibers in a one-step process with almost no loss of the agents. However, nanofibers incorporated with an agent always inevitably show an initial burst release effect[3]. This could be a result of the large surface area of the nanofibers as well as the incompatibility between the polymer and the incorporated agent. One of the reasons why electrospinning is such an attractive technique is the ease with which a wide range of polymers can be processed into nanofibers. These polymers include both commonly used synthetic polymers and biopolymers.

Electrospun nanofibers obtained through hydrophilic or hydrophobic polymers can be used to overcome the burst effect. In this study, four different polymers, poly (vinyl alcohol) (PVA), chitosan, poly (ethylene-co-vinyl alcohol) (EVOH) and poly (styrene-co-maleic anhydride) (SMA), all different in their hydrophilic-hydrophobic nature are used. PVA and chitosan have excellent properties such as being biocompatible, biodegradable and nontoxic, which make the polymers ideal for controlled release systems[4-7]. PVA and chitosan are exploited for use in delivery systems due to their hydrophilic nature. EVOH and SMA both consist of hydrophilic and hydrophobic parts. The non-biodegradable property of these polymers makes them applicable as a delivery system, but has not been studied as extensively as PVA and chitosan.

In terms of this study, 2,3-dihydroxybenzoic acid was selected as the active agent. 2,3-Dihydroxybenzoic acid (DHBA) is a minor product of the metabolic breakdown of aspirin, excreted by the kidneys. DHBA is a salicylate derived from acetyl salicylic acid which is a non-steroidal anti-inflammatory agent widely used in the relief of pain[8]. Salicylates have the ability to scavenge free radicals and offer neuroprotection[9]. The incorporation of DHBA into polymer matrices and the release behavior of this agent have not been significantly explored. Research concerning the incorporation of this agent into polymer nanofibers has been done by Ahire[10]. That study did not focus on controlling the release of DHBA. DHBA is a water-soluble agent which poses a challenge controlling the release in aqueous systems. The higher the agent solubility in the release medium, the faster is the release[11]. In this study we were interested in controlling the release of DHBA, and understanding the factors that control the burst effect as well as the rate of subsequent release from the different polymers.

1.2 Goals and Objectives

The main goal of this study was to develop polymeric artifacts (nanofibers and films) infused with an antimicrobial agent, 2,3-dihydroxybenzoic acid and study the release of DHBA as a function of the structure and properties of selected polymers. The effect of hydrophilic and hydrophobic polymers on the release behavior was the main focus of this study. The objectives of this study were therefore:

- The processing of PVA, chitosan, EVOH and SMA into polymer nanofibers via electrospinning.
- Investigating the influence of the different parameters namely, concentration, applied voltage, flow rate and spinning distance on the average fiber diameter.
- Incorporation of DHBA into the nanofibers and characterization thereof.
- Study the release of DHBA from films and nanofibers.
- Control the release of DHBA.

1.3 Outline of Document

This thesis comprises of six chapters. In chapter 1, a brief introduction into why controlling the release of an agent is important, is given and the objectives set out to achieve.

Chapter 2: An overall review on the fundamental theory of this study is given as well as a background on the polymers being used. The electrospinning technique and the parameter affecting the fiber diameter will also be discussed.

Chapter 3: Describes the materials and methodologies used. The techniques used for analysis are also described.

Chapter 4: Results and discussion of the electrospinning of PVA, chitosan, EVOH and SMA and the different parameters affecting the fiber diameter and morphology. Incorporation of DHBA into the various matrices, interaction with polymers and the affect it has on the thermal stability are also reported.

Chapter 5: Results from release behavior of DHBA from the films and nanofibers are discussed and how the release could be controlled.

Chapter 6: Comprises of general conclusions from this study and recommendations for future research in this field.

References

1. Langer, R.; Peppas, N. Present and future applications of biomaterials in controlled drug delivery systems. *Biomaterials* **1981,** *2,* 201-214.

2. Sohrabi, A.; Shaibani, P.; Etayash, H.; Kaur, K.; Thundat, T. Sustained drug release and antibacterial activity of ampicillin incorporated poly (methyl methacrylate)–nylon6 core/shell nanofibers. *Polymer* **2013,** *54,* 2699-2705.

3. Li, J.; Feng, H.; He, J.; Li, C.; Mao, X.; Xie, D.; Ao, N.; Chu, B. Coaxial electrospun zein nanofibrous membrane for sustained release. *J. Biomater. Sci, Polymer Edition* **2013,** *24,* 1923-1934.

4. Merkle, V.; Zeng, L.; Teng, W.; Slepian, M.; Wu, X. Gelatin shells strengthen polyvinyl alcohol core–shell nanofibers. *Polymer* **2013,** *54,* 6003-6007.

5. Koski, A.; Yim, K.; Shivkumar, S. Effect of molecular weight on fibrous PVA produced by electrospinning. *Mater. Lett.* **2004,** *58,* 493-497.

6. Rao, S.B.; Sharma, C.P. Use of chitosan as a biomaterial: studies on its safety and hemostatic potential. *J. Biomed. Mater. Res.* **1997,** *34,* 21-28.

7. Rinaudo, M. Chitin and chitosan: properties and applications. *Progr. Polym. Sci.* **2006,** *31,* 603-632.

8. Sandrini, M.; Ottani, A.; Vitale, G.; Pini, L.A. Acetylsalicylic acid potentiates the antinociceptive effect of morphine in the rat: involvement of the central serotonergic system. *Eur. J. Pharmacol.* **1998,** *355,* 133-140.

9. Guerrero, A.; González-Correa, J.; Arrebola, M.; Munoz-Marın, J.; De La Cuesta, F Sánchez; De La Cruz, J. Antioxidant effects of a single dose of acetylsalicylic acid and salicylic acid in rat brain slices subjected to oxygen-glucose deprivation in relation with its antiplatelet effect. *Neurosci. Lett.* **2004,** *358,* 153-156.

10. Ahire, J.J.; Neppalli, R.; Heunis, T.D.; van Reenen, A.J.; Dicks, L.M. 2, 3-dihydroxybenzoic acid electrospun into poly (d, l-lactide)(PDLLA)/poly (ethylene oxide)(PEO) nanofibers inhibited the growth of Gram-positive and Gram-negative bacteria. *Curr. Microbiol.* **2014,** *69,* 587-593.

11. Zilberman, M. Active implants and scaffolds for tissue regeneration. Springer: **2011**; 8, 57-85.

Chapter 2

Literature review

This chapter starts with a discussion on the controlled release of antimicrobial agents as background to understanding the various systems to be used and the importance in controlling the release of these agents. One of the systems to be used is through electrospinning and the parameters affecting the resultant nanofibers will be discussed.

2.1 Controlled release of antimicrobial agents

2.1.1 Background

Controlled delivery technology represents one of the most rapidly advancing areas of science. Such delivery systems offer numerous advantages compared to conventional dosage forms including improved efficacy, reduced toxicity, and improved patient compliance and convenience. All controlled release systems aim to improve the effectiveness of drug therapy[1]. Numerous studies have been carried out in order to design, characterize and develop drug delivery systems, but with limited success[2]. In controlled delivery systems an active agent is incorporated into a polymeric network structure in such a way that the agent is released from the material in a predetermined manner[3].

2.1.2 Need for controlled release systems

The phenomenon of an initial burst release of agents from delivery systems has been under investigation for years. This is most common for nano delivery systems with high surface area[4].

The need for polymer systems in which the agents are released at a slower rate to water from the aqueous environment are highly in demand. This can be achieved by a polymer coating or matrix that dissolve at a slower rate than the agent. The insoluble polymer matrix inhibits the fast release of the molecules where molecules must travel through complex pathways to exit the device[1]. An encapsulating system is ideally designed to provide a controlled release pattern where the molecules are released at a constant rate[5].

Development of micro/nano-encapsulation techniques for effective delivery of molecules has been on the rise. Recently, electrospinning has gained much attention as delivery systems for its potential to minimize burst release of agents. This is due to the continuously long and high-order aligned structure of molecules as well as to the large surface area of the electrospun fibers. The bursting depends on the surrounding medium, polymers used as well as encapsulant. A common way of controlling agent delivery is by incorporating the agent into the polymer matrix. Agent dissolution and diffusion through the polymers are important phenomena in controlling the

release characteristics of the formulation. The electrospun fibrous mats have gained rapid interest as potential controlled release candidate in food, pharmaceutical, and medical applications[5].

2.1.3 Scope of polymer systems for controlled release

Polymeric delivery systems have numerous advantages compared to conventional delivery systems; they are able to improve therapeutic effect, reduce toxicity, and more convenient for the patients by delivering the agents at a constant rate over a period of time to the site of action[6]. The limited capacity of delivery and burst release of agents are still problematic in these systems; attempts to overcome the burst have been made, but with varying degrees of success[2, 7, 8].

The use of polymers as carriers is expanding continuously. Various delivery systems using biodegradable polymers have been fabricated in order to achieve controlled release. These include nano- or microparticles[9, 10], hydrogels[11, 12], micelles[13-15], films[16, 17] and fibrous scaffolds[5, 18]. These systems have been studied widely for their release profiles but all with similar limitations.

2.1.3.1 Nano- or microparticles

Nano- or microparticles are submicron-sized polymeric colloidal particles which vary in size from 10 to 1000 nm[19]. Agents can be dissolved, entrapped, adsorbed, attached and/or encapsulated into or onto a nano-matrix. The release characteristics and properties of the nanoparticles can be controlled by the method of preparation for the best delivery or encapsulation of agents[20].

Over the past few decades, there has been considerable interest in developing biodegradable nanoparticles as effective delivery devices. Polymeric nanoparticles possess certain advantages such as to increase the stability of agents against degradation and have useful controlled release properties[20, 21]. The majority of studies on nanoparticles (NPs) have dealt with microparticles created from poly(D,L-lactide), poly(lactic acid) (PLA), poly(D,L-glycolide) (PLG), poly(lactide-co-glycolide) (PLGA), and polycyanoacrylate (PCA)[22].

According to Calvo *et al*[23], the release can be controlled by coating the NPs. The release takes place by the partitioning of the agent; however, the main factor controlling the release is the

volume of the aqueous medium. A faster and complete release of the agent took place with a higher dilution of the dissolution medium. Lu *et al*[24] reported that the release of Bovine Serum Albumin (BSA) from PLA nanocapsules depends on the molecular mass of the polymer, which indicated that the release may be due to diffusion across the polymer coating and not partitioning of the BSA.

The use of particle carriers where the agent can be encapsulated inside each particle is not easy in controlling the release because of the large surface area and the potential coagulation of the agents and are still under investigation as potential carriers[25].

2.1.3.2 Hydrogels

Hydrogels are networks of hydrophilic polymeric materials that do not dissolve in water at physiological temperature and pH, but are able to swell considerably in an aqueous medium while maintaining its structure. They are widely used as controlled release carriers of agents because of their good tissue compatibility, easy manipulation under swelling condition, and solute permeability[26-28].

Hydrogels have several characteristics that make them excellent delivery systems. Firstly, the polymers used in the preparation of hydrogels have mucoadhesive and bioadhesive characteristics that enhance agent resistance time and tissue permeability[29, 30]. Secondly, the dimension of a hydrogel can vary significantly, ranging from nanometers to centimeters in width. They can deform into any shape of to which they are confined[31]. The method in which the agents are loaded determines the release. Three approaches are common, namely through direct addition, entrapment, or covalent attachment to the hydrogel-forming polymer as shown in Figure 2.1. Depending on the method, the release of agents can be controlled[32, 33].

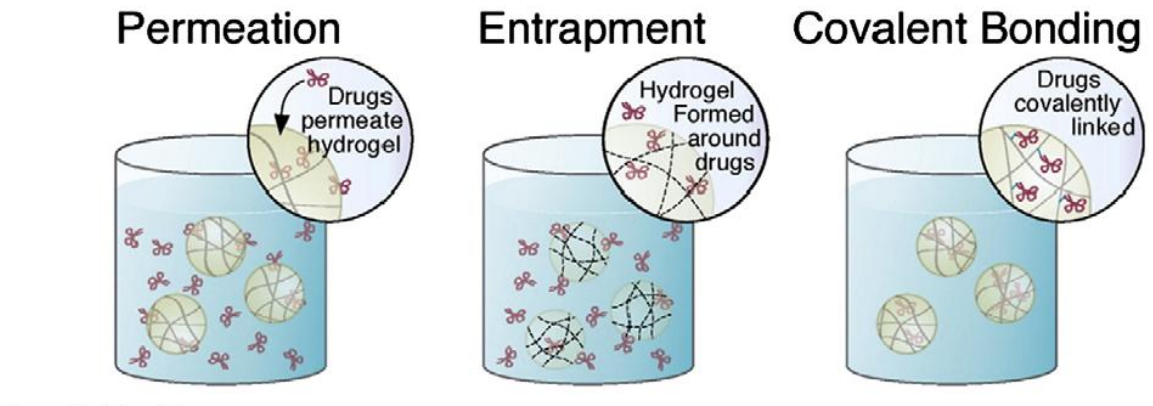

Figure 2.1: Three different loading strategies for hydrogels[32].

The high water content of most hydrogels typically results in relatively rapid release of agents from the matrix. The release rate can be reduced by either interactions between the agent and the hydrogel matrix or by increasing the diffusive barrier for the release of the agent[34].

2.1.3.3 Micelles

Polymeric micelles have been of increasing interest as potential carriers for poorly soluble agents in the past few years. They are characterized by a core-shell structure; where they can solubilize the water in-soluble agents in their inner core[35]. Research has been mainly focused on polymers having an A-B diblock structure as shown in Figure 2.2 with A, the hydrophilic polymer (shell) and B, the hydrophobic polymer (core), respectively[36].

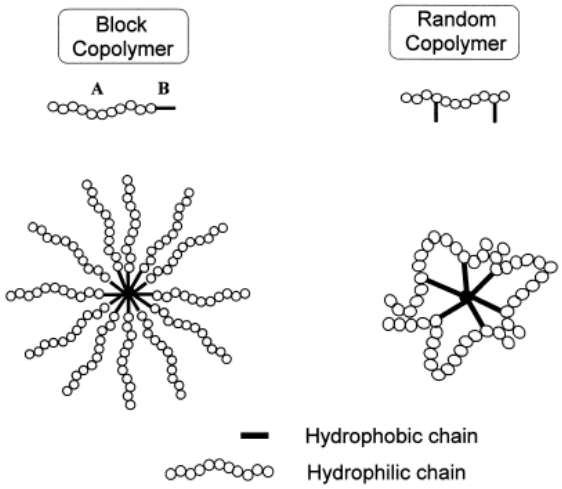

Figure 2.2: Schematic representation of block and random copolymer micelles[37].

Loading of insoluble agents into the micelles can be done in different methods; which include simple equilibrium, dialysis, O/W emulsion, solution casting and freeze-drying[15]. The different methods can affect the preparation of agent-loading polymeric micelles and alter the properties of the end product.

2.1.3.4 Films

The uses of films are well known to be applicable in food packaging applications and several studies have dealt with this subject[38-40]. The results obtained are quite limited because the studies have been restricted to the case of release of the antimicrobial agents from hydrophobic polymeric matrices. The release of a hydrophilic agent from a hydrophobic film affects the release rate critically; the hydrophobic surface results in slower release rates of the agents[41, 42]. Xu *et al*[43] investigated the surface wettability and release of agent from a hydrophobic matrix, polyvinyl butyral (PVB), by electrospinning nano-structures on the surface. The release of two hydrophilic agents, acetaminophen and 5-fluorourasil could be controlled by depositing different amounts of PVB nanofibers on the surface of the polymer films.

Layer-by-layer deposition of films is a versatile technique that has shown great promise in delivery systems. These films are formed by exploiting electrostatic, hydrogen bonding, and

covalent interactions between film components. The release of the agents is usually through diffusion and film degradation when placed in an aqueous environment. Cationic poly (B-amino esters) has been used for this application in several studies. A burst release is observed at first followed by zero-order release via degradation. These types of systems are ideally for complex release architectures where multiple agents can be incorporated directly or through a carrier which results in multi-agent release[44].

2.1.3.5 Fibrous scaffolds

In the last decade, electrospun nanofibers have been explored and attracted increasing attention for their use in biomedical applications including tissue engineering scaffolds[45], wound dressing materials[45-47] and controlled delivery carriers[8, 48-50]. The interconnected, three dimensional porous structures with a high specific surface area help agent particles diffuse out of the matrix more efficiently. Unlike other common techniques, electrospinning have several advantages over the conventional delivery system, including the agent release profile, which can be finely tailored by modulation of the morphology, porosity and composition of the nanofiber membrane and the small diameter of nanofibers with a high surface area are helpful for mass transfer and efficient release[33, 51].

The introduction of the electrospinning technique where the electrospun fibers can serve as effective delivery systems inspired a new era of investigations. Two types of delivery systems could be designed by means of the electrospun fibers: matrices and reservoirs[52, 53].

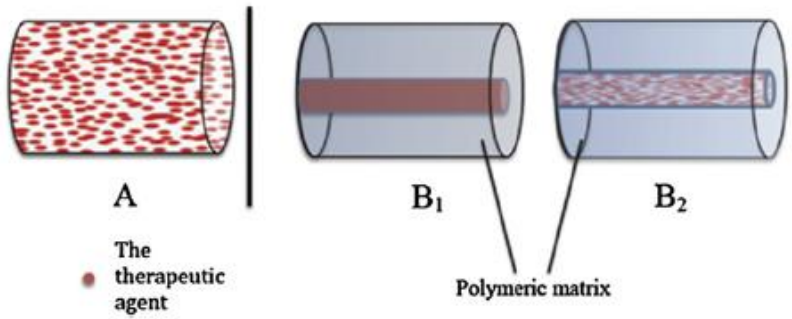

Figure 2.3: Possible configurations for delivery systems by means of the electrospun fibers[54].

As depicted in Figure 2.3A; the agent can be dispersed homogeneously in the electrospun fiber matrix. Kenawy *et al*[55] published the first report concerning electrospun fibers as delivery systems. They used poly (lactic acid) (PLA), poly (ethylene-co-vinyl acetate) (PEVA) or 50:50 blend electrospun fiber mats as delivery vehicles while using tetracycline hydrochloride as a model agent. The release profiles showed promising results when they were compared to a commercially available delivery system - Actisite® (Alza Corporation, Palo Alto, CA), as well as to the corresponding cast films.

The matrix system is known to release the agent in a burst manner followed by a constant decrease on the release rate since the agent required a longer diffusion path for release. Ignatious and Baldoni[56] described electrospun polymer nanofibers which can be designed to provide a rapid, intermediate, delayed, or modified dissolution, such as sustained and/or pulsatile release characteristics. However, the low deliver efficiency and burst release are some of the problems with these systems; therefore core-shell structures nanofibers have been developed to overcome the problem of burst release[57].

The reservoir type system utilizes a core-shell structure in which the agent can be incorporated in two ways. As shown in Figure 2.3B; the pure agent could be encapsulated inside a polymeric shell (B_1) or the agent could be initially dispersed in a polymeric matrix and then encapsulated with another polymer (B_2)[58, 59].

2.1.3.5.1 Electrospun nanofibers

Electrospun polymer nanofibers have potential applications as release systems and to protect the activity of the encapsulated agents or proteins for tissue engineering applications. It has been shown that release patterns from nanofibrous meshes can be tailored by various formulation conditions such as polymer type[60, 61], polymer concentration[8], blending of different polymers[61, 62], surface coating[63], and the state of molecules in an electrospinning medium[64, 65].

A good number of polymers have been used for electrospinnng as the matrix for delivery systems. Poly(lactic acid) (PLA) and poly(ethylene-co-vinyl acetate) (PEVA) were successfully electrospun in the presence of tetracycline hydrochloride (an antibiotic) as a model agent by Kenawy *et al*[55]. Zong *et al*[55] also used PLA as the matrix and mefoxin as the model agent. Both

came to same conclusion that the total percentage agent released from the cast films was lower than that from the as-spun fiber mats due to the much lower surface area. The table below contains a list of polymers that have been successfully electrospun and used as delivery systems.

Table 2.1: Electrospun polymes for delivery systems

No.	Polymer	Solvent	Fiber diameter	Nozzle configuration	Application (cell type/drug)	Ref.
1	(a) Poly(e-caprolactone) (shell) (b) Poly(ethylene glycol)(PEG) (core)	(a) 2,2,2-trifluoroethanol (b) Water	270 - 380 nm	Coaxial	D.D.S. (fitcBSA)	67
2	(a) Poly(e-caprolactone) and poly(ethylene glycol) (shell) (b) Dextran (core)	(a) Chloroform and DMF (b) Water	1.1 - 5.7 µm	Coaxial	D.D.S. (BSA)	68
3	(a) Poly(e-caprolactone) (shell) (b) Poly(ethylene glycol) (core)	(a) Chloroform and DMF (b) Water	545 - 774 nm	Coaxial	D.D.S. (BSA and lysozyme)	50
4	Poly(e-caprolactone-co-ethyl ethylene phosphate)	DCM and PBS	0.46 - 5.01 µm	Single nozzle	D.D.S. (b-nerve growth factor and BSA)	69
5	Poly(D,L-lactic-co-glycolic acid), PEG-b-PLA, and PLA	DMF	260 - 360 nm	Single nozzle	D.D.S. (Mefoxin, cefoxitin sodium)	70
6	Poly(D,L-lactic-co-glycolic acid)	DCM	0.03 - 10 µm	Single nozzle	D.D.S. (Paclitaxel)	71
7	Poly(L-lactide-co-glycolide) and PEG-PLLA	Chloroform	690 - 1350 nm	Single nozzle	D.D.S. (BCNU)	72
8	Poly(e-caprolactone), Poly (ethylene oxide), PLLA and PLGA	Chloroform and DMSO	0.99 - 1.43 µm	Single nozzle	D.D.S. (Lysozyme)	61
9	Poly(L-lactide), Poly(ethylene imine) and Poly(L-lysin)	Chloroform	336 - 525 nm	Single nozzle	D.D.S. (Cytochrome C)	8
10	(a) Cellulose Acetate (shell) (b) PEG and Gelatin	(a) Acetic acid and water (b) Acetic acid and water	296 - 900 nm	Coaxial	D.D.S. (Gelatin)	5
11	(a) Polyvinylpyrrolidone (shell) (b) Ethyl Cellulose (core)	(a) Ethanol and N,N-dimethylacetamide (DMAc) (b) Ethanol	580 - 1020 nm	Coaxial	D.D.S. (ketoprofen (KET) and Methylene blue)	73
12	Poly(vinyl alcohol) and Poly(vinyl acetate)	Acetic acid and water	145 - 448 nm	Single nozzle	D.D.S. (Ciprofloxacin HCl (CipHCl))	51
13	Poly(ethylene-co-vinyl alcohol) (EVOH)	Propan-2-ol and water	59 nm - 3 µm	Single nozzle	D.D.S. (Ag nanoparticle)	74

Abbreviations: D.D.S.: drug delivery systems; DMF: N,N-dimethylformamide; DCM: dichloromethane; DMSO: dimethylsulfoxide, PBS: phosphate buffered saline; HCl: hydrochloric acid; BSA: bovine serum albumin; PLA: poly (lactic acid); PLLA: poly (L-lactic acid); PLGA: poly (lactide-co-glycolic acid); fitcBSA: fluorescein isothiocyanate – bovine serum albumin; BCNU: 1,3-bis (2-chloroethyl)-1-nitrosourea; Ag: silver

One of the obvious advantages of the electrospinning process over the conventional film-casting technique is the highly porous structure of electrospun fiber mats which exhibit much greater surface area that assumingly could allow molecules to diffuse out from the matrix much more conveniently[55, 66].

2.1.3.5.2 Core-shell nanofibers

Core-shell nanofibers have been studied intensely and are ideal for when thin, delicate structures are needed for better release profile control where biologically active molecules are incorporated within the fibers[75, 76].

Core-shell structures are one of the several approaches used to obtain a controlled release profile. Jiang *et al*[50] used polycaprolactone (PCL) as the shell and protein-containing poly (ethylene glycol) (PEG) as the core. They showed the release of the protein can be controlled by the thickness of the core and shell by adjusting the feed rate of the inner syringe. Jiang *et al*[68] also find similar findings when Poly (ε-caprolactone) was used as the shell and bovine serum albumin (BSA)-containing dextran as core. The release rate of BSA could be varied by the feed rate of the inner syringe during electrospinning. With an increase in the feed rate, there was an accelerated release of BSA[68].

The coaxial electrospinning technique has the advantages of being facile, has high loading efficiency, mild preparation, and controllable release behavior of the incorporated agents[68].

2.1.3.6 Release of antimicrobial agents

The ability to incorporate a variety of antimicrobial agents into polymeric matrices is of increasing interest especially in the biomedical field. Various agents and proteins such as antibiotics[77], silver nanoparticles[78], analgesics[79], growth factors[80], vitamins[81], antifungal agents[82], etc. have been incorporated into electrospun nanofibers for controlled release. The release profile is influenced by the polymer-agent interactions and solubility of the agent in the polymer solution[83]. Stronger agent-polymer interactions allows for slower, more linear release while

negative or lack of interaction promotes burst or rapid release[64]. Controlled release of hydrophilic molecules from biodegradable polymer matrices has always presented a challenge. In general, there is a considerable amount of initial burst release, caused mainly by inadequate solubility of the molecule in the polymer matrix. If on the other hand, a hydrophilic polymer is used as the matrix, the polymer swells in aqueous media, accelerating the release[2].

Entrapment and sustained release of water-soluble agents by conventional electrospinning techniques remains challenging. Reza *et al*[60] investigated the release of water-soluble agents from different matrices. They showed that the release of water-soluble agents with higher solubility was higher from a hydrophilic polymer matrix than a hydrophobic one. Karuppuswamy *et al*[84] incorporated a hydrophilic agent, tetracycline hydrochloride into a hydrophobic polycaprolactone nanofiber. With an increase in agent concentration, the surface of the fibers became more hydrophilic, resulting in a faster release of the agent.

2.2 Polymers

In the next section, a brief introduction will be given on the various polymers that were used in this study as well as the importance of using them as a possible delivery system.

2.2.1 Poly (vinyl alcohol)

Poly (vinyl alcohol) (PVA) is a water-soluble synthetic polymer produced industrially by hydrolysis of poly (vinyl acetate)[85, 86]. PVA is the world's largest volume synthetic polymer produced for its excellent chemical resistance and physical properties and complete biodegradability, which has led to broad practical applications such as biomedical, plastic and textile fields[87-89].

PVA was first prepared by Herman and Haehnel in 1924 by hydrolyzing polyvinyl acetate in ethanol with potassium hydroxide. It is commercially produced from polyvinyl acetate by a continuous process. As shown in Figure 2.4, the acetate groups are hydrolyzed by ester interchange with methanol in the presence of aqueous sodium hydroxide. Its physical

characteristics and end uses depend on the degree of hydrolysis and polymerization[88]. The solubility of PVA in water increases greatly as its degree of hydrolysis increases. Properties such as water solubility, high tensile strength, and tack are determined by the degree of hydrolysis[90].

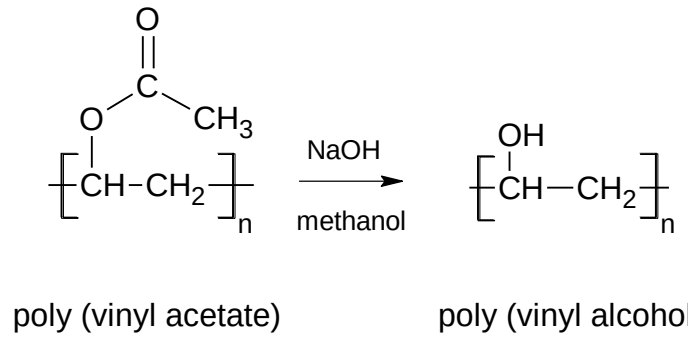

Figure 2.4: Preparation of PVA from Poly (vinyl acetate)[91].

Because of its flexibility and swelling capability in an aqueous medium, PVA has been much studied as a wound dressing; however, its poor stability in water has limited its use in aqueous systems, particularly for delivery applications. To overcome this problem, PVA has been made insoluble by copolymerizing[92], grafting[93] and crosslinking[94].

However, PVA is exploited for use in delivery systems due to its high hydrophilicity, ease of processing, good mechanical and thermal stability, high biocompatibility, and its non-toxic and biodegradable nature[95].

2.2.1.1 PVA nanofibers

Over the past few years, many researchers have investigated various parameters affecting the morphology of electrospun PVA fibers for example the solution concentration, solution flow rate, degree of hydrolysis, applied electric potential, collection distance, ionic salt addition, molecular weight of PVA , and pH. PVA nanofibers have several interesting characteristics, such as high surface area to mass ratio, significant possibilities for surface functionalization, and high mechanical performance. These properties make electrospun PVA fibers possible for many applications, such as filtration[96], wound dressings[51], tissue engineering[97, 98], and as releasing carriers[51, 62, 99].

The electrospinning of PVA has been studied extensively due to the use of water-based solvents. Taepaibon *et al*[62] dissolved PVA in distilled water and reported the successful electrospinning of PVA nanofibers as carriers of agents used as transdermal delivery systems. They proved that the agent-loaded electrospun PVA mats exhibited better release characteristics of four model agents than the loaded as-cast films.

The use of PVA nanofibers as wound dressings has its limitations due to the biodegradability of PVA; it swells considerably in aqueous medium and results in a burst release of agents. To overcome this problem, crosslinking of the fibers can be done. Yang *et al*[6] crosslinked PVA/Gelatin bicomponent nanofibers with glutaraldehyde vapour and investigated the release of Raspberry ketone (RK). They showed that the release of RK can be controlled with different crosslinking times, a longer time resulted in a slower release of RK. Another approach that can be considered is to coat the electrospun nanofibers. In a study done by Zeng *et al*[100], they coated loaded-PVA nanofibers with poly (p-xylylene) (PPX) by chemical vapour deposition. Burst release of BSA was noted with uncoated PVA nanofibers, where PPX-coated nanofibers exhibited a significantly retarded release of BSA depending on the coating thickness.

2.2.2 Chitosan

Chitosan (CS) (structure shown in Figure 2.5), a cationic natural biopolymer, is a linear polysaccharide consisting of β(1,4)-linked 2-amino-deoxy-β-D-glucan, is a deacetylated derivative of chitin, which is the second most abundant polysaccharide found in nature after cellulose. Chitosan has aroused great interest as a promising material for biomedical applications because it possesses excellent biological properties such as good biocompatibility, biodegradability, antimicrobial activity, nontoxicity, and wound healing properties[101-103]. These attractive properties make the polymer an ideal candidate for controlled release systems.

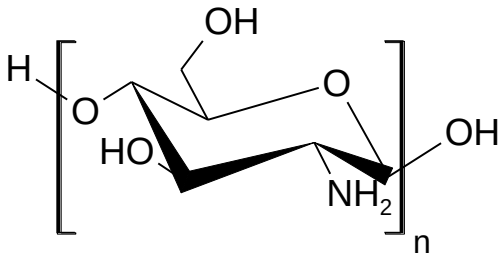

Figure 2.5: Structure of Chitosan

The antimicrobial activity of chitosan is dependent on the type of chitosan; particularly the degree of deacetylation, molecular weight, target organism, the pH of the medium, ionic strength and presence of solutes which can affect or completely block the reactivity of the active amine group. It has been reported that low molecular weight chitosan, has a higher reactivity towards the active sites of the targeted microorganisms than high molecular weights because it is more soluble in aqueous media. Low pH values, up to 5.5 increased the antimicrobial activity of chitosan because of its higher solubility and protonation in the acidic pH interval[104]. It has been recognized that yeasts and moulds are the most sensitive groups to chitosan, followed by Gram-positive and Gram-negative bacteria[105]. Due to its antimicrobial properties, it has been applied to wound treatments in various physical forms, such as beads, powders, gels, sponges, tubes, films, and fibers[102].

2.2.2.1 Chitosan nanofibers

Chitosan is an attractive material for electrospinning. However, it is difficult to electrospin into a nanofibrous structure because it has a polycationic character in acidic aqueous solutions due to many amino groups in its backbone, its limited solubility in most organic solvents, its three-dimensional networks of strong hydrogen bonds, its molecular weight, and its wide molecular weight distribution. The polycationic nature of chitosan increases the surface tension of the solution considerably and requires a strong electrical field to successfully electrospin chitosan[106]. Successful electrospinning of chitosan have been reported but the electrospinning conditions are limited in terms of concentration, molecular weight, and degree of deacetylation[107].

Okhawa *et al*[108] managed to electrospin chitosan dissolved in trifluoroacetic acid (TFA): dichloromethane (DCM) but these solvents are environmentally harmful and toxic. Concentrated acetic acid has also been used as solvent for the electrospinning of chitosan[109]. The use of toxic solvents makes it difficult to be used in wound healing applications.

The electrospinning ability of chitosan can be improved by mixing/blending it with other synthetic or natural polymers which are easy to electrospin and have good miscibility with chitosan. A number of polymers have been used to blend with chitosan which includes: poly (lactic acid) PLA[110], poly (vinyl alcohol) PVA[111], poly (ethylene oxide) PEO[112], Sericin[113], Gelatin[114], etc. and have been widely investigated. The electrospinning of chitosan blends remained difficult with high chitosan content. It was proven by Xu *et al*[110] with a chitosan/PLA blend, smooth nanofibers were obtained with increasing amount of PLA; the bead formation decreased. Bead-free nanofibers of the electrospun chitosan/PVA blend nanofibers were obtained when the weight ratio of chitosan/PVA in the polymer blend was lower than 95:5[111].

2.2.3 Poly (ethylene-co-vinyl alcohol)

Poly (ethylene-co-vinyl alcohol) (EVOH) is a random copolymer consisting of hydrophobic ethylene and hydrophilic vinyl alcohol units. EVOH is produced by a hydrolysis reaction of a parent ethylene-co-vinyl acetate copolymer (EVA) where the acetoxy groups are converted to a secondary alcohol[115] as shown in Figure 2.6.

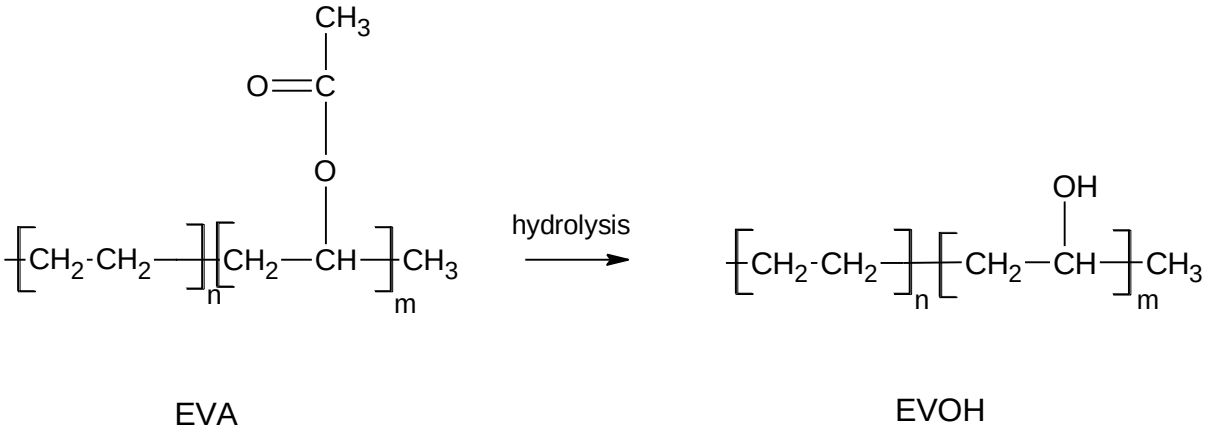

Figure 2.6: Conversion of EVA into EVOH[116].

EVOH are commercially available in two variations. The first variation is where the EVOH has a high ethylene content (82-90 mole %) and are normally used for adhesives. The second variation consists of an ethylene content of 25-45% and 60-75 mole% vinyl alcohol. This type of EVOH has excellent barrier properties to gases such as oxygen, nitrogen, carbon dioxide and helium and is usually used as packaging material[117].

EVOH is very sensitive to humidity and it can change the resistance of the polymers to oxygen diffusion[118]. The content of the vinyl alcohol influences the properties of EVOH. The more the increase in the vinyl alcohol content, the more the polymer will be influenced by moisture and humidity; it will also increase the hardness of the polymer[119]. Due to the presence of the hydroxyl groups, the polymer is hydrophilic whilst still being water-insoluble. Other properties such as biocompatibility, thermal resistance and non-biodegradability make it applicable to be used in tissue engineering, delivery systems and wound treatments[120, 121].

2.2.3.1 EVOH nanofibers

EVOH can be electrospun and used as nanofibrous mats for cell growth, as membranes[122] and in tissue engineering[121]. The surface modification of nanofibers as mentioned above, is much easier than a polymer in any other form. The modification of the surface of EVOH nanofibers will encourage the use of this material in various applications[123].

Electrospinning is a straightforward approach to fabricate highly porous EVOH materials for medical applications. Silver nanoparticles have been encapsulated into EVOH nanofibers by Xu *et al*[74]; they concluded that the silver nanoparticles encapsulated EVOH nanofibers showed inflammation control capacity and potential for applications in skin wound treatment. Electrospun EVOH mats have been shown to support the culturing of smooth muscle cells and fibroblasts[124]. Chao Xu[125] also investigated the electrospinning of EVOH encapsulated with silver nanoparticles for medical applications. He looked at the degradation of EVOH nanofibers and reported that the mechanical property of the materials is stable in vitro, indicating that it is a good candidate for wound dressing applications.

The reason for choosing EVOH as dressing material is due to its good biocompatibility and proven use in the preparation of nanofibers by means of electrospinning[120].

2.2.4 Poly (styrene-co-maleic anhydride)

Poly (Styrene-co-maleic anhydride) (SMA), shown in Figure 2.7 below, can be synthesized by conventional polymerization of styrene and maleic anhydride comonomers[126]. SMA is an important reactive thermoplastic copolymer as its anhydride groups on the backbone of the structure can react with other reagents, such as alcohols, amines, and water etc. to produce many derivatives. Because of the presence of aromatic and anhydride functionalities, the molecular and segmental structures of SMA can be easily modified. The degree of hydrophilicity can be modified by adjusting the styrene-maleic ratio. SMA copolymers with relatively high anhydride content have been used for various coating additives and binder applications[127].

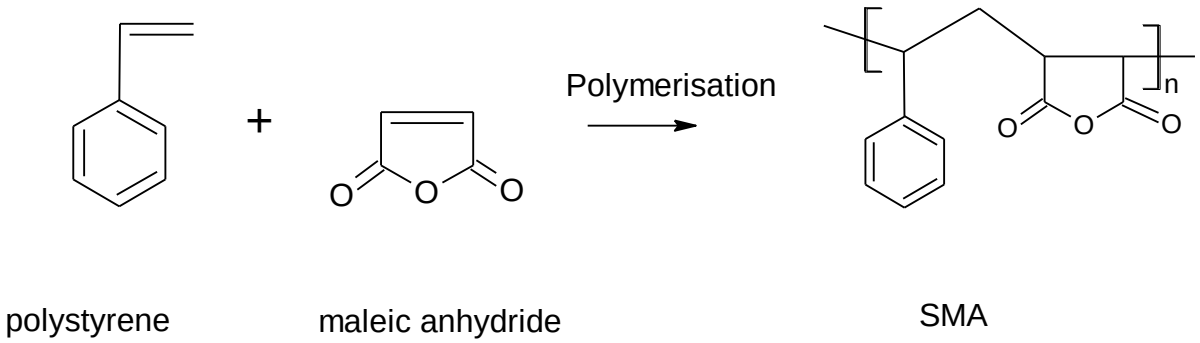

Figure 2.7: Schematic illustration of the synthesis of polystyrene maleic anhydride.

Maeda *et al*[128] investigated the use of SMA as a delivery system. An antitumor protein, neucarzinostatin was incorporated into SMA copolymers. They concluded that they significantly improved the pharmacological properties of the protein by increasing both its circulatory half-life and its lipid solubility as well as it's been clinically effective in treating liver cancer[128, 129].

The grafting of a hydrophilic monomer, acrylic acid onto SMA has been done by Kaur *et al*[127]. The introduction of acrylic acid induced swelling behaviour and can be a suitable option for delivery. The agent release from this polymer showed the effectiveness (swelling, pH

responsiveness, functional groups of the polymer etc.) of the polymer to be used as a vehicle for agent loading and delivery.

2.2.4.1 SMA nanofibers

Polystyrene (PS) is one of the first polymers to be electrospun because it is a chemically and structurally versatile polymer making it easy to synthesize by several polymerization mechanisms[130, 131]. Polystyrene maleic anhydride is a copolymer that is even more chemically versatile because of the highly charged maleic anhydride (MA) moiety. The presence of maleic anhydride moieties makes it possible to be modified before or after electrospinning which can change the properties of the polymer that affects the electrospinnability of the polymer[132].

SMAs are appropriate polymers for enzyme immobilization since they are easily available, possess relatively low toxicity and provide reactive anhydride groups for further functionalization. The electrospinning of poly (styrene-co-maleic anhydride) P(St-co-MA) in DMF and methylene chloride was successfully done by Ignatova *et al*[133] and showed potential as suitable carriers for enzyme immobilization.

The anhydride groups are not only purposeful for modifications of the surface properties, but can also be used for covalent binding of biologically active compounds. This allows the preparation of electrospun materials with long term antimicrobial activity that can be used in a wide range of applications, such as antimicrobial filters, medical devices, antimicrobial bandages and even as delivery systems[134]. The preparations of these types of systems which are covalently bonded are still scarce[135, 136]. Ignatova *et al*[134] reported the covalent attachment between antibacterial agents; 5-amino-8-hydroquinoline and chlorhexidine, and SMA electrospun mats. These mats with antimicrobial activity had the ability to prevent bacteria adhesion and showed great promise for use in medical devices, bandages, etc.

2.3 Electrospinning

2.3.1 Introduction

Electrospinning, firstly reported in 1934, has been used for more than 60 years. Since the 1980s and especially in recent years, the electrospinning process has regained more attention due to interest in nanotechnology, developing ultrafine fibrous structures of various polymers with diameters in the micro/nano-meter range[4].

A background on single-needle electrospinning will be given followed by a brief description of some of the parameters influencing the electrospinning process and resultant fibers.

2.3.1.1 Single-needle electrospinning

Electrospinning is a highly versatile and straightforward method to produce polymer fibers from polymer solutions, with diameters ranging from a few micrometers to a few nanometers[137]. Figure 2.8 shows a schematic illustration of the basic setup for electrospinning. It consists of three major components: a high-voltage power supply, a spinneret (a needle) and a collector which is grounded.

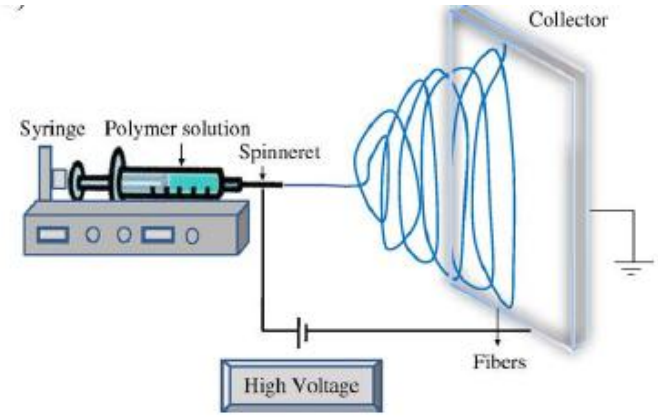

Figure 2.8: Schematic illustration of the electrospinnng setup[138].

The polymer solution is driven from a syringe into a needle by a syringe pump at a constant and controllable rate. A high voltage is applied to the syringe needle and a pendent droplet of polymer solution at the tip of the needle will become highly electrified. The droplet will experience two types of electrostatic forces: the electrostatic repulsion between the charged

surface and the Coulomb forces exerted by the external electric field. Under the influence of these electrostatic interactions, the droplet is deformed into a conical shape known as the Taylor cone. On further increase in the voltage, a critical voltage is exceeded where the repulsive force within the charged solution is larger than its surface tension; a jet would erupt from the tip of the Taylor cone and the jet moves towards a ground collector acting as counter electrode. The discharged polymer solution jet undergoes an elongation and whipping process, leading to the formation of long and thin fibers. Reneker and Doshi[139] suggested that the whipping process results from repulsive forces originating from the charged elements within the electrospinning jet. The solvent evaporates immediately after the jet is formed, leaving behind a charged polymer fiber which forms a non-woven fabric on the collector.

These non-woven nanofiber membranes have growing interest due to their unique physical, mechanical and electrical properties with their very high surface area and small pore sizes in comparison with commercial textiles[139]. The polymer used must have certain properties to be spinnable which includes, insolubility, electrical conductivity, mechanical resilience, and adhesiveness and should have chemoselective reactivity[140].

2.3.2 Parameters

There are a variety of parameters that influence the shapes and dimensions of the fibers formed during electrospinning. These include:

a) Solution parameters such as viscosity, conductivity and surface tension,
b) Process parameters such as applied voltage, distance between the capillary tip and the collector, feed rate and ambient parameters (temperature and humidity)[141, 142]

For the purpose of my study, nanofibers had to be obtained from the different polymers with similar average fiber diameters. Although numerous studies concerning the parameters exist, only those affecting the fiber diameter will be discussed further. The fiber diameter can be manipulated by varying the parameters of the electrospinning process. The major parameters affecting the diameter of the fibers are the concentration of the solution, conductivity, the electrical field strength, the flow rate of the solution and the distance between the capillary and collector[143].

2.3.2.1 Solution concentration

The polymer concentration determines if a polymer is able to be electrospun. The viscosity of a polymer solution is affected by the polymer solution concentration and molar mass of the polymer. With increasing solution concentration and molar mass of the polymer, the higher the viscosity of the solution is.

The fiber diameter is dependent on the viscosity of the solution; the lower the solution viscosity, the thinner the fibers are[144]. The higher the viscosity of the solution, the more polymer chain entanglements are present and the greater the resistance of the solution to be stretched, resulting in an increase in fiber diameter[142, 145, 146]. The fiber diameter will increase with an increase in polymer concentration until a certain concentration is reached where the solution viscosity will be too high, blocking the capillary and no electrospinning will occur[140, 147]. At too low concentrations, the polymer solution will not contain enough polymer chain entanglements to stabilize the jet and beaded fibers are formed[120, 148]. With an increase in the concentration this can be prohibited until smooth nanofibers are obtained without breaking of the jet[149].

2.3.2.2 Solution conductivity

Solution conductivity, while playing a smaller role, can affect the fiber size. The conductivity of the solution is the ability of the solution to carry charges. The extent of whipping and stretching of the polymer solution is determined by the conductivity of the solution because of the repulsion of the mutual charges present on the surface. Solutions with high conductivity have a greater charge carrying capacity than solutions with low conductivity, resulting in more whipping and stretching taking place, thus lower fiber diameters[148, 150].

For electrospinning to occur the solution must have conductivity. Conductivity can be increased by the addition of salt, increase in temperature or using a different solvent. Zhang *et al*[85] examined the effect of adding NaCl to a PVA/water solution on the diameter of electrospun fibers. The fiber diameters decreased with increasing NaCl concentration in the solution, due to the increased net charge density imparted by the NaCl causing an increased in the conductivity of the solution.

2.3.2.3 Applied voltage and electrical field strength

The strength of the applied electrical field controls formation of fibers from several microns in diameter to tens of nanometers. The applied voltage will initiate the electrospinning process; it is responsible for the surface charge on the jet. The polymer solution induces electrostatic forces by the applied voltage and when the electrostatic forces overcome the surface tension of the solution, the polymers will be electrospun.

An increase in applied voltage alters the shape of the surface at which the Taylor cone and fiber jet are formed[142] as shown in Figure 2.9.

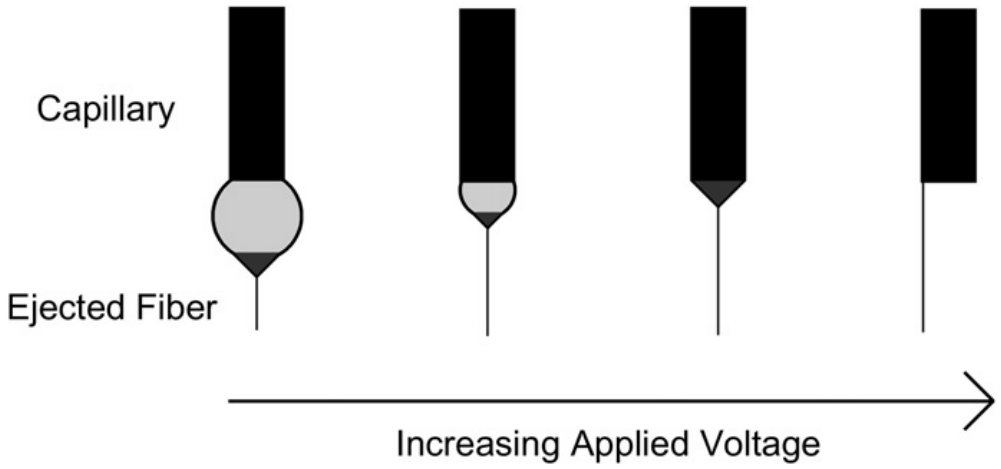

Figure 2.9: The effect of increasing applied voltage on the formation of the Taylor cone[18].

At low voltages a pendant droplet (light gray) is formed at the tip of the capillary; the Taylor cone (dark gray) forms at the tip of the pendant droplet. With an increase in voltage, the size of the pendant droplet decreases while the Taylor cone is formed. With a further increase in the voltage, the jet is ejected from the capillary. This charged jet undergoes whipping and stretching due to electrostatic repulsive charges within the jet. The higher the voltage, the more stretching occurs, decreasing the fiber diameter continuously until all the solvent has evaporated and collected on the collector as dry fibers[142].

2.3.2.4 Flow rate of the solution

Polymer flow rate has an influence on fiber size, and additionally can influence fiber porosity and fiber shape. Polymer flow rate is defined as the rate at which the solution is pumped through the capillary. The amount of solution that is available to be electrospun is determined by the flow rate.

The fiber diameter increases with an increase in the polymer flow rate[66, 151] because more solution is drawn from the tip of the capillary. Lower flow rates are more desirable as there is sufficient time for solvent evaporation and stretching of the polymer jet that leads to reduced fiber diameters[152]. If the flow rate is too low, the Taylor cone disappears, resulting in a discontinuous jet from the polymer solution. When the flow rate is too high, droplets are formed at the tip of the capillary and there is insufficient time for solvent evaporation which may result in wet fibers forming, having a ribbon-like structure[151].

2.3.2.5 Spinning distance

The spinning distance is the distance between the capillary tip and the collector surface. The distance influences the time allowed for whipping and solvent evaporation before fiber collection. With an increase in the distance, a decrease in the fiber diameter occurs. At a longer distance, the jet is able to stretch and elongate more, leading to a smaller fiber diameter[153].

A minimum distance is required to give the fibers sufficient time to dry before reaching the collector. At a shorter distance, the solvent may not have enough time to evaporate, resulting in fibers merging and forming a connected mesh; beads have also been observed at close distances[109, 154, 155].

References

1. Uhrich, K.E.; Cannizzaro, S.M.; Langer, R.S.; Shakesheff, K.M. Polymeric systems for controlled drug release. *Chem. Rev.* **1999,** *99,* 3181-3198.

2. Tiwari, S.K.; Tzezana, R.; Zussman, E.; Venkatraman, S.S. Optimizing partition-controlled drug release from electrospun core–shell fibers. *Int. J. Pharm.* **2010,** *392,* 209-217.

3. Misra, A.; Jogani, V.; Jinturkar, K.; Vyas, T. Recent patents review on intranasal administration for CNS drug delivery. *Recent patents on drug delivery & formulation* **2008,** *2,* 25-40.

4. Yu, D.; Zhu, L.; White, K.; Branford-White, C. Electrospun nanofiber-based drug delivery systems. *Health* **2009,** *1,* 67.

5. Sakuldao, S.; Yoovidhya, T.; Wongsasulak, S. Coaxial electrospinning and sustained release properties of gelatin-cellulose acetate core-shell ultrafine fibres. *Science Asia* **2011,** *37,* 335-343.

6. Yang, D.; Li, Y.; Nie, J. Preparation of gelatin/PVA nanofibers and their potential application in controlled release of drugs. *Carbohydr. Polym.* **2007,** *69,* 538-543.

7. Zeng, J.; Xu, X.; Chen, X.; Liang, Q.; Bian, X.; Yang, L.; Jing, X. Biodegradable electrospun fibers for drug delivery. *J. Controlled Release* **2003,** *92,* 227-231.

8. Maretschek, S.; Greiner, A.; Kissel, T. Electrospun biodegradable nanofiber nonwovens for controlled release of proteins. *J. Controlled Release* **2008,** *127,* 180-187.

9. Huang, Y.; Chung, T.; Tzeng, T. A method using biodegradable polylactides/polyethylene glycol for drug release with reduced initial burst. *Int. J. Pharm.* **1999,** *182,* 93-100.

10. Jeong, Y.; Kang, M.; Sun, H.; Kang, S.; Kim, H.; Moon, K.; Lee, K.; Kim, S.; Jung, S. All-trans-retinoic acid release from core-shell type nanoparticles of poly (ε-caprolactone)/poly (ethylene glycol) diblock copolymer. *Int. J. Pharm.* **2004,** *273,* 95-107.

11. Gupta, P.; Vermani, K.; Garg, S. Hydrogels: from controlled release to pH-responsive drug delivery. *Drug Discov. Today* **2002,** *7,* 569-579.

12. Graham, N.; McNeill, M. Hydrogels for controlled drug delivery. *Biomaterials* **1984,** *5,* 27-36.

13. Li, Y.; Lokitz, B.S.; Armes, S.P.; McCormick, C.L. Synthesis of reversible shell cross-linked micelles for controlled release of bioactive agents. *Macromolecules* **2006,** *39,* 2726-2728.

14. Gaucher, G.; Dufresne, M.; Sant, V.P.; Kang, N.; Maysinger, D.; Leroux, J. Block copolymer micelles: preparation, characterization and application in drug delivery. *J. Controlled Release* **2005,** *109,* 169-188.

15. Kataoka, K.; Harada, A.; Nagasaki, Y. Block copolymer micelles for drug delivery: design, characterization and biological significance. *Adv. Drug Deliv. Rev.* **2001,** *47,* 113-131.

16. Dong, Z.; Wang, Q.; Du, Y. Alginate/gelatin blend films and their properties for drug controlled release. *J. Membr. Sci.* **2006,** *280,* 37-44.

17. Wang, Q.; Dong, Z.; Du, Y.; Kennedy, J.F. Controlled release of ciprofloxacin hydrochloride from chitosan/polyethylene glycol blend films. *Carbohydr. Polym.* **2007,** *69,* 336-343.

18. Sill, T.J.; von Recum, H.A. Electrospinning: applications in drug delivery and tissue engineering. *Biomaterials* **2008,** *29,* 1989-2006.

19. Panyam, J.; Labhasetwar, V. Biodegradable nanoparticles for drug and gene delivery to cells and tissue. *Adv. Drug Deliv. Rev.* **2003,** *55,* 329-347.

20. Singh, R.; Lillard, J.W. Nanoparticle-based targeted drug delivery. *Exp. Mol. Pathol.* **2009,** *86,* 215-223.

21. Soppimath, K.S.; Aminabhavi, T.M.; Kulkarni, A.R.; Rudzinski, W.E. Biodegradable polymeric nanoparticles as drug delivery devices. *J. Controlled Release* **2001,** *70,* 1-20.

22. Pitt, G.; Gratzl, M.; Kimmel, G.; Surles, J.; Sohindler, A. Aliphatic polyesters II. The degradation of poly (DL-lactide), poly (ε-caprolactone), and their copolymers in vivo. *Biomaterials* **1981,** *2*, 215-220.

23. Calvo, P.; Vila-Jato, J.L.; Alonso, M.J. Comparative in vitro evaluation of several colloidal systems, nanoparticles, nanocapsules, and nanoemulsions, as ocular drug carriers. *J. Pharm. Sci.* **1996,** *85*, 530-536.

24. Lu, Z.; Bei, J.; Wang, S. A method for the preparation of polymeric nanocapsules without stabilizer. *J. Controlled Release* **1999,** *61*, 107-112.

25. Gref, R.; Minamitake, Y.; Peracchia, M.T.; Trubetskoy, V.; Torchilin, V.; Langer, R. Biodegradable long-circulating polymeric nanospheres. *Science* **1994,** *263*, 1600-1603.

26. Qiu, Y.; Park, K. Environment-sensitive hydrogels for drug delivery. *Adv. Drug Deliv. Rev.* **2012,** *64*, 49-60.

27. Kim, S.W.; Bae, Y.H.; Okano, T. Hydrogels: swelling, drug loading, and release. *Pharm. Res.* **1992,** *9*, 283-290.

28. Kim, S.J.; Park, S.J.; An, K.H.; Kim, N.G.; Kim, S.I. Water behavior of poly (vinyl alcohol)/poly (vinylpyrrolidone) interpenetrating polymer network hydrogels. *J Appl. Polym. Sci.* **2003,** *89*, 24-27.

29. Peppas, N.; Bures, P.; Leobandung, W.; Ichikawa, H. Hydrogels in pharmaceutical formulations. *Eur. J. Pharm. Biopharm.* **2000,** *50*, 27-46.

30. Peppas, N.A.; Sahlin, J.J. Hydrogels as mucoadhesive and bioadhesive materials: a review. *Biomaterials* **1996,** *17*, 1553-1561.

31. Hamidi, M.; Azadi, A.; Rafiei, P. Hydrogel nanoparticles in drug delivery. *Adv. Drug Deliv. Rev.* **2008,** *60*, 1638-1649.

32. Bhattarai, N.; Gunn, J.; Zhang, M. Chitosan-based hydrogels for controlled, localized drug delivery. *Adv. Drug Deliv. Rev.* **2010,** *62*, 83-99.

33. Choi, J.S.; Choi, S.H.; Yoo, H.S. Coaxial electrospun nanofibers for treatment of diabetic ulcers with binary release of multiple growth factors. *J. Mater. Chem.* **2011,** *21*, 5258-5267.

34. Hoare, T.R.; Kohane, D.S. Hydrogels in drug delivery: progress and challenges. *Polymer* **2008,** *49*, 1993-2007.

35. Kwon, G.S.; Okano, T. Polymeric micelles as new drug carriers. *Adv. Drug Deliv. Rev.* **1996,** *21*, 107-116.

36. Kabanov, A.V.; Chekhonin, V.; Alakhov, V.Y.; Batrakova, E.; Lebedev, A.; Melik-Nubarov, N.; Arzhakov, S.; Levashov, A.; Morozov, G.; Severin, E. The neuroleptic activity of haloperidol increases after its solubilization in surfactant micelles: micelles as microcontainers for drug targeting. *FEBS Lett.* **1989,** *258*, 343-345.

37. Jones, M.; Leroux, J. Polymeric micelles–a new generation of colloidal drug carriers. *Eur. J. Pharm. Biopharm.* **1999,** *48*, 101-111.

38. Ogawa, T.; Ima, S.; Wakamatsu, K. Films for food packaging. Google patents: **1992.**

39. Appendini, P.; Hotchkiss, J.H. Review of antimicrobial food packaging. *Innov. Food Sci. Emerg. Technol.* **2002,** *3*, 113-126.

40. Dutta, P.; Tripathi, S.; Mehrotra, G.; Dutta, J. Perspectives for chitosan based antimicrobial films in food applications. *Food Chem.* **2009,** *114*, 1173-1182.

41. Yohe, S.T.; Herrera, V.L.; Colson, Y.L.; Grinstaff, M.W. 3D superhydrophobic electrospun meshes as reinforcement materials for sustained local drug delivery against colorectal cancer cells. *J. Controlled Release* **2012,** *162*, 92-101.

42. Yohe, S.T.; Colson, Y.L.; Grinstaff, M.W. Superhydrophobic materials for tunable drug release: using displacement of air to control delivery rates. *J. Am. Chem. Soc.* **2012,** *134,* 2016-2019.

43. Xu, H.; Li, H.; Chang, J. Controlled drug release from a polymer matrix by patterned electrospun nanofibers with controllable hydrophobicity. *J. Mater. Chem. B* **2013,** *1,* 4182-4188.

44. Moskowitz, J.S.; Blaisse, M.R.; Samuel, R.E.; Hsu, H.; Harris, M.B.; Martin, S.D.; Lee, J.C.; Spector, M.; Hammond, P.T. The effectiveness of the controlled release of gentamicin from polyelectrolyte multilayers in the treatment of Staphylococcus aureus infection in a rabbit bone model. *Biomaterials* **2010,** *31,* 6019-6030.

45. Yarin, A. Coaxial electrospinning and emulsion electrospinning of core–shell fibers. *Polym. Adv. Technol.* **2011,** *22,* 310-317.

46. Bazilevsky, A.V.; Yarin, A.L.; Megaridis, C.M. Co-electrospinning of core-shell fibers using a single-nozzle technique. *Langmuir* **2007,** *23,* 2311-2314.

47. Moghe, A.; Gupta, B. Co-axial Electrospinning for Nanofiber Structures: Preparation and Applications. *Polym. Rev.* **2008,** *48,* 353-377.

48. Luong-Van, E.; Grøndahl, L.; Chua, K.N.; Leong, K.W.; Nurcombe, V.; Cool, S.M. Controlled release of heparin from poly (ε-caprolactone) electrospun fibers. *Biomaterials* **2006,** *27,* 2042-2050.

49. Huang, X.; Brazel, C.S. On the importance and mechanisms of burst release in matrix-controlled drug delivery systems. *J. Controlled Release* **2001,** *73,* 121-136.

50. Jiang, H.; Hu, Y.; Li, Y.; Zhao, P.; Zhu, K.; Chen, W. A facile technique to prepare biodegradable coaxial electrospun nanofibers for controlled release of bioactive agents. *J. Controlled Release* **2005,** *108,* 237-243.

51. Jannesari, M.; Varshosaz, J.; Morshed, M.; Zamani, M. Composite poly (vinyl alcohol)/poly (vinyl acetate) electrospun nanofibrous mats as a novel wound dressing matrix for controlled release of drugs. *Int. J. Nanomed.* **2011,** *6*, 993-1003.

52. Brannon-Peppas L Polymers in controlled drug delivery. *Med. Plast. Biomater.* **1997,** 34-44.

53. Langer, R.; Peppas, N.A. Advances in biomaterials, drug delivery, and bionanotechnology. *AIChE J.* **2003,** *49*, 2990-3006.

54. Sohrabi, A.; Shaibani, P.; Etayash, H.; Kaur, K.; Thundat, T. Sustained drug release and antibacterial activity of ampicillin incorporated poly (methyl methacrylate)–nylon6 core/shell nanofibers. *Polymer* **2013,** *54*, 2699-2705.

55. Kenawy, E.; Bowlin, G.L.; Mansfield, K.; Layman, J.; Simpson, D.G.; Sanders, E.H.; Wnek, G.E. Release of tetracycline hydrochloride from electrospun poly (ethylene-co-vinylacetate), poly (lactic acid), and a blend. *J. Controlled Release* **2002,** *81*, 57-64.

56. Ignatious, F.; Baldoni, J. Electrospun pharmaceutical compositions. WO 0154667, **2001.**

57. Su, Y.; Su, Q.; Liu, W.; Lim, M.; Venugopal, J.R.; Mo, X.; Ramakrishna, S.; Al-Deyab, S.S.; El-Newehy, M. Controlled release of bone morphogenetic protein 2 and dexamethasone loaded in core–shell PLLACL–collagen fibers for use in bone tissue engineering. *Acta Biomaterialia* **2012,** *8*, 763-771.

58. Xiaoqiang, L.; Yan, S.; Rui, C.; Chuanglong, H.; Hongsheng, W.; Xiumei, M. Fabrication and properties of core-shell structure P (LLA-CL) nanofibers by coaxial electrospinning. *J. Appl. Polym. Sci.* **2009,** *111*, 1564-1570.

59. Chen, W.; Li, D.; Ahmed, E.; El-Newehy, M.; EI-Hamshary, H.A.; Al-Deyab, S.S.; He, C.; Mo, X. Dexamethasone loaded core–shell SF/PEO nanofibers via green electrospinning reduced endothelial cells inflammatory damage. *Colloids Surf., B.* **2015,** *126*, 561-568.

60. Reza, M.S.; Quadir, M.A.; Haider, S.S. Comparative evaluation of plastic, hydrophobic and hydrophilic polymers as matrices for controlled-release drug delivery. *J. Pharm. Pharm. Sci.* **2003,** *6,* 274-291.

61. Kim, T.G.; Lee, D.S.; Park, T.G. Controlled protein release from electrospun biodegradable fiber mesh composed of poly (ε -caprolactone) and poly (ethylene oxide). *Int. J. Pharm.* **2007,** *338,* 276-283.

62. Taepaiboon, P.; Rungsardthong, U.; Supaphol, P. Drug-loaded electrospun mats of poly (vinyl alcohol) fibres and their release characteristics of four model drugs. *Nanotechnology* **2006,** *17,* 2317.

63. Almodóvar, J.; Kipper, M.J. Coating Electrospun Chitosan Nanofibers with Polyelectrolyte Multilayers Using the Polysaccharides Heparin and N, N, N-Trimethyl Chitosan. *Macromol. Biosci.* **2011,** *11,* 72-76.

64. Geiger, B. Dual Drug Release from CO2-Infused Nanofibers via Hydrophobic and Hydrophilic Interactions. Honors thesis, Ohio State University, **2014.**

65. Li, J.; Feng, H.; He, J.; Li, C.; Mao, X.; Xie, D.; Ao, N.; Chu, B. Coaxial electrospun zein nanofibrous membrane for sustained release. *J. Biomater. Sci., Polymer Edition* **2013,** *24,* 1923-1934.

66. Zong, X.; Kim, K.; Fang, D.; Ran, S.; Hsiao, B.S.; Chu, B. Structure and process relationship of electrospun bioabsorbable nanofiber membranes. *Polymer* **2002,** *43,* 4403-4412.

67. Zhang, Y.; Wang, X.; Feng, Y.; Li, J.; Lim, C.; Ramakrishna, S. Coaxial electrospinning of (fluorescein isothiocyanate-conjugated bovine serum albumin)-encapsulated poly (ε-caprolactone) nanofibers for sustained release. *Biomacromolecules* **2006,** *7,* 1049-1057.

68. Jiang, H.; Hu, Y.; Zhao, P.; Li, Y.; Zhu, K. Modulation of protein release from biodegradable core–shell structured fibers prepared by coaxial electrospinning. *J. Biomed. Mater. Res. B: Appl. Biomater.* **2006,** *79,* 50-57.

69. Chew, S.Y.; Wen, J.; Yim, E.K.; Leong, K.W. Sustained release of proteins from electrospun biodegradable fibers. *Biomacromolecules* **2005,** *6,* 2017-2024.

70. Xu, X.; Chen, X.; Xu, X.; Lu, T.; Wang, X.; Yang, L.; Jing, X. BCNU-loaded PEG–PLLA ultrafine fibers and their in vitro antitumor activity against Glioma C6 cells. *J. Controlled Release* **2006,** *114,* 307-316.

71. Liang, D.; Luu, Y.K.; Kim, K.; Hsiao, B.S.; Hadjiargyrou, M.; Chu, B. In vitro non-viral gene delivery with nanofibrous scaffolds. *Nucleic Acids Res.* **2005,** *33,* e170.

72. Xie, J.; Wang, C. Electrospun micro-and nanofibers for sustained delivery of paclitaxel to treat C6 glioma in vitro. *Pharm. Res.* **2006,** *23,* 1817-1826.

73. Yu, D.; Wang, X.; Li, X.; Chian, W.; Li, Y.; Liao, Y. Electrospun biphasic drug release polyvinylpyrrolidone/ethyl cellulose core/sheath nanofibers. *Acta Biomaterialia* **2013,** *9,* 5665-5672.

74. Xu, C.; Xu, F.; Wang, B.; Lu, T. Electrospinning of poly (ethylene-co-vinyl alcohol) nanofibres encapsulated with Ag nanoparticles for skin wound healing. *J. Nanomater.* **2011,** *2011,* 3.

75. Elahi, M.F.; Lu, W.; Guoping, G.; Khan, F. Core-shell Fibers for Biomedical Applications-A Review. *J Bioeng.r & Biomed. Sci 3: 121.doi* **2013.**

76. Tong, H.; Zhang, X.; Wang, M. A new nanofiber fabrication technique based on coaxial electrospinning. *Mater. Lett.* **2012,** *66,* 257-260.

77. Kim, K.; Luu, Y.K.; Chang, C.; Fang, D.; Hsiao, B.S.; Chu, B.; Hadjiargyrou, M. Incorporation and controlled release of a hydrophilic antibiotic using poly (lactide-co-glycolide)-based electrospun nanofibrous scaffolds. *J. Controlled Release* **2004,** *98,* 47-56.

78. Atiyeh, B.S.; Costagliola, M.; Hayek, S.N.; Dibo, S.A. Effect of silver on burn wound infection control and healing: review of the literature. *Burns* **2007,** *33,* 139-148.

79. Yu, D.; Shen, X.; Branford-White, C.; White, K.; Zhu, L.; Bligh, S.A. Oral fast-dissolving drug delivery membranes prepared from electrospun polyvinylpyrrolidone ultrafine fibers. *Nanotechnol.* **2009,** *20,* 055104.

80. Richardson, T.P.; Peters, M.C.; Ennett, A.B.; Mooney, D.J. Polymeric system for dual growth factor delivery. *Nat. Biotechnol.* **2001,** *19,* 1029-1034.

81. Taepaiboon, P.; Rungsardthong, U.; Supaphol, P. Vitamin-loaded electrospun cellulose acetate nanofiber mats as transdermal and dermal therapeutic agents of vitamin A acid and vitamin E. *Eur. J. Pharm. Biopharm.* **2007,** *67,* 387-397.

82. Shukla, A.; Fleming, K.E.; Chuang, H.F.; Chau, T.M.; Loose, C.R.; Stephanopoulos, G.N.; Hammond, P.T. Controlling the release of peptide antimicrobial agents from surfaces. *Biomaterials* **2010,** *31,* 2348-2357.

83. Heunis, T.d.J. Development of an antimicrobial wound dressing by co-electrospinning bacteriocins of lactic acid bacteria into polymeric nanofibers. PhD Thesis, University of Stellenbosch **2012,** 48.

84. Karuppuswamy, P.; Venugopal, J.R.; Navaneethan, B.; Laiva, A.L.; Ramakrishna, S. Polycaprolactone nanofibers for the controlled release of tetracycline hydrochloride. *Mater. Lett.* **2015,** *141,* 180-186.

85. Zhang, C.; Yuan, X.; Wu, L.; Han, Y.; Sheng, J. Study on morphology of electrospun poly (vinyl alcohol) mats. *Eur. Polym. J.* **2005,** *41,* 423-432.

86. Kang, Y.O.; Yoon, I.; Lee, S.Y.; Kim, D.; Lee, S.J.; Park, W.H.; Hudson, S.M. Chitosan-coated poly (vinyl alcohol) nanofibers for wound dressings. *J. Biomed. Mater. Res. Part B Appl. Biomater.* **2010,** *92,* 568-576.

87. Merkle, V.; Zeng, L.; Teng, W.; Slepian, M.; Wu, X. Gelatin shells strengthen polyvinyl alcohol core–shell nanofibers. *Polymer* **2013,** *54,* 6003-6007.

88. Finch, C.A. *P*olyvinyl alcohol; properties and applications. John Wiley & Sons: **1973**.

89. Wang, Z.; Hao, X.; Deng, W.; Que, Y. Research and application of PVA in slow-release material [J]. *Pack. Eng.* **2008,** *9,* 011.

90. Peppas, N.A.; Mongia, N.K. Ultrapure poly (vinyl alcohol) hydrogels with mucoadhesive drug delivery characteristics. *Eur. J. Pharm. Biopharm.* **1997,** *43,* 51-58.

91. Haweel, C.; Ammar, S. Preparation of polyvinyl alcohol from local raw material. *Iraqi J.Chem.Pet.Eng.(IJCPE)* **2008,** *9,* 15-21.

92. Şanlı, O.; Ay, N.; Işıklan, N. Release characteristics of diclofenac sodium from poly (vinyl alcohol)/sodium alginate and poly (vinyl alcohol)-grafted-poly (acrylamide)/sodium alginate blend beads. *Eur. J. Pharm. Biopharm.* **2007,** *65,* 204-214.

93. Kurihara, S.; Sakamaki, S.; Mogi, S.; Ogata, T.; Nonaka, T. Crosslinking of poly (vinyl alcohol)-graft-N-isopropylacrylamide copolymer membranes with glutaraldehyde and permeation of solutes through the membranes. *Polymer* **1996,** *37,* 1123-1128.

94. Philipp, W.H.; Hsu, L. Three Methods for In Situ Cross-Linking of Polyvinyl Alcohol Films for Application as Ion-Conducting Membranes in Potassium Hydroxide Electrolyte. NASA Technical Paper **1979**, 1-15.

95. Koski, A.; Yim, K.; Shivkumar, S. Effect of molecular weight on fibrous PVA produced by electrospinning. *Mate. Lett.* **2004,** *58,* 493-497.

96. Jin, X.; Hsieh, Y. pH-responsive swelling behavior of poly (vinyl alcohol)/poly (acrylic acid) bi-component fibrous hydrogel membranes. *Polymer* **2005,** *46,* 5149-5160.

97. Shalumon, K.; Binulal, N.; Selvamurugan, N.; Nair, S.; Menon, D.; Furuike, T.; Tamura, H.; Jayakumar, R. Electrospinning of carboxymethyl chitin/poly (vinyl alcohol) nanofibrous scaffolds for tissue engineering applications. *Carbohydr. Polym.* **2009,** *77,* 863-869.

98. Pham, Q.P.; Sharma, U.; Mikos, A.G. Electrospinning of polymeric nanofibers for tissue engineering applications: a review. *Tissue Eng.* **2006,** *12,* 1197-1211.

99. Liu, F.; Nishikawa, T.; Shimizu, W.; Sato, T.; Usami, H.; Amiya, S.; Ni, Q.; Murakami, Y. Preparation of fully hydrolyzed polyvinyl alcohol electrospun nanofibers with diameters of sub-200 nm by viscosity control. *Text. Res. J.* **2012,** *82*, 1635-1644.

100. Zeng, J.; Aigner, A.; Czubayko, F.; Kissel, T.; Wendorff, J.H.; Greiner, A. Poly (vinyl alcohol) nanofibers by electrospinning as a protein delivery system and the retardation of enzyme release by additional polymer coatings. *Biomacromolecules* **2005,** *6*, 1484-1488.

101. Rao, S.B.; Sharma, C.P. Use of chitosan as a biomaterial: studies on its safety and hemostatic potential. *J. Biomed. Mater. Res.* **1997,** *34*, 21-28.

102. Rinaudo, M. Chitin and chitosan: properties and applications. *Prog. Polym. Sci.* **2006,** *31*, 603-632.

103. Jayakumar, R.; Prabaharan, M.; Kumar, P.S.; Nair, S.; Tamura, H. Biomaterials based on chitin and chitosan in wound dressing applications. *Biotechnol. Adv.* **2011,** *29*, 322-337.

104. Tsai, G.; Su, W. Antibacterial activity of shrimp chitosan against Escherichia coli. *J. Food Prot.* **1999,** *62*, 239-243.

105. Ralston, G.; Tracey, M.; Wrench, P.M. The inhibition of fermentation in baker's yeast by chitosan. *Biochim. et Biophys. Acta (BBA)-General Subjects* **1964,** *93*, 652-655.

106. Min, B.; Lee, S.W.; Lim, J.N.; You, Y.; Lee, T.S.; Kang, P.H.; Park, W.H. Chitin and chitosan nanofibers: electrospinning of chitin and deacetylation of chitin nanofibers. *Polymer* **2004,** *45*, 7137-7142.

107. De Vrieze, S.; Westbroek, P.; Van Camp, T.; Van Langenhove, L. Electrospinning of chitosan nanofibrous structures: feasibility study. *J. Mater. Sci.* **2007,** *42*, 8029-8034.

108. Ohkawa, K.; Cha, D.; Kim, H.; Nishida, A.; Yamamoto, H. Electrospinning of chitosan. *Macromol. Rapid Commun.* **2004,** *25*, 1600-1605.

109. Geng, X.; Kwon, O.; Jang, J. Electrospinning of chitosan dissolved in concentrated acetic acid solution. *Biomaterials* **2005,** *26*, 5427-5432.

110. Xu, J.; Zhang, J.; Gao, W.; Liang, H.; Wang, H.; Li, J. Preparation of chitosan/PLA blend micro/nanofibers by electrospinning. *Mater. Lett.* **2009,** *63*, 658-660.

111. Zhou, Y.; Yang, D.; Nie, J. Electrospinning of chitosan/poly (vinyl alcohol)/acrylic acid aqueous solutions. *J. Appl. Polym. Sci.* **2006,** *102*, 5692-5697.

112. Duan, B.; Dong, C.; Yuan, X.; Yao, K. Electrospinning of chitosan solutions in acetic acid with poly (ethylene oxide). *J. Biomater. Sci. Polym. Ed.* **2004,** *15*, 797-811.

113. Zhao, R.; Li, X.; Sun, B.; Zhang, Y.; Zhang, D.; Tang, Z.; Chen, X.; Wang, C. Electrospun chitosan/sericin composite nanofibers with antibacterial property as potential wound dressings. *Int. J. Biol. Macromol.* **2014,** *68*, 92-97.

114. Zhuang, X.; Cheng, B.; Kang, W.; Xu, X. Electrospun chitosan/gelatin nanofibers containing silver nanoparticles. *Carbohydr. Polym.* **2010,** *82*, 524-527.

115. Lopez-Rubio, A.; Lagaron, J.M.; Gimenez, E.; Cava, D.; Hernandez-Muñoz, P.; Yamamoto, T.; Gavara, R. Morphological alterations induced by temperature and humidity in ethylene-vinyl alcohol copolymers. *Macromolecules* **2003,** *36*, 9467-9476.

116. Du Toit, M.L. Incorporation of polysaccharide nanowhiskers into a poly (ethylene-co-vinyl alcohol) matrix. MSc Thesis, University of Stellenbosch **2013,** 6.

117. Keulder, L. The preparation of polyolefin nanofibres by solution electrospinning. PhD Thesis, University of Stellenbosch. **2013,** 11.

118. Ait-Kadi, A.; Bousmina, M.; Yousefi, A.; Mighri, F. High performance structured polymer barrier films obtained from compatibilized polypropylene/ethylene vinyl alcohol blends. *Polym. Eng. Sci.* **2007,** *47*, 1114-1121.

119. Fonseca, C.; Pereña, J.; Benavente, R.; Cerrada, M.L.; Bello, A.; Pérez, E. Microhardness and thermal study of the annealing effects in vinyl alcohol-ethylene copolymers. *Polymer* **1995,** *36,* 1887-1892.

120. Kenawy, E.; Layman, J.M.; Watkins, J.R.; Bowlin, G.L.; Matthews, J.A.; Simpson, D.G.; Wnek, G.E. Electrospinning of poly (ethylene-co-vinyl alcohol) fibers. *Biomaterials* **2003,** *24,* 907-913.

121. Ogata, N.; Lu, G.; Iwata, T.; Yamaguchi, S.; Nakane, K.; Ogihara, T. Effects of ethylene content of poly (ethylene-co-vinyl alcohol) on diameter of fibers produced by melt-electrospinning. *J. Appl. Polym. Sci.* **2007,** *104,* 1368-1375.

122. Young, T.; Hu, W. Covalent bonding of lysine to EVAL membrane surface to improve survival of cultured cerebellar granule neurons. *Biomaterials* **2003,** *24,* 1477-1486.

123. Cerrada, M.; Sánchez-Chaves, M.; Ruiz, C.; Fernandez-Garcia, M. Recognition abilities and development of heat-induced entangled networks in lactone-derived glycopolymers obtained from ethylene-vinyl alcohol copolymers. *Biomacromolecules* **2009,** *10,* 1828-1837.

124. de Biotecnología, G. Poly (vinylalcohol-co-ethylene) biodegradation on semi solid fermentation by Phanerochaete chrysosporium. *Acta Farm.Bonaerense* **2004,** *23,* 123-128.

125. Xu, C. Electro-spinning of poly (ethylene-co-vinyl alcohol) (EVOH) nanofibers for medical applications and its mechanical properties. PhD Thesis, Brunel University **2012,** 78-90.

126. Mpitso, K. Synthesis and characterization of styrene–maleic anhydride copolymer derivatives MSc Thesis, University of Stellenbosch **2009,** 31.

127. Kaur, I.; Kumari, V.; Singh, B. Synthesis and characterization of acrylic acid grafted styrene-maleic anhydride copolymer. *Der Chemica Sinica***, 2012,** *3,* 343-358.

128. Maeda, H.; Ueda, M.; Morinaga, T.; Matsumoto, T. Conjugation of poly (styrene-co-maleic acid) derivatives to the antitumor protein neocarzinostatin: pronounced improvements in pharmacological properties. *J. Med. Chem.* **1985,** *28,* 455-461.

129. Maeda, H. SMANCS and polymer-conjugated macromolecular drugs: advantages in cancer chemotherapy. *Adv. Drug Deliv. Rev.* **2001,** *46,* 169-185.

130. Eda, G.; Liu, J.; Shivkumar, S. Solvent effects on jet evolution during electrospinning of semi-dilute polystyrene solutions. *Eur. Polym. J.* **2007,** *43*, 1154-1167.

131. Jarusuwannapoom, T.; Hongrojjanawiwat, W.; Jitjaicham, S.; Wannatong, L.; Nithitanakul, M.; Pattamaprom, C.; Koombhongse, P.; Rangkupan, R.; Supaphol, P. Effect of solvents on electro-spinnability of polystyrene solutions and morphological appearance of resulting electrospun polystyrene fibers. *Eur. Polym. J.* **2005,** *41,* 409-421.

132. Cronje, L. Surface modification of styrene maleic anhydride nanofibers for efficient capture of Mycobacterium tuberculosis. PhD Thesis, University of Stellenbosch **2012,** 30.

133. Ignatova, M.; Stoilova, O.; Manolova, N.; Mita, D.; Diano, N.; Nicolucci, C.; Rashkov, I. Electrospun microfibrous poly (styrene-alt-maleic anhydride)/poly (styrene-co-maleic anhydride) mats tailored for enzymatic remediation of waters polluted by endocrine disruptors. *Eur. Polym. J.* **2009,** *45*, 2494-2504.

134. Ignatova, M.; Stoilova, O.; Manolova, N.; Markova, N.; Rashkov, I. Electrospun mats from styrene/maleic anhydride copolymers: modification with amines and assessment of antimicrobial activity. *Macromol. Biosci.* **2010,** *10,* 944-954.

135. Chen, L.; Bromberg, L.; Hatton, T.A.; Rutledge, G.C. Electrospun cellulose acetate fibers containing chlorhexidine as a bactericide. *Polymer* **2008,** *49,* 1266-1275.

136. Yao, C.; Li, X.; Neoh, K.; Shi, Z.; Kang, E. Surface modification and antibacterial activity of electrospun polyurethane fibrous membranes with quaternary ammonium moieties. *J. Membr. Sci.* **2008,** *320*, 259-267.

137. Bognitzki, M.; Czado, W.; Frese, T.; Schaper, A.; Hellwig, M.; Steinhart, M.; Greiner, A.; Wendorff, J.H. Nanostructured fibers via electrospinning. *Adv Mater* **2001,** 70.

138. Bhardwaj, N.; Kundu, S.C. Electrospinning: a fascinating fiber fabrication technique. *Biotechnol. Adv.* **2010,** *28,* 325-347.

139. Doshi, J.; Reneker, D.H. Electrospinning process and applications of electrospun fibers. *J. Electrost.* **1993,** 35**,** 1698-1703.

140. Greiner, A.; Wendorff, J.H. Electrospinning: a fascinating method for the preparation of ultrathin fibers. *Angew. Chem. Int.l Ed.* **2007,** *46,* 5670-5703.

141. Kim, B.; Kim, I. Recent nanofiber technologies. *Polym. Rev.* **2011,** *51,* 235-238.

142. Deitzel, J.; Kleinmeyer, J.; Harris, D.; Tan, N.B. The effect of processing variables on the morphology of electrospun nanofibers and textiles. *Polymer* **2001,** *42,* 261-272.

143. Li, D.; Xia, Y. Electrospinning of nanofibers: reinventing the wheel? *Adv. Mater* **2004,** *16,* 1151-1170.

144. Wang, C.; Yan, K.; Lin, Y.; Hsieh, P.C. Biodegradable core/shell fibers by coaxial electrospinning: processing, fiber characterization, and its application in sustained drug release. *Macromolecules* **2010,** *43,* 6389-6397.

145. Yördem, O.; Papila, M.; Menceloğlu, Y.Z. Effects of electrospinning parameters on polyacrylonitrile nanofiber diameter: An investigation by response surface methodology. *Mater. Design* **2008,** *29,* 34-44.

146. Dersch, R.; Steinhart, M.; Boudriot, U.; Greiner, A.; Wendorff, J. Nanoprocessing of polymers: applications in medicine, sensors, catalysis, photonics. *Polym. Adv. Technol.* **2004,** *16,* 276-282.

147. Venugopal, J.; Zhang, Y.; Ramakrishna, S. Electrospun nanofibres: biomedical applications. *Proc. Inst. Mech. Eng. N. J. Nanoeng. Nanosyst.* **2004,** *218,* 35-45.

148. Kilic, A.; Oruc, F.; Demir, A. Effects of polarity on electrospinning process. *Text. Res. J.* **2008,** *78,* 532-539.

149. Teo, W.; Gopal, R.; Ramaseshan, R.; Fujihara, K.; Ramakrishna, S. A dynamic liquid support system for continuous electrospun yarn fabrication. *Polymer* **2007,** *48*, 3400-3405.

150. Uyar, T.; Besenbacher, F. Electrospinning of uniform polystyrene fibers: The effect of solvent conductivity. *Polymer* **2008,** *49*, 5336-5343.

151. Megelski, S.; Stephens, J.S.; Chase, D.B.; Rabolt, J.F. Micro-and nanostructured surface morphology on electrospun polymer fibers. *Macromolecules* **2002,** *35*, 8456-8466.

152. Yuan, X.; Zhang, Y.; Dong, C.; Sheng, J. Morphology of ultrafine polysulfone fibers prepared by electrospinning. *Polym. Int.* **2004,** *53*, 1704-1710.

153. Seeram, R.; Kazutoshi, F.; LT-C, T.W.; Zuwei, M. An introduction to electrospinning and nanofibers. World Scientific Publishing Co. Pte. Ltd: Singapore, **2005.**

154. Lee, J.S.; Choi, K.H.; Ghim, H.D.; Kim, S.S.; Chun, D.H.; Kim, H.Y.; Lyoo, W.S. Role of molecular weight of atactic poly (vinyl alcohol)(PVA) in the structure and properties of PVA nanofabric prepared by electrospinning. *J. Appl. Polym. Sci.* **2004,** *93*, 1638-1646.

155. Ki, C.S.; Baek, D.H.; Gang, K.D.; Lee, K.H.; Um, I.C.; Park, Y.H. Characterization of gelatin nanofiber prepared from gelatin–formic acid solution. *Polymer* **2005,** *46*, 5094-5102.

Chapter 3

Experimental

This chapter describes the materials and procedures used for the electrospinning and the incorporation of the antimicrobial agent, DHBA into the electrospun mats and films. The characterization techniques used to study these electrospun fibers will also be discussed.

3.1 Materials

The materials are summarized in the following table. The materials were used as received from the supplier.

Table 3.1: Materials used during study.

Materials	Supplier
Poly (vinyl alcohol) , (99+ hydrolyzed, Mw=89 000-98 000 g/mole)	Sigma-Aldrich
Chitosan (Medium Mw = 129 000 g/mole)	Sigma-Aldrich
Poly (ethylene-co-vinyl alcohol) , (EVOH with an ethylene content of 44%)	Sigma-Aldrich
Poly (styrene-co-maleic anhydride) (Mw = 6 400g/mole, 28% anhydride content)	Polyscope Polymers
2,3-Dihydroxybenzoic acid	Merck
Trifluoroacetic acid	Sigma-Aldrich
Dichloromethane	Merck
Isopropanol	Merck
N,N-dimethylformamide	Sigma-Aldrich
Acetic acid	Merck
Glutaraldehyde (50% in water)	Fluka

3.2 Methodology

The conventional single-needle electrospinning technique was used to electrospin polymer solutions and solvent casting was used for the preparation of the films. The preparation of electrospinning solutions and conditions used during the electrospinning process are reported in subsequent sections as well as the solvent casting technique used to make the films.

3.2.1 Electrospinning

3.2.1.1 Preparation of electrospinning solutions

The polymer solutions were prepared as shown in table 3.2 below. The solvent system used for each polymer[1-4] was chosen because it gave the smoothest fibers and also made for stable electrospinning solutions that displayed minimal blocking of the capillaries during electrospinning. For the incorporation of DHBA, 30 mg of DHBA was added to the solution prior to electrospinning.

Table 3.2: Preparation of polymer solutions.

Polymer	Concentration (wt%)	Solvent system	Temperature (°C)	Time (hours)
PVA	10-14	Distilled water	90	3
EVOH	5-7	Isopropanol:H_2O (70:30)	80	3
Chitosan	2-6	TFA:DCM (70:30)	R.T	2
SMA	30-50	Acetone:DMF (2:1)	R.T	2

3.2.1.2 Electrospinning set-up and conditions

The electrospinning of the polymer solutions was carried out on a horizontal electrospinning setup as illustrated in Figure 3.1. This set-up consists of a high voltage power supply unit (0-50 kV), a syringe pump, a spinneret connected to the positive terminal as well as a grounded collector plate covered with aluminum foil connected to the negative terminal of the power supply unit. All spinning was conducted inside a fume-hood (without the extraction fan operating) and both temperature and relative humidity were monitored and controlled at 23-25 °C and ~40% rH, respectively. The parameters which influence the average fiber diameter, such

as the concentration, voltage, flow rate of the solution and the spinning distance between the needle tip and the collector were varied to investigate the effect it has on the average fiber diameter.

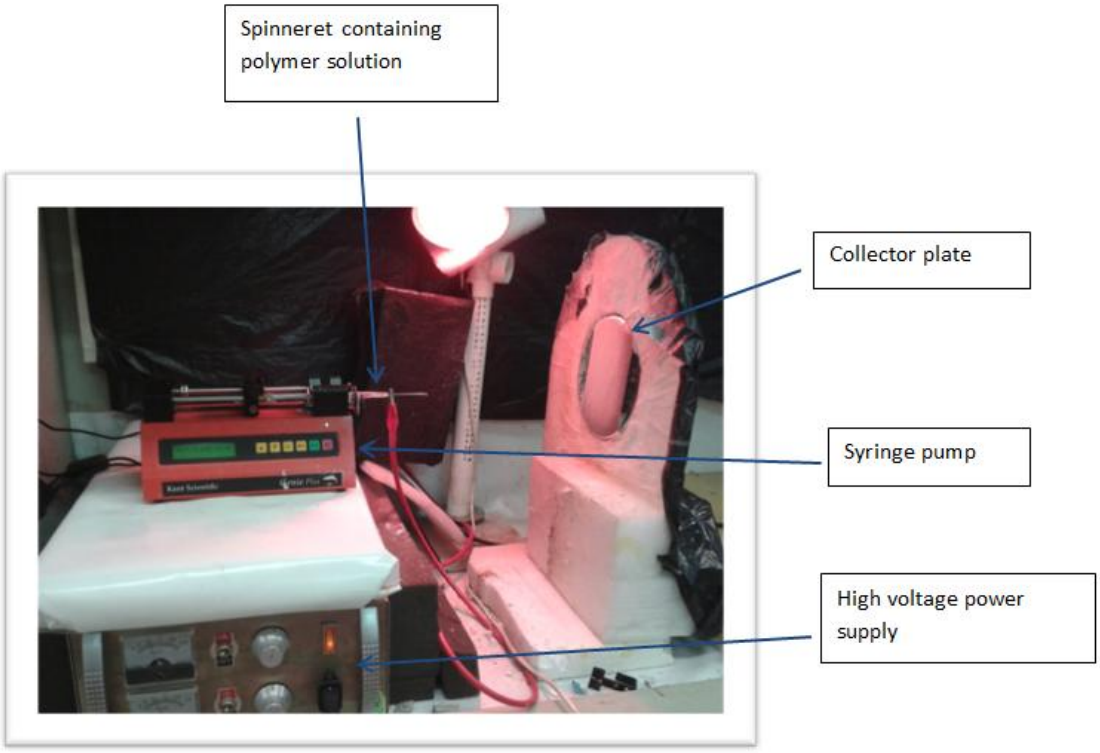

Figure 3.1: Electrospinning set-up used to electrospin the various polymer solutions.

3.2.2 Solvent casting

Cast films were made from the polymer solutions described in Section 3.2.1.1. For comparison purposes between different polymers, the concentrations were kept constant at 5wt% for all polymers. The amount of DHBA that was added was also kept constant at 30 mg. The solutions were cast into petri dishes of 5 cm in diameter and left at room temperature for most of the solvents to evaporate. They were dried under vacuum to completely remove any residual solvents. The weights of all samples were recorded before any further analysis.

3.3 Methods of characterization of DHBA-loaded electrospun nanofibers

3.3.1 Analysis of resultant fiber diameter: Scanning Electron Microscopy (SEM)

All samples were fixed to SEM stubs and gold coated before analysis for 3 min. SEM analysis was performed with a Leo® 1430VP scanning electron microscope at the Central Analytical Facility of Stellenbosch University to study the morphology of the electrospun fiber mats. The average fiber diameters were determined with custom image analysis software (SEM Image Studio). About 25 measurement were taken for the calculation as shown in Figure 3.2.

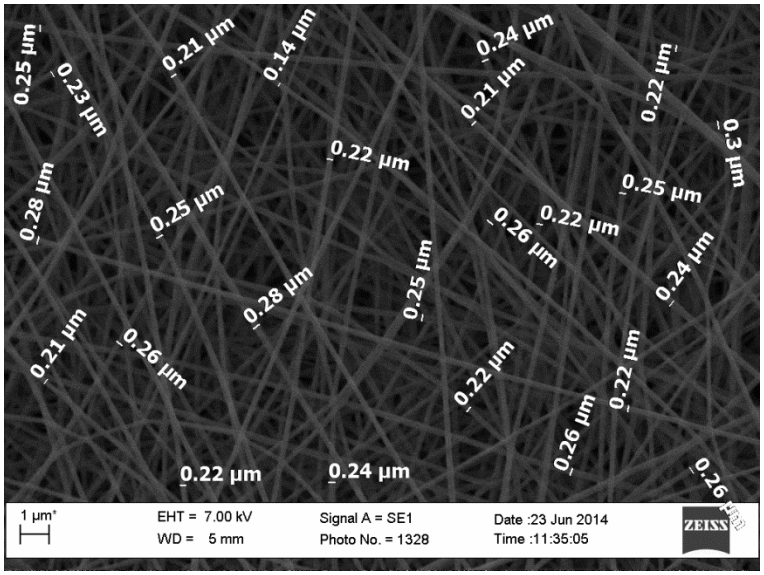

Figure 3.2: SEM image of PVA showing measurement of fiber diameter.

3.3.2 Interaction of DHBA with polymers and stability of DHBA

3.3.2.1 Attenuated total reflectance - Fourier transform infrared spectroscopy (ATR-FTIR)

ATR-FTIR is an effective and simple instrument to identify and study the presence of specific functional groups in a molecule. It was used to monitor the presence of DHBA within the polymer matrices and also to identify the interaction of DHBA with the matrices. Analysis of samples with and without DHBA was done at room temperature using a Thermo Fisher Nicolet

iS10 Attenuated Total Reflectance – Fourier Transform Infrared spectrometer. The spectra were recorded at a number of scans set at 64 and with a resolution of 4 cm^{-1}.

3.3.2.2 Thermogravimetric analysis (TGA)

TGA is a technique that studies the thermal stability of a compound; it measures the weight loss of a material as a function of temperature under a controlled atmosphere. These changes in weight loss of a material are due to decomposition, oxidation or dehydration. Stability of the incorporated DHBA matrices was studied by thermogravimetric analysis (TGA), using a Perkin Elmer TGA7 instrument. Samples of 20 mg were analysed. All tests were performed from 25-900 °C, at a heating rate of 10 °C/min in a nitrogen atmosphere.

3.3.2.3 Differential scanning calorimetry (DSC)

The effect of DHBA on the melting temperature of the polymers was studied using differential scanning calorimetry. The melting behavior of all the samples with and without DHBA was studied using a Q100 (TA Instrument). The instrument was calibrated using Indium metal according to a standard procedure. About 5 mg of each sample was weighed off and sealed in a standard DSC pan for analysis. All the measurements were conducted in a nitrogen atmosphere. The procedure consisted of three cycles and a heating/cooling ramp of 10 °C/min was used.

The following conditions were used for the different polymers:

Table 3.3: DSC temperature ranges used for each polymer matrix.

Samples with and without DHBA	Temperature range (°C)
PVA	-40-270
Chitosan	0-300
EVOH	25-200
SMA	25-300

3.4 Release study

3.4.1 Determination of DHBA release with time

DHBA-containing nanofibers and films (5 cm in diameter) were placed in 100 ml distilled water. At pre-determined time intervals up to 1 week[5], samples were taken and the DHBA concentration in the nanofibers and films was determined using a UV Spectrophotometer (SmartSpec™ plus, Biorad) at a wavelength of 310 nm. The percentage DHBA released from the mats and films was back-calculated from a calibration curve.

3.4.2 Swelling behavior

To evaluate the swelling behavior, the DHBA-loaded cast films with known weights were put in 100 ml distilled water for up to 24 hours. The samples were removed at specified times (1, 4 and 24 hours) where the water on the sample surfaces was removed with tissue paper and the samples were weighed. The degree of swelling was calculated according to the following equation for each sample[6]:

Degree of swelling (%): $\frac{M-M_d}{M_d} \times 100$

M is the weight of the samples after immersion in water and M_d is the weight of the samples in dry state.

3.4.3 Controlling the release of DHBA from the films

The release of DHBA from the coated DHBA-loaded films was studied. This was done as illustrated in Figure 3.3. The bottom film was incorporated with DHBA and coated with another polymer film[7]. The release of DHBA from these films was studied using UV spectroscopy at specified time-intervals as discussed above.

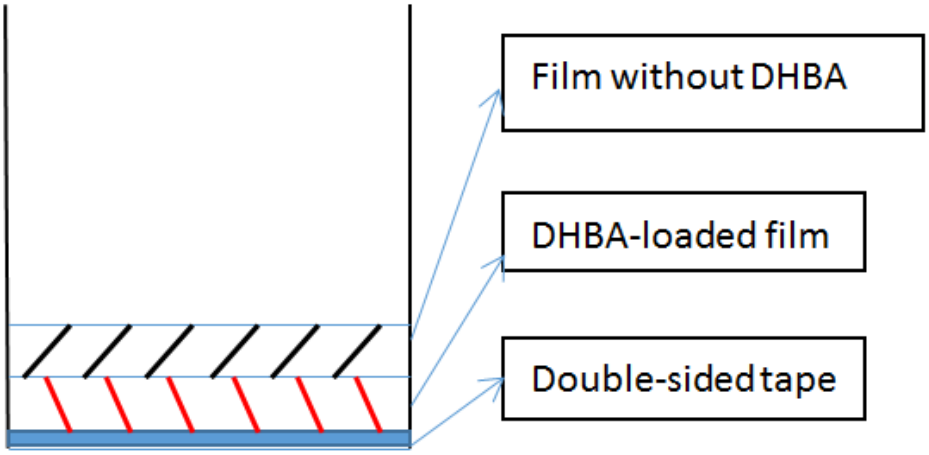

Figure 3.3: Schematic illustration of the film-film formation.

3.4.4 Actual DHBA content in electrospun mats

The actual amount of DHBA in the DHBA-loaded electrospun mats was quantified by dissolving the mats in 5 ml of an appropriate solvent as shown in table 3.2. After this, 0.5 ml of the solution was added into 5 ml of distilled water. Each DHBA-containing dilute solution the amount of DHBA was determined using a UV-spectrophotometer at a wavelength of 310 nm. The amount of DHBA present in the electrospun mats was back-calculated from the obtained data against a pre-determined calibration curve for each electrospun mat. The results were reported as averages from at least five measurements.

3.4.5 Degradation effects

In order to determine the stability of the electrospun fibers in aqueous media, the nanofiber mats were immersed in distilled water at room temperature for 24 hours. They were dried under hood and then viewed under SEM to observe morphological changes.

3.4.6 Effect of crosslinking on the release behavior

The effect of crosslinking on the morphological stability and the release rate of DHBA from the DHBA-loaded electrospun mats was investigated. The fiber mats were crosslinked in a vaporizing chamber with a 50% glutaraldehyde solution. The effect of two crosslinking times, 24 and 48 hours, was investigated. The fiber mats were dried to remove any residual glutaraldehyde on the surface and the morphology was studied using SEM. The release of DHBA from these crosslinked samples was analysed using UV spectroscopy as discussed above.

3.4.7 Controlling the release of DHBA from the electrospun mats

Nanofiber mats incorporated with DHBA were coated with 1% polymer solutions for 60 min[8]. The mats were weighed before immersion into various polymer solutions. Each polymer was coated with three other polymer solutions where-after it was dried and weighed again. The morphology of the coated DHBA-electrospun mats was studied using SEM, and FTIR was used to confirm the coating of the electrospun mats. The release of DHBA from these coated DHBA-electrospun mats was investigated by UV spectroscopy.

References

1. Park, J.; Ito, T.; Kim, K.; Kim, K.; Kim, B.; Khil, M.; Kim, H.; Kim, I. Electrospun poly (vinyl alcohol) nanofibers: effects of degree of hydrolysis and enhanced water stability. *Polym. J.* **2010,** *42,* 273-276.

2. Du Toit, M.L. Incorporation of polysaccharide nanowhiskers into a poly (ethylene-co-vinyl alcohol) matrix. MSc Thesis, University of Stellenbosch, **2013,** 21-22.

3. Ohkawa, K.; Cha, D.; Kim, H.; Nishida, A.; Yamamoto, H. Electrospinning of chitosan. *Macromol. Rapid Commun.***2004,** *25,* 1600-1605.

4. Tang, C.; Ye, S.; Liu, H. Electrospinning of poly (styrene-co-maleic anhydride) (SMA) and water-swelling behavior of crosslinked/hydrolyzed SMA hydrogel nanofibers. *Polymer* **2007,** *48,* 4482-4491.

5. Jannesari, M.; Varshosaz, J.; Morshed, M.; Zamani, M. Composite poly (vinyl alcohol)/poly (vinyl acetate) electrospun nanofibrous mats as a novel wound dressing matrix for controlled release of drugs. *Int. J. Nanomed.* **2011,** *6,* 993-1003.

6. Meng, Z.; Xu, X.; Zheng, W.; Zhou, H.; Li, L.; Zheng, Y.; Lou, X. Preparation and characterization of electrospun PLGA/gelatin nanofibers as a potential drug delivery system. *Colloids Surf., B* **2011,** *84,* 97-102.

7. Arya, A.; Chandra, A.; Sharma, V.; Pathak, K. Fast dissolving oral films: an innovative drug delivery system and dosage form. *Int. J. Chem. Tech. Res.* **2010,** *2,* 576-583.

8. Kang, Y.O.; Yoon, I.; Lee, S.Y.; Kim, D.; Lee, S.J.; Park, W.H.; Hudson, S.M. Chitosan-coated poly (vinyl alcohol) nanofibers for wound dressings. *J. Biomed. Mater. Res. Part B Appl. Biomater.* **2010,** *92,* 568-576.

Chapter 4

Characterization of electrospun fibers with and without DHBA

In this chapter the utilization of the electrospinning process is described with a closer look at the parameters affecting the average fiber diameter. An antimicrobial agent, 2, 3-dihydroxybenzoic acid is added to the various polymer solutions to obtain nanofibers with antimicrobial properties. These electrospun mats and films were characterized and analysed with various techniques in order to get a better understanding of how the DHBA influences the properties of the polymer itself.

4.1 Electrospinning

As mentioned in Chapter 2, there are many factors that can affect the final morphology and fiber diameter of the electrospun fibers including polymer solution concentration, conductivity, and applied voltage, spinning distance, flow rate of polymer solution, needle diameter, temperature and humidity[1, 2]. By manipulating these processing variables and parameters during electrospinning, the final morphology and fiber diameter of the fibers can be controlled. The main objective for the electrospinning was not to do a comprehensive investigation of factors affecting nanofiber morphology. Instead it focused on investigating the effect the parameters has on the average fiber diameter and finding optimum conditions for the various polymers to have similar fiber diameters. This would be important in the case of release rate comparisons.

The electrospinning of PVA, chitosan, EVOH and SMA are well documented in literature[3-10] although an in-depth study on the various parameters affecting the fiber diameter has not been done. The effect of the different parameters on each polymer will be discussed separately. The fibers produced were observed using scanning electron microscopy (SEM) to determine the average fiber diameter.

4.1.1 Electrospinning of poly (vinyl alcohol)

The electrospinning of PVA solution has been extensively studied for the preparation of biodegradable mats. The dissolution of PVA depends on the temperature and the extent of hydrolysis in the polymer. The solubility of PVA in water increases greatly as its degree of hydrolysis increases[11]. Various morphologies have been produced, mostly including beads, beaded fibers and fibers[3, 12].

PVA was dissolved in water at 80 °C for 3 hours until it was completely dissolved. The concentration of the PVA solution was varied from 10wt% to 14wt% while keeping the voltage, spinning distance and flow rate constant. With an increase in the concentration, an increase in the average fiber diameter (238±48 nm to 361±41 nm) was observed as shown in Figure 4.1. On increasing the solution concentration the viscosity increases[13]. The morphology changes from beads-like structure to smooth fibers with an increase in concentration. Although smooth fibers

were obtained at 14wt%, the viscosity was such that blockage of the needle occurred and a continuous electrospinning process was not possible.

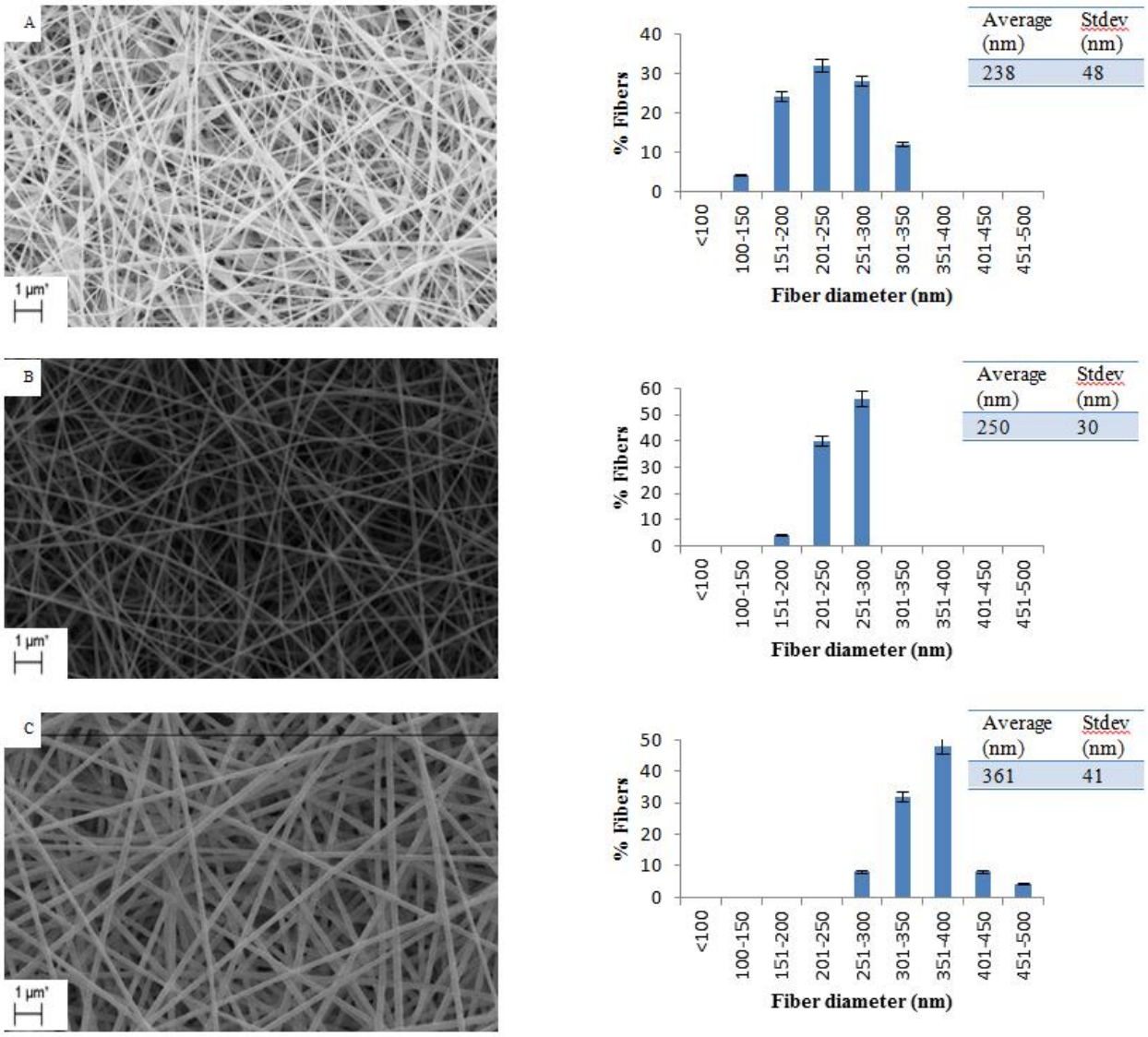

Figure 4.1: SEM images of PVA at different concentrations: A – 10wt%, B – 12wt%, and C – 14wt%, all spun under the same conditions, 10 kV, FR: 0.01 ml/min and SD: 10 cm.

A narrow fiber distribution was obtained at 12wt% PVA solution which indicates homogenous and complementary parameter (solution, process and ambient) combinations[14]. For this reason, the concentration was kept constant at 12wt% while investigating the other parameters.

The effect of varying the voltage is shown in Figure 4.2. A slight increase in the average fiber diameter was observed with an increase in voltage from 10 to 15 kV. In most cases higher voltage will lead to reduction in fiber diameter, due to better stretching of the solution[15]. Beaded fibers with lumps in-between were also obtained at a higher voltage. Some researchers have shown that when the voltage increases, the tendency of bead formation also increases[2, 16, 17]. The reason for an increase in fiber diameter is that at a higher voltage more solution gets drawn out of the needle and results in thicker fibers and not enough stretching of the solution. The lumps or fused droplets indicate insufficient stretching and solvent evaporation because of the slow evaporation of water during the electrospinning process.

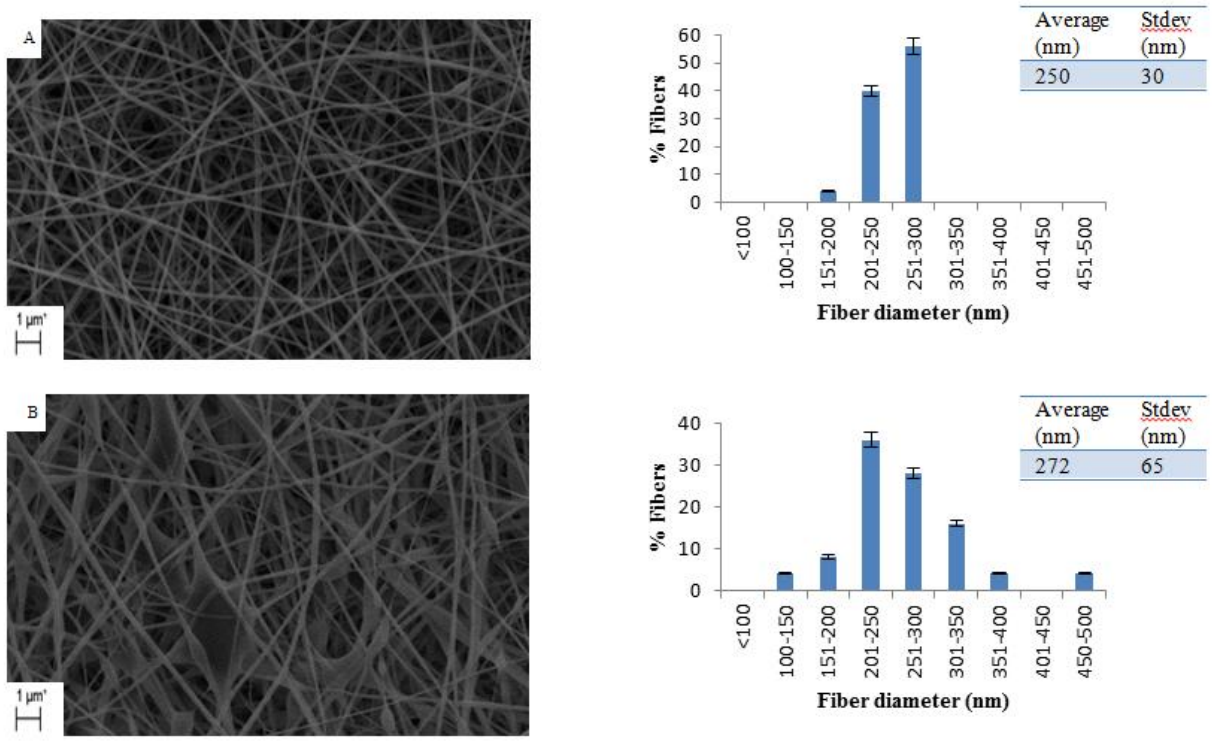

Figure 4.2: SEM images of 12wt% PVA while varying the voltage, A – 10 kV and B – 15 kV.

In Figure 4.3 the results of varying the flow rate are presented. The concentration, voltage and distance were kept constant at 12wt%, 10 kV and 10 cm respectively. The flow rate of the solution was varied from 0.01 ml/min to 0.03 ml/min. The fiber diameter tends to increase when increasing the flow rate and produced bead-free fibers. It is expected that with an increase in the

flow rate that an increase in the average fiber diameter will occur. With an increase in flow rate, more polymer solution will be present at the tip of the needle and more material will lead to thicker fibers being produced. The thinnest fibers of 244±63 nm were however produced using the highest flow rate of 0.03 ml/min. At a certain point where the amount of the solution supplied at the needle tip equals the rate at which it is taken away, an increase in the flow rate will increase the charges on the jet, which in turn will allow the jet to be stretched more and thinner fibers will be obtained[15].

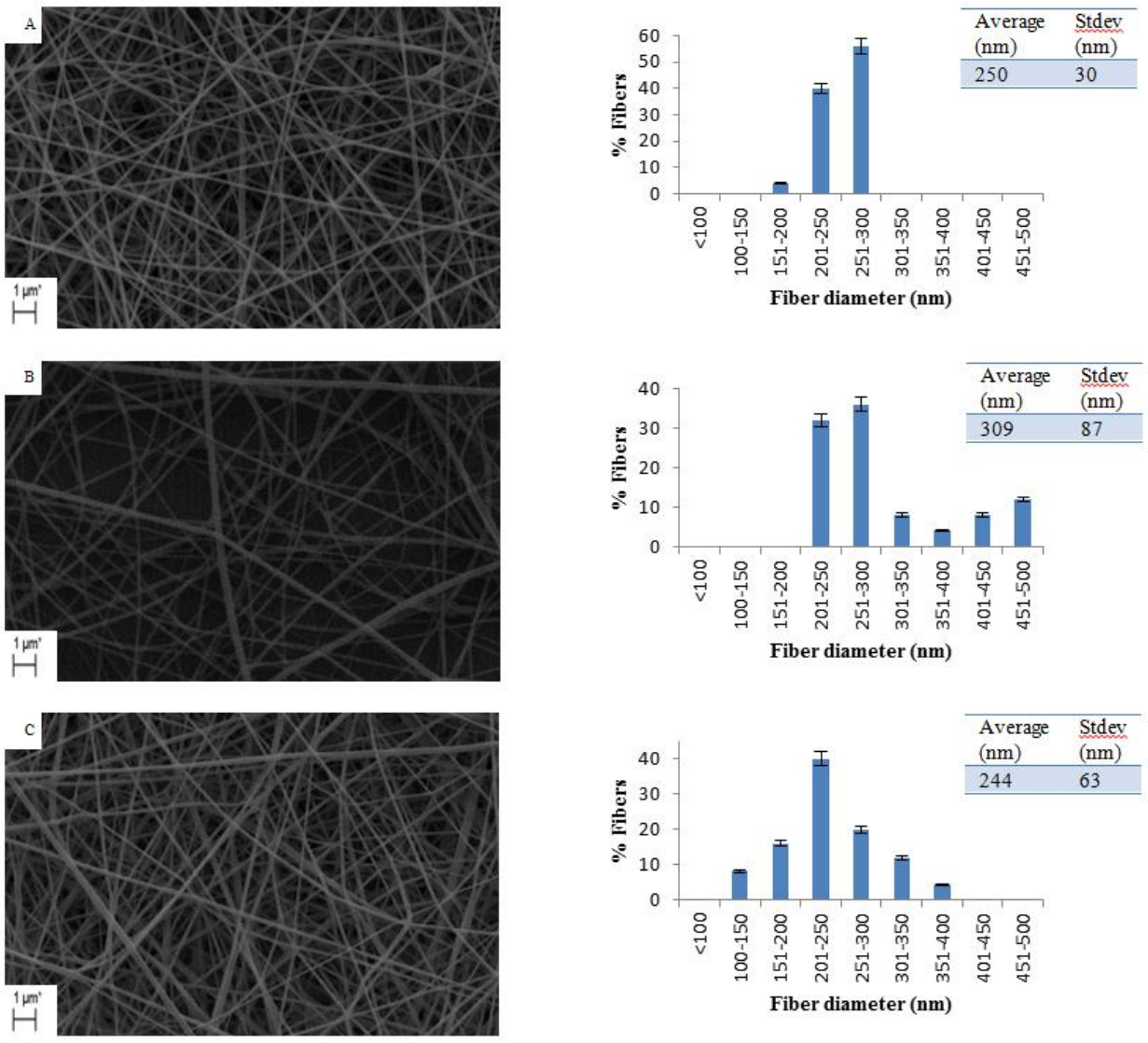

Figure 4.3: SEM images of 12wt% PVA with increasing flow rate: A - 0.01 ml/min, B - 0.02 ml/min and C - 0.03 ml/min.

The last parameter to be studied was the spinning distance. The concentration was kept constant at 12wt%, voltage at 10 kV and the flow rate at 0.01 ml/min. The distance was varied between 10, 15 and 20 cm. As shown in Figure 4.4, smooth, bead-free fibers were produced at all the distances. The average fiber diameter decreased with an increase in distance as would be expected. At a longer distance, the polymer has more time to be stretched before reaching the collector.

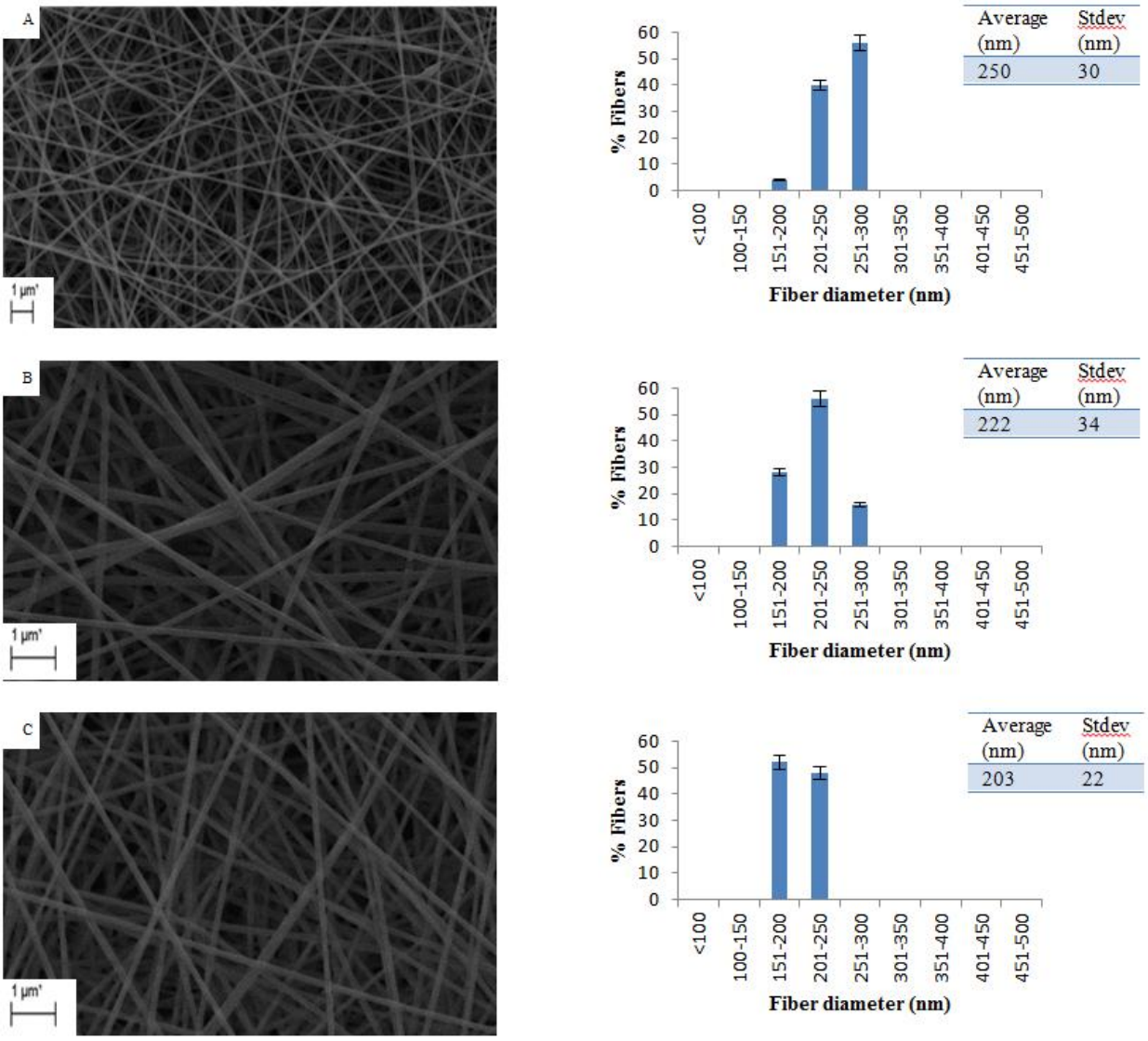

Figure 4.4: SEM images of 12wt% PVA while varying the spinning distance, A – 10 cm, B – 15 cm, C – 20 cm.

From the different parameters it can clearly be seen that the voltage played the biggest role in the formation of beads. Bead-free fibers were produced while varying the flow rate and the distance. The average fiber diameter could be manipulated by varying the flow rate and the spinning distance.

4.1.2 Electrospinning of chitosan

Chitosan is known to be difficult to electrospin due to its polycationic nature in acidic solutions[18]. Successful electrospinning of chitosan have been done by Okhawa *et al*[5]. They tried different solvents and solvent ratios comprising of diluted hydrochloric acid, acetic acid, neat formic acid, and trifluoroacetic acid (TFA). TFA was the only solvent that was able to produce fibers and with the introduction of dichloromethane (DCM) in a 70:30 (TFA:DCM) ratio, the homogeneity of the electrospun chitosan fibers was improved.

TFA is a toxic, harmful solvent which is not suitable for use in the biomedical field. For this reason, a 1% acetic acid solution was initally investigated as an appropriate solution for electrospinning of chitosan. Although the use of an acetic acid solution for the electrospinning of chitosan had been reported[19], it seemed to be impossible to obtain fibers on our set-up and only beads were formed as shown in Figure 4.5. Geng *et al*[19] confirmed that the acetic acid concentration in water strongly influenced the surface tension of a chitosan solution, which was remarkably important in the electrospinning of chitosan. Reasons for our failure may be that the molecular weight of the chitosan was too high, the voltage supply unit could not supply a high enough electric field or that temperature and humidity played a role[20, 21, 19].

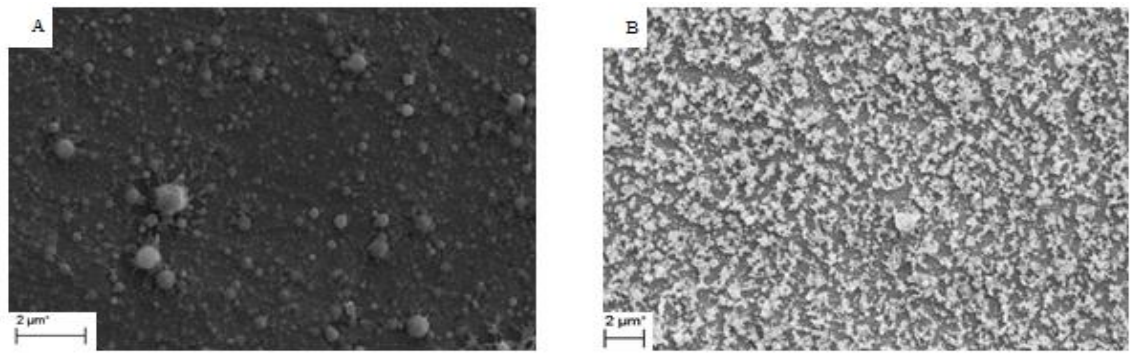

Figure 4.5: SEM images of A - 4wt%CS, 15 kV, 15 cm, 0.02 ml/min and B - 2wt%CS, 10 kV, 10 cm, 0.02 ml/min.

There are two reasons why the use of TFA for the electrospinning of chitosan has been successful in the past: (1) TFA forms salts with the amino groups if chitosan[22] and this salt formation destroys the rigid interactions between the chitosan molecules, making them ready to

be electrospun and (2) the high volatility of TFA is advantageous for the rapid solidification of the electrified jet of the chitosan-TFA solution. It was found when using only TFA as the solvent, small beads and interconnected fibers were still found, suggesting that optimization of the electrospinning conditions is necessary and with the introduction of DCM which is a volatile organic solvent this can be done[5]. For this reason, the use of a TFA:DCM (70:30) solvent combination was chosen.

The first parameter that was investigated was the concentration of the solution. The concentration was varied from 2wt% to 6wt% while keeping the voltage, distance and flow rate constant (Figure 4.6). At 2wt%, beads were observed with fine fibers but not enough fibers to determine the average fiber diameter. The occurrence of beads is the result of insufficient stretching of the polymer solution, clearly not enough to encourage fiber formation. With increasing the concentration, smooth fibers were obtained in the fiber diameter range of 248±55 nm. A further increase in concentration led to a higher fiber diameter however a broad fiber distribution was observed, which is because of the smaller and larger fibers produced. At 6wt%, the viscosity of the solution was very high which may cause the formation of an unstable jet resulting in a combination of electrospinning and electrospraying[2].

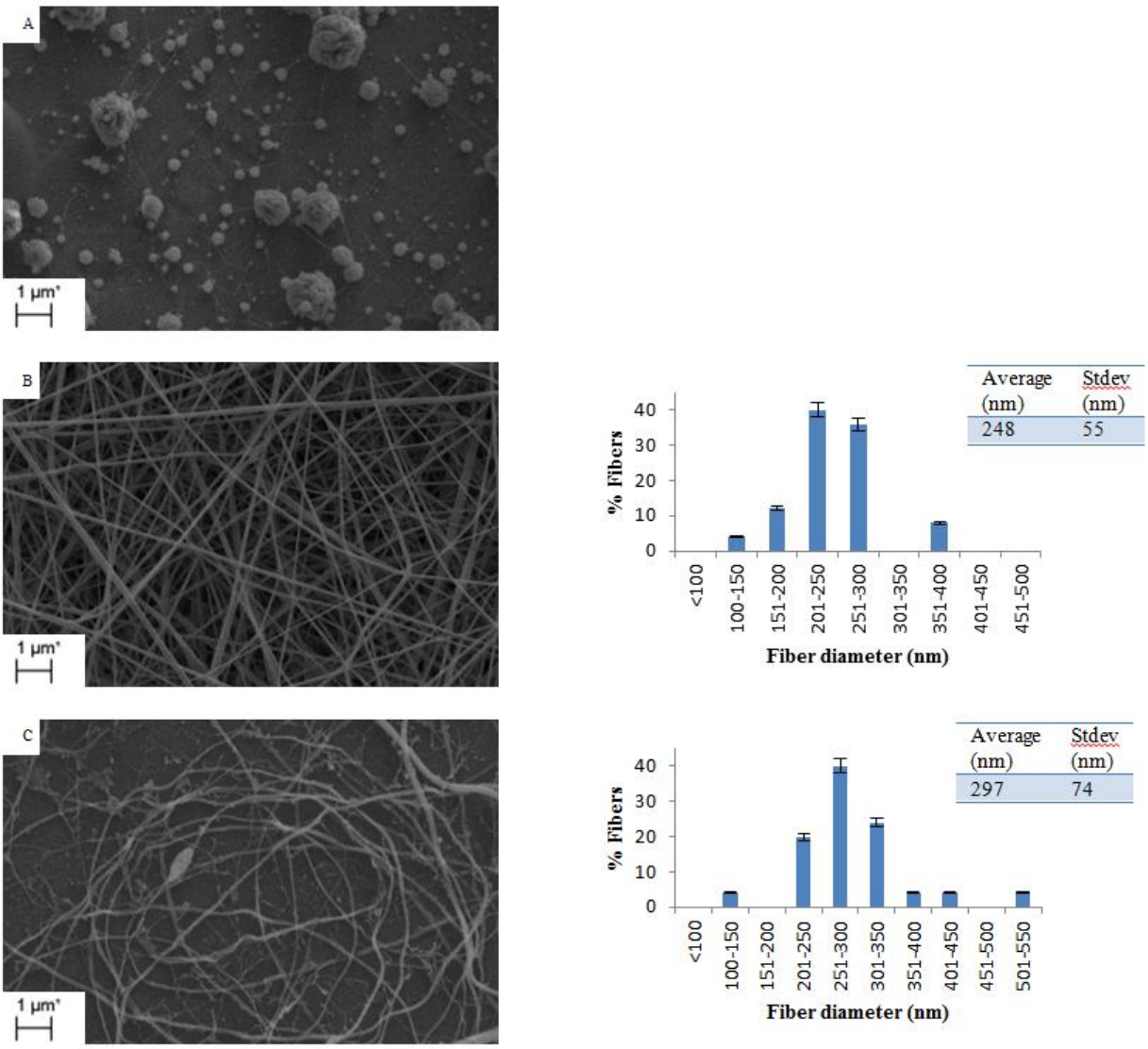

Figure 4.6: SEM images of chitosan at different concentrations: A – 2wt%, B – 4wt%, and C – 6wt%, all spun at the same conditions, 15 kV, FR: 0.02 ml/min and SD: 15 cm.

At low polymer concentration there are not enough chain entanglements to withstand the electrostatic and coulombic repulsion forces and this leads to the formation of beads. As the polymer concentration is increased, the solution viscosity increases resulting in enough chain entanglements for the electrospinning to occur and smooth nanofibers are formed. As a critical limit of concentration is reached, the viscosity is too high, disrupting the flow of the polymer solution through the needle[23, 24]. Okhawa *et al*[6] investigated the relationship between

concentration and viscosity and came to the conclusion, with an increase in concentration, the viscosity increases resulting in the failure of the spinning jet.

As the voltage was increased from 10 kV to 15 kV, smooth nanofibers were obtained. Varying the voltage did not have a big effect on the fiber morphology, and only a slight decrease in the average fiber diameter was observed from 254±54 nm at 10 kV to 248±55 nm at 15 kV. A higher voltage leads to greater stretch of the solution, which directly affects the morphology of the fibers and increases the possibility of bead formation. As shown in Figure 4.7, an increase in voltage not only decreases and refines nanofiber diameter, but also improves the quality of the electrospun nanofibers[25].

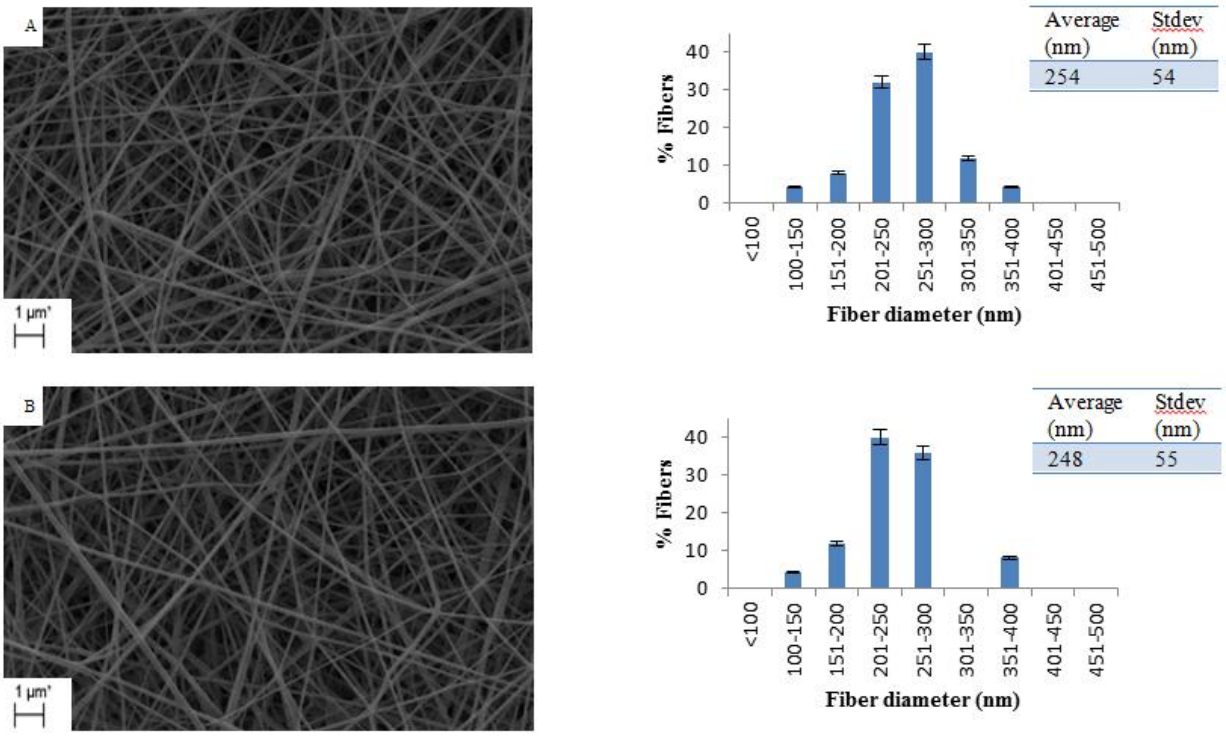

Figure 4.7: SEM images of 4wt% chitosan while varying the voltage, A – 10 kV and B – 15 kV.

The flow rate was the next parameter which was studied. The concentration was fixed at 4wt%, with the voltage and distance at 15 kV and 15 cm, respectively. As one would expect, with an increase in the flow rate, the average fiber diameter increased from 213±77 nm to 303±65 nm (Figure 4.8). Bead-free fibers indicated that the spinning distance did not have an effect on the morphology of the electrospun fibers.

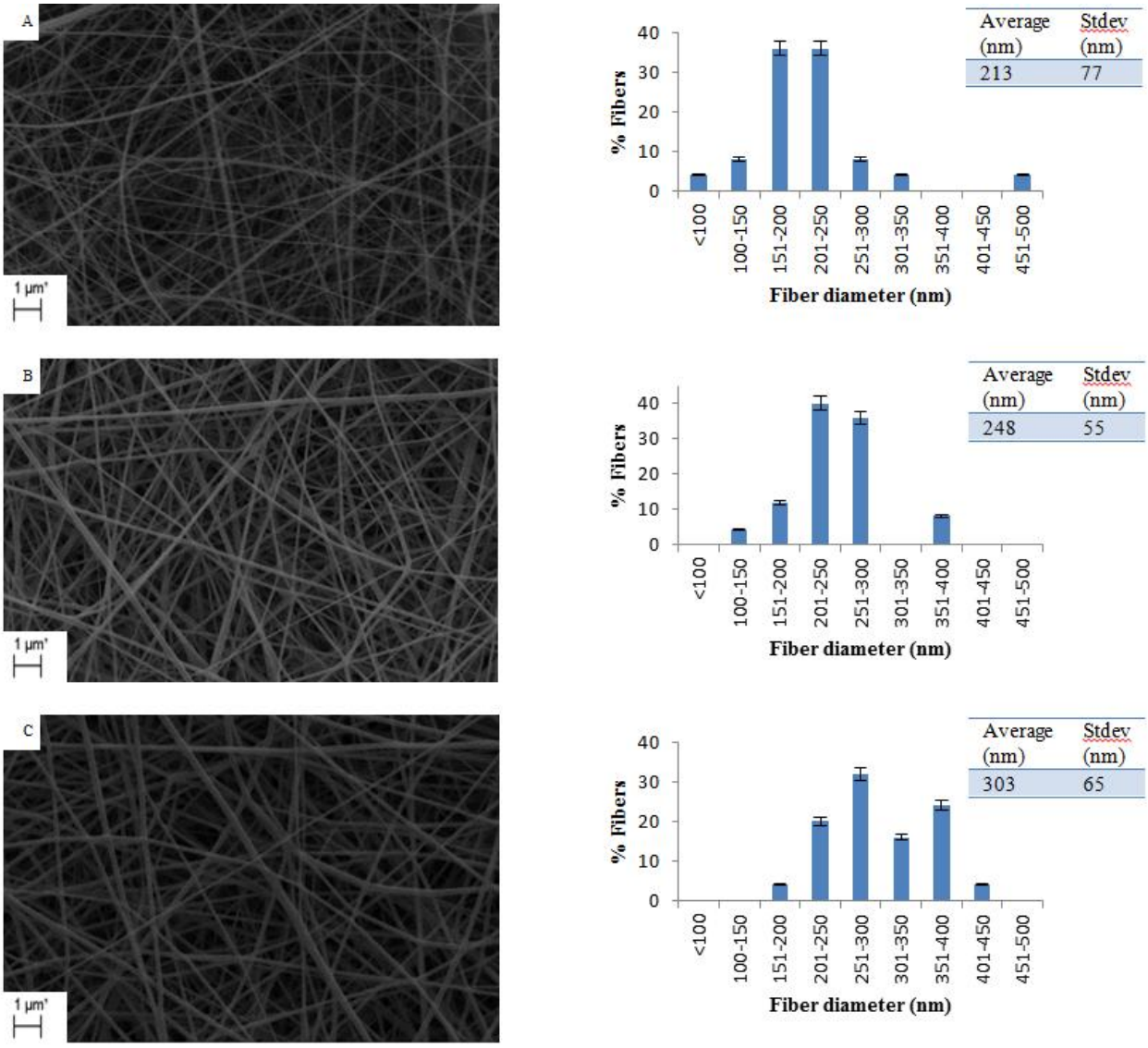

Figure 4.8: SEM images of 4wt% chitosan showing the effect of varying the flow rate: A - 0.01 ml/min, B - 0.02 ml/min, C - 0.03 ml/min.

The effect of spinning distance showed no linear relationship with the fiber diameter obtained. The fiber diameter increased from 216±46 nm to 248±55 nm when increasing the distance from 10 to 15 cm, as shown in Figure 4.9. Although it is expected that the fiber diameter decreases with increasing spinning distance, the opposite occurs at 10 to 15 cm. This might be explained if it is assumed that the distance becomes too large, the electrostatic field strength weakens to the

point where elongation of the jet no longer occurs[26]. A decrease in fiber diameter was observed with a further increase in the spinning distance to 20 cm. With an increase in spinning distance the polymer has more time to be stretched before reaching the collector. Beads as well as a variety of fiber sizes were observed at 20 cm. With chitosan, the solution is viscous and in high electrical fields, splitting of the jet could occur. The evaporation of the solvent and the elongation of the jet may cause changes in the shape of the jet and will become unstable. For stabilization of the jet, a smaller jet will form from the surface of the primary jet resulting in smaller and larger fibers[27].

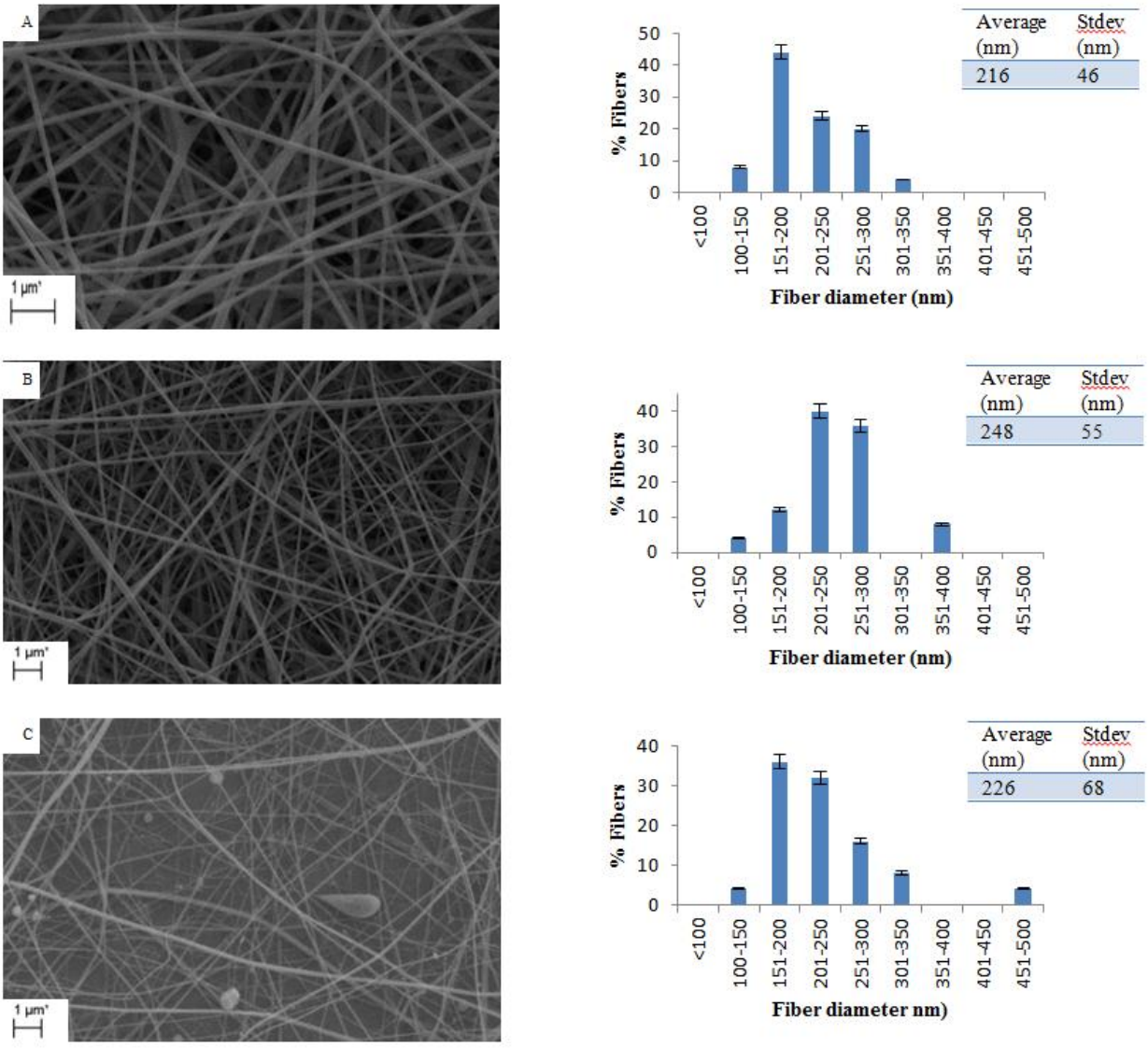

Figure 4.9: SEM images of 4wt% chitosan with increasing spinning distance, A – 10 cm, B – 15 cm and C – 20 cm.

Concentration and spinning distance had the greatest effect on the fiber morphology while the flow rate influenced the average fiber diameter mostly. With a too low or too high concentration, fibers with beads were observed indicating the viscosity of the solution played a major role in the electrospinning of chitosan. Spinning distance had an effect on the overall electrostatic field resulting in an unstable jet and producing fibers with beads. By optimizing the concentration and spinning distance, smooth, bead-free fibers were produced.

4.1.3 Electrospinning of EVOH

The use of EVOH in electrospinning remains intriguing due to its hydrophilic-hydrophobic nature. The vinyl alcohol repeat units contributed to the hydrophilic character while being water-insoluble due to the ethylene repeat units[7, 28]. EVOH is a polymer that has been electrospun in various solutions. The reason for this is that EVOH can dissolve quite easily in a number of conductive solvents, which is ideal for electrospinning[29, 30].

The polymer we used was a commercial EVOH copolymer containing 44% ethylene. The most common solvent system used is a 2-isopropanol/water combination in a 70:30 ratio. Kenawy *et al*[7] reported the successful electrospinning of EVOH copolymers with 56-71wt% vinyl alcohol in a 2-isopropanol/water solvent combination. The polymer stayed in solution for a few hours before precipitating. EVOH is often used in the biomedical field, making the 2-isopropanol/water solvent system quite suitable[31, 32].

Different concentrations (5, 6 and 7wt%) of EVOH were dissolved in isopropanol/water (70:30) at 80 °C for 3 hours whereafter it was electrospun. SEM images shown in Figure 4.10 clearly show that an increase in concentration, the average fiber diameter increases. The fiber morphology changes from beads-on-string (5wt%) , to smooth nanofibers at 6wt% and at 7wt%, fibers as well as fused polymer droplets were seen. At low concentration, stretching of the polymer did take place but not enough to prohibit the formation of beads. With an increase in concentration, the beads disappear resulting in the formation of smooth nanofibers. Seeram *et al*[15] explained it by saying that the surface tension decreases the surface area per unit mass. So at a low concentration, there is a high concentration of free solvent molecules and they tend to agglomerate and the surface tension will then cause the molecules to assume a spherical shape. With a higher concentration there is more interaction between the polymer molecules and the solvent molecules. When the solution is stretched, the solvent molecules will not agglomerate but rather expand over the entangled polymer molecules. This should lead to more chain entanglement and therefore we could have expected bead-free fibers[13]. When the concentration is further increased to 7wt%, fibers were obtained but with fused droplets. In this case, the viscosity of the solution might have been too high resulting in an unstable jet. The jet might not have had enough time to be fully stretched and solvent evaporation was not satisfactory, resulting in larger fibers and large fused droplets in between them.

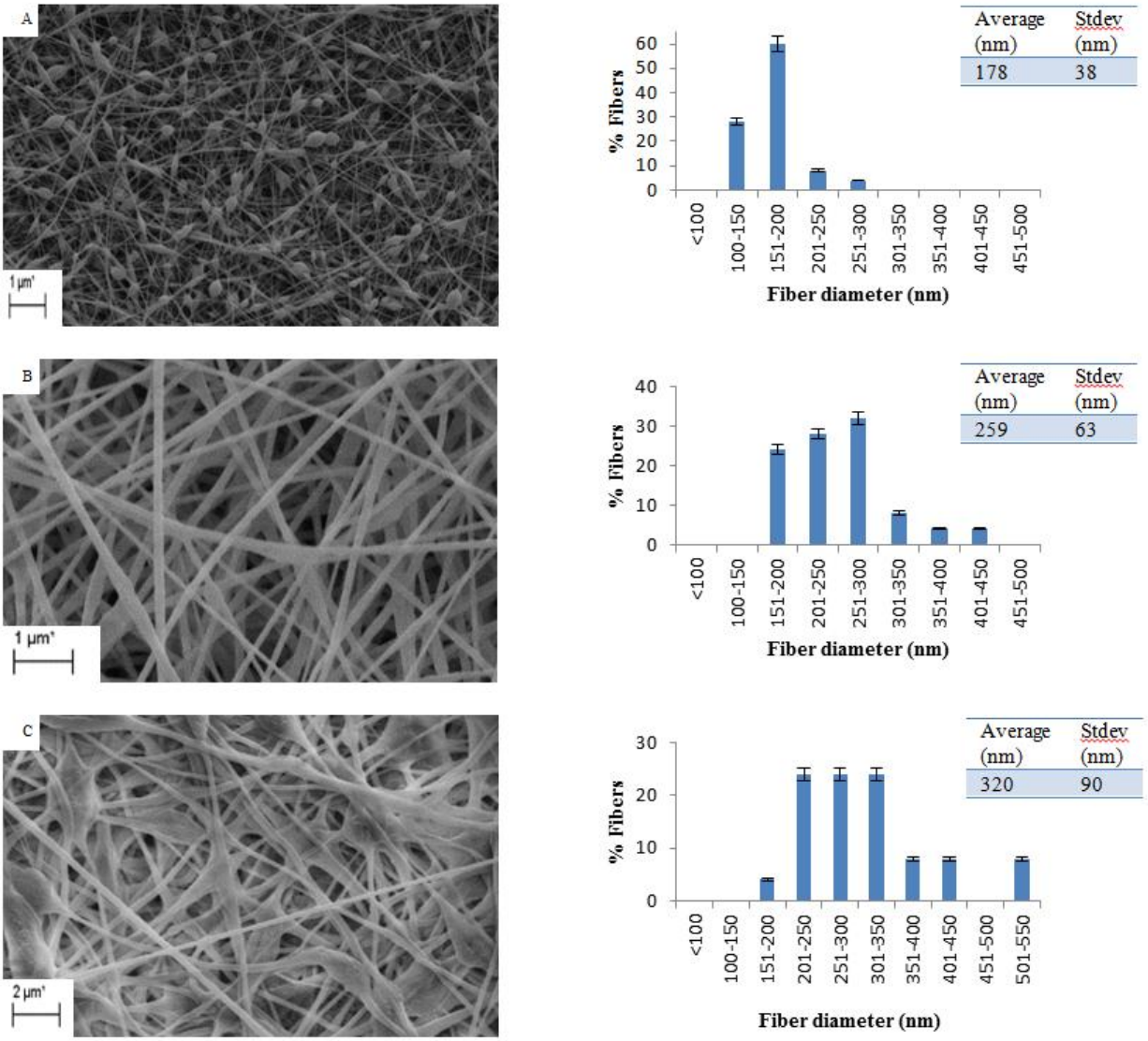

Figure 4.10: SEM images of EVOH at different concentrations: A – 5wt%, B – 6wt%, and C – 7wt%, all spun at the same conditions, 10 kV, FR: 0.03 ml/min and SD: 15 cm.

Varying the voltage and keeping the distance at 15cm and flow rate at 0.03ml/min constant are shown in Figure 4.11. Increasing the voltage from 10 kV to 15 kV had quite a significant effect on the fiber diameter, decreasing the fiber diameter from 259±63 nm to 198±46 nm. In most cases, a higher voltage causes greater stretching of the solution due to larger columbic forces within the jet and a stronger electric field, thus reducing the fiber diameter[33-35]. However, the higher voltage can also shorten the flight time of the electrospinning jet, providing less time for the fibers to stretched before it reaches the collector which is associated with a greater tendency

to form beads, due to greater instability of the jet as shown when increasing the voltage to 15 kV[16, 17].

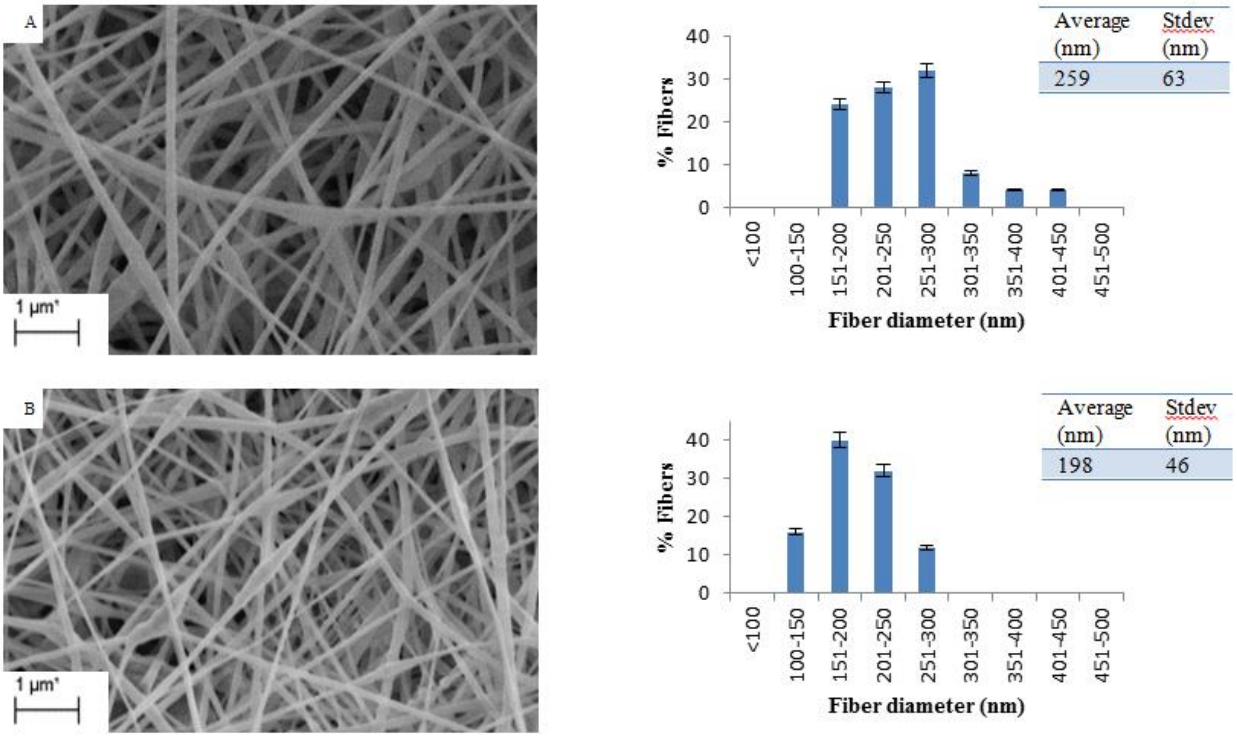

Figure 4.11: SEM images of 6wt% EVOH with increasing voltage, A – 10 kv and B – 15 kV.

From varying concentration and the voltage, it can be seen that the smoothest fibers were produced at 6wt% and a voltage of 10 kV. These parameters were kept constant when the flow rate was varied. The spinning distance was kept constant at 15 cm. Increasing the flow rate increases the amount of polymer in the electrospinning jet, thus increasing the fiber diameter as shown in Figure 4.12. When the flow rate is increased from 0.01 ml/min to 0.03 ml/min, the average fiber diameter also increased from 211±47 nm to 274±53 nm. At too high flow rate there is insufficient time for the solvent to evaporate and the fibers appeared to be flat. This morphology was also observed by Hsu and Shivkumar[36] who postulated that this is caused by incomplete solvent evaporation by the time the fibers reach the collector. These wet fibers can coalesce or re-dissolve, leading to flat, big fibers. Another reason could be that some solvent is

trapped inside the collected fibers and as the solvent evaporates the fibers will collapse, leading to flat fibers which have a broader fiber diameter distribution[37].

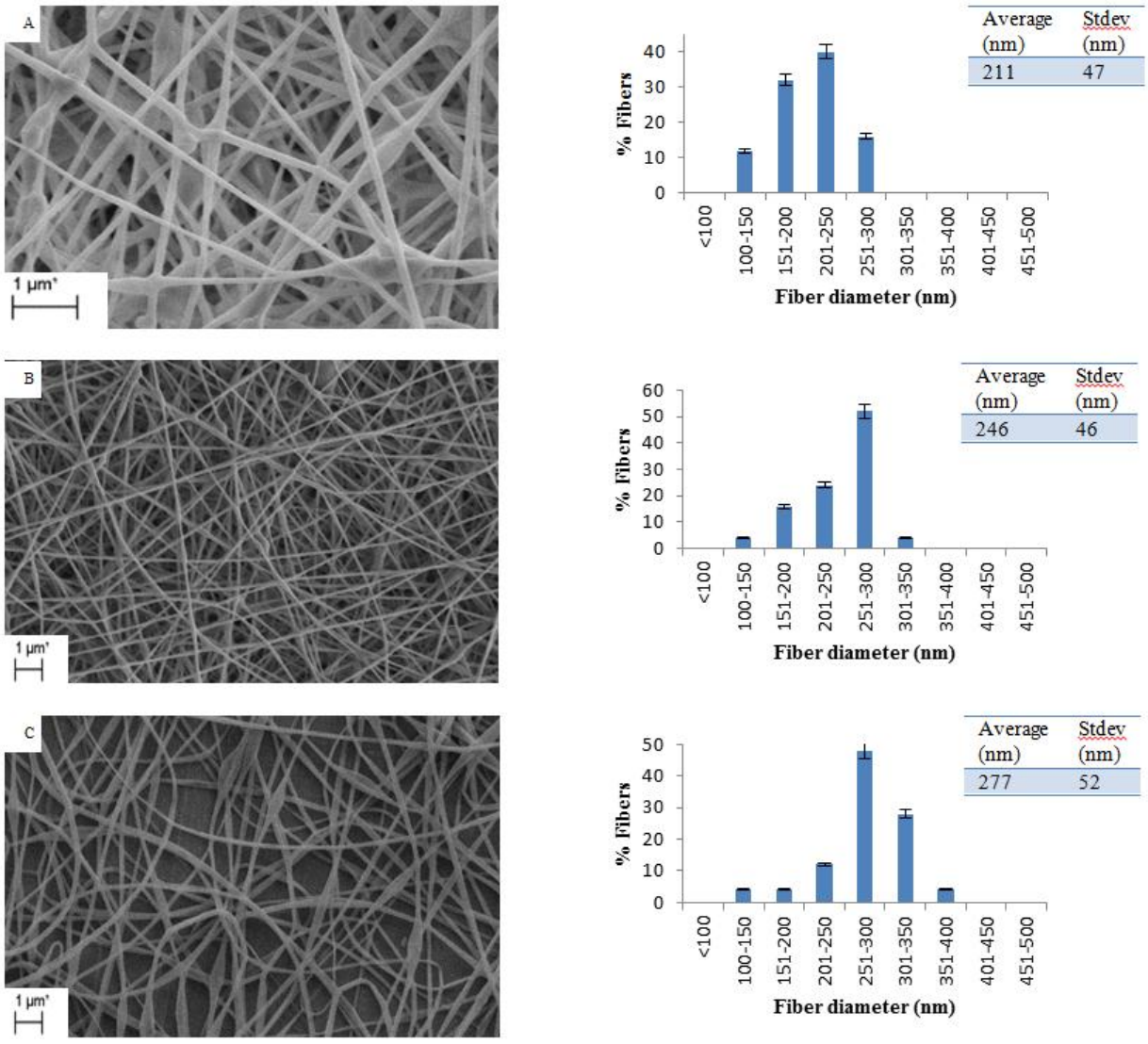

Figure 4.12: SEM images of 6wt% EVOH while varying the flow rate, A - 0.01ml/min, B - 0.015ml/min, C - 0.03 ml/min.

A possible way to overcome this problem is to change or vary the spinning distance. By increasing the distance, the jet has further to travel before reaching the collector, meaning the

solvent has a longer time to evaporate. The effect of varying the spinning distance is shown in Figure 4.13.

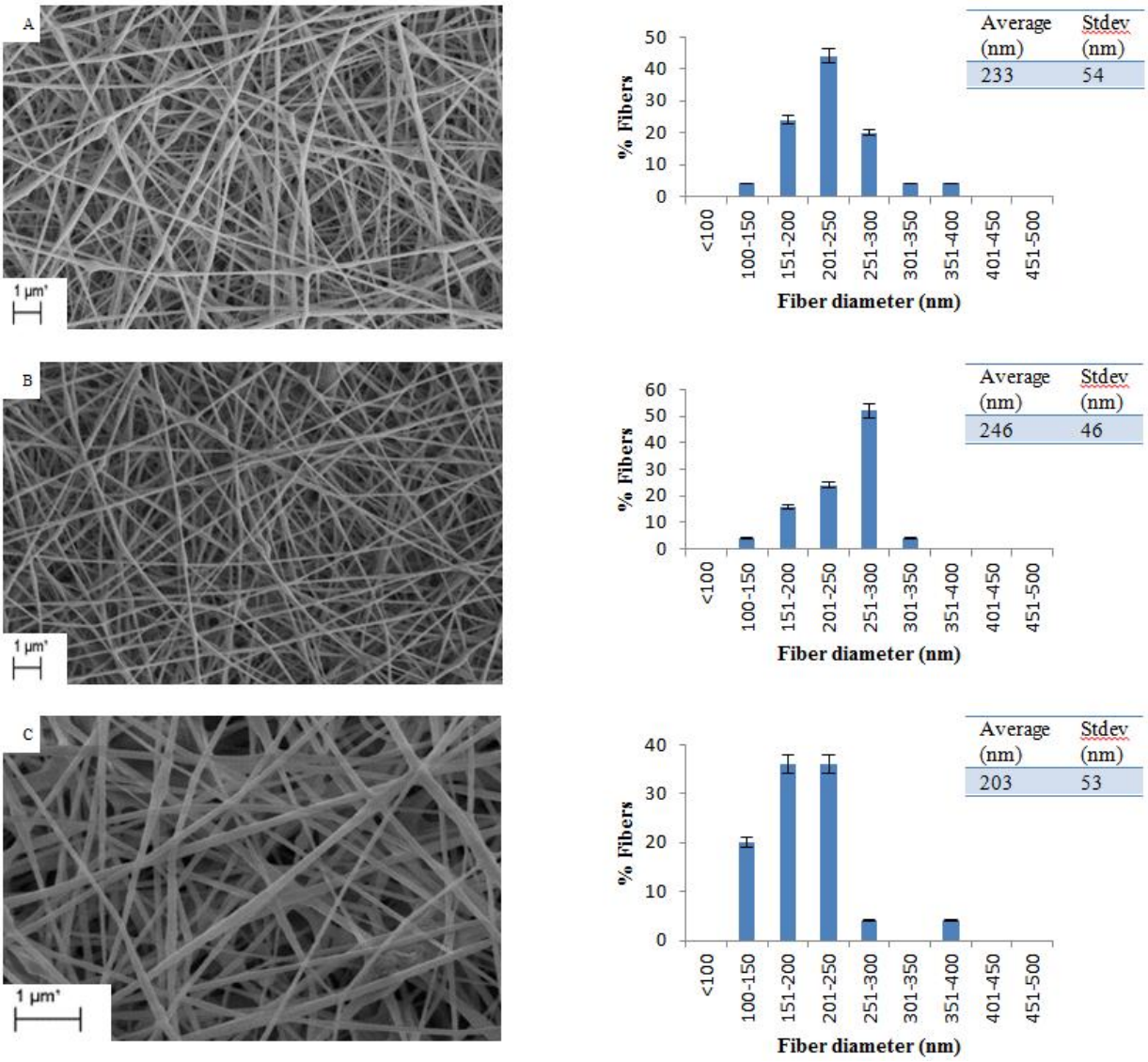

Figure 4.13: SEM images of 6wt% EVOH with increasing spinning distance: A – 10 cm, B – 15 cm, C – 20 cm.

Similar results were obtained when compared with chitosan. The average fiber diameter increased with increasing distance from 10 to 15 cm whereafter it decreased with a further increase in distance from 15 to 20 cm. As shown by Xu[8], the fiber diameter decreased with increasing distance, providing enough distance for the fibers to stretch and dry out before

reaching the collector. The decrease in fiber diameter at 10 cm compared to 15 cm spinning distance can be attributed to the fact that the electrical field strength is very high at a short distance and could lead to an increase in the elongation of the jet[2, 26, 38]. The thinnest fibers were produced at the longer spinning distance of 20 cm. The jet is able to travel further, allowing it to be stretched more and also giving the solvent enough time to be evaporated.

The average fiber diameter was mostly influenced by the applied voltage while the flow rate and the spinning distance influenced the evaporation of the solvent. By manipulating these parameters, the average fiber diameter could be controlled.

4.1.4 Electrospinning of SMA

SMA mats were prepared as described in Chapter 3. SMA is known to give the smoothest fibers in a 2:1 acetone:DMF solutions. Tang *et al*[9] studied the use of pure acetone or DMF as solvents and their ratios. Large sized fibers were obtained from the SMA/acetone solutions, while ultrafine fibers were produced from SMA/DMF solutions. The acetone evaporates very quickly as compared to DMF where the fibers can be stretched more before reaching the collector. With the DMF content being increased in the acetone:DMF solution, the average fiber diameter decreased. DMF is one of the solvents known to improve the fibers morphology and is usually added to the solution to increase the dielectric property of the solution[39, 40].

SEM images of different concentrations of SMA are shown in Figure 4.14. A‘beads-on-string’ morphology was found for 30wt% and 40wt% SMA solutions. With increasing the SMA concentration to 50wt%, bead-free nanofibers were obtained. Beaded fibers are often observed in the electrospinning of many polymer solutions at low concentration[41-43]. This happens when the jet cannot withstand the surface tension and the electrostatic force exerted on it, and forms a stable beads-on-string structure. The flat ribbon-like structure also observed at lower concentration is a consequence of rapid evaporation of acetone from the surface of the fibers, trapping solvent inside the fibers. At a later stage, the solvent in the inside of the fibers will evaporate resulting in a collapsed structure[44].

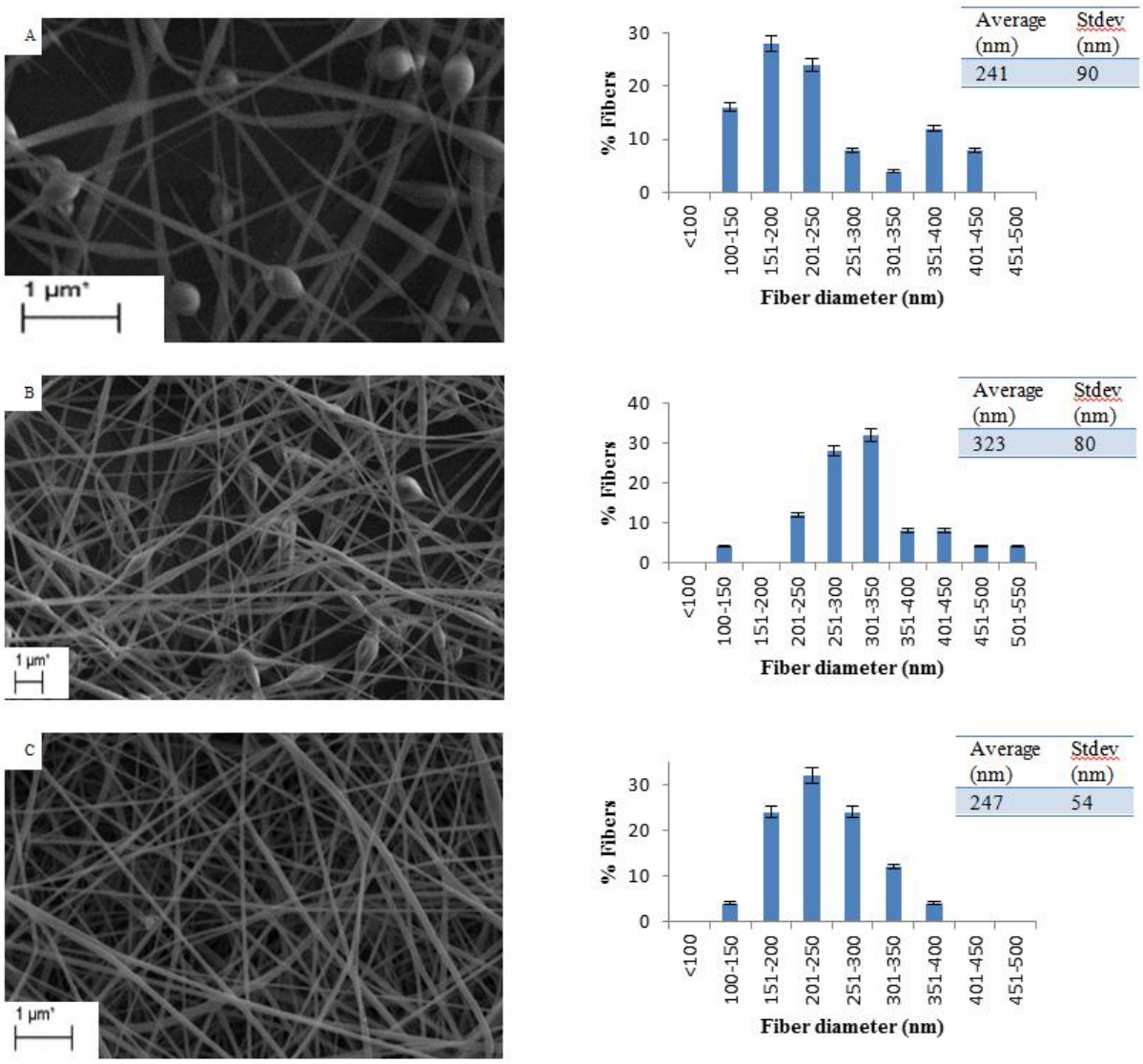

Figure 4.14: SEM images of SMA fibers spun at different concentrations: A – 30wt%, B – 40wt%, and C – 50wt%, all spun at the same conditions, 10 kV, FR: 0.01 ml/min and SD: 15 cm.

The increase in voltage from 10 kV to 15 kV did not have a significant effect on the average fibers diameter. The fiber diameter stayed more or less the same (Figure 4.15). However, the morphology changed from round to flat-like fibers with increasing voltage. At higher voltage the electrical field could be unstable, the Taylor cone may draw back into the needle, leading to an unstable jet[2, 15].

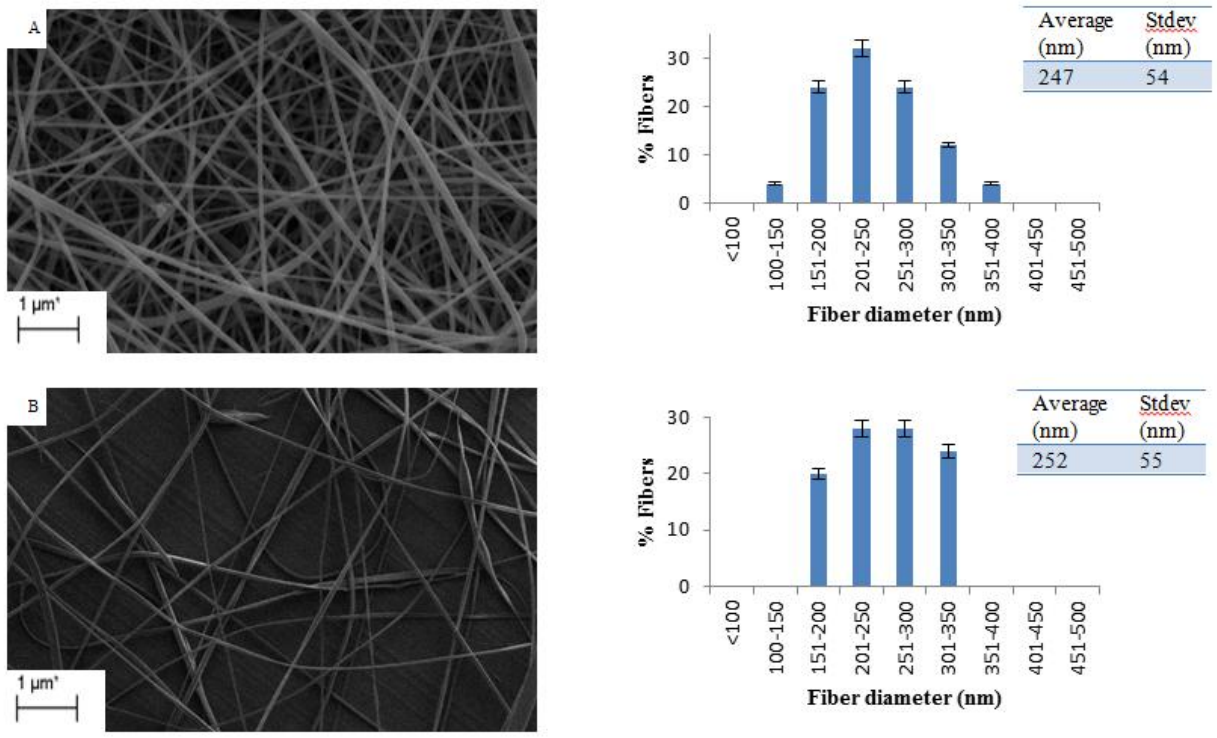

Figure 4.15: SEM images of 50wt% SMA while varying the voltage, A – 10 kV, B – 15 kV.

The formation of flat-collapsed fibers can be attributed to insufficient solvent evaporation. This reason can be two-fold: (1) the flow rate can result in insufficient time for solvent evaporation and (2) the distance between the needle tip and the collector might not be far enough.

To investigate these allegations, the flow rate and spinning distance were varied as shown in Figure 4.16 and Figure 4.17 respectively. Megelski *et al*[35] showed that with an increase in diameter of electrospun polystyrene nanofibers, to be associated with an increased flow rate of the polymer solution.

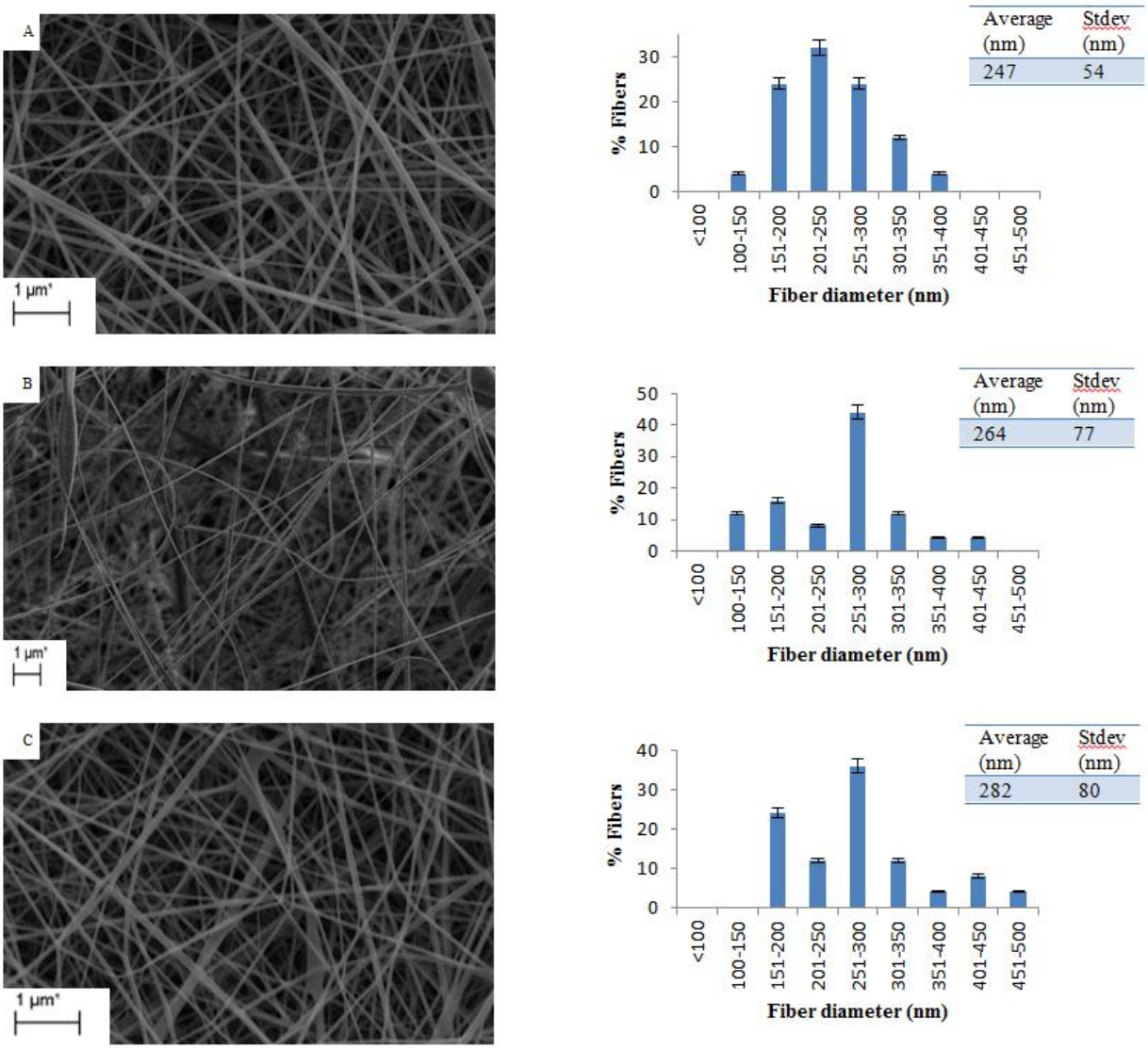

Figure 4.16: SEM images of 50wt% SMA with increasing the flow rate: A - 0.01 ml/min, B - 0.02 ml/min and C - 0.03 ml/min.

As the flow rate increases, the available polymer volume became higher which increased the nanofiber diameter. When the flow rate was too high, the nanofibers were unable to dry completely before reaching the collector, resulting in flat-structured fibers. Similar results were obtained as shown in Figure 4.16 when the flow rate was increased from 0.01 ml/min to 0.03 ml/min. The larger diameter was attributed to the larger droplet at the tip of the needle, due to the higher flow rate, resulting in the solution having a faster trajectory and resulting in incomplete drying.

In the case of varying the spinning distances, an overall decrease was observed with increasing distance. The same trend was seen for PVA, which can be explained that with an increase in distance, the jet has a longer distance to travel, being able to stretch more and finally having a smaller fiber diameter[2]. At a shorter distance the jet will accelerate faster, since the electrical field is stronger. The jet will arrive at the collector plate in a short time and the fibers might not have enough time to be elongated as much as at a longer distance. The effect of varying the distance on the morphology and the average fiber diameter are shown in Figure 4.17. The average fiber diameter decreased from 286±59 nm to 231±49 nm.

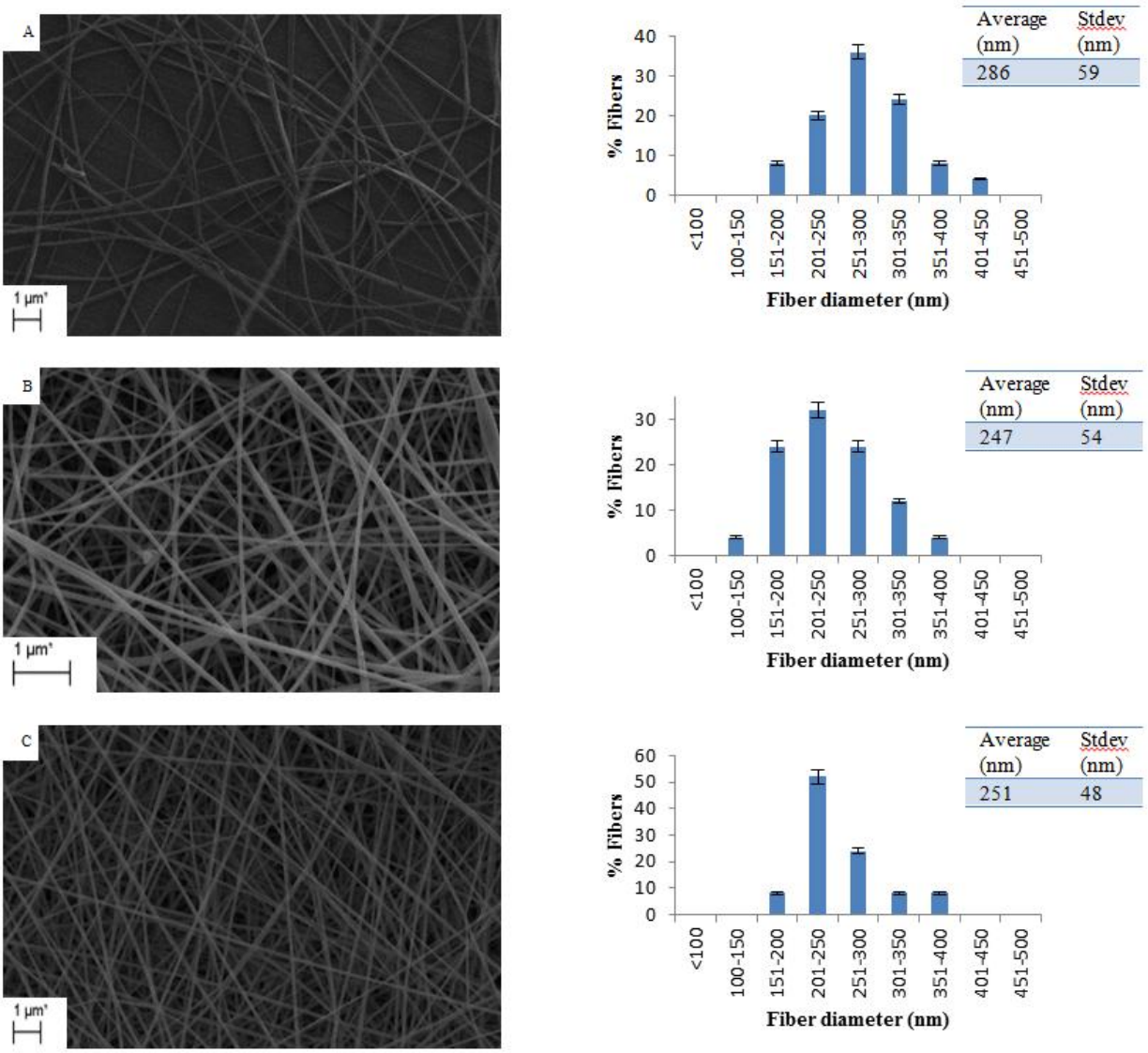

Figure 4.17: SEM images of 50wt% SMA with increasing the spinning distance, A – 10 cm, B – 15 cm, C – 20 cm.

Bead-free fibers were only produced at a high concentration, while the voltage, spinning distance and flow rate influenced the average fiber diameter the greatest. By manipulating the flow rate and the spinning distance, the problem of solvent evaporation was overcome and the average fiber diameter was controlled.

4.2 Average fiber diameter

The results of the fiber characterization show that the nanofiber size can be controlled by regulating the concentration, the applied voltage, flow rate and the spinning distance of the electrospinning process. To continue further with this study, the average fiber diameters of PVA, chitosan, EVOH and SMA had to be similar for comparison purposes in the release study section. The effect of different sized fibers on the release behavior is not an objective in this study, but rather the comparison of the different polymers, this is why it is necessary for the polymer fibers to have similar fiber diameter[45, 46].

By taking the different parameters into consideration the final optimum conditions for each polymer were chosen. In Figure 4.18 the average fiber diameter for each polymer is shown. The concentration of the polymer solution and the conditions (shown in table 4.1) used for electrospinning were chosen to be used in further analysis because they all have similar average fiber diameters.

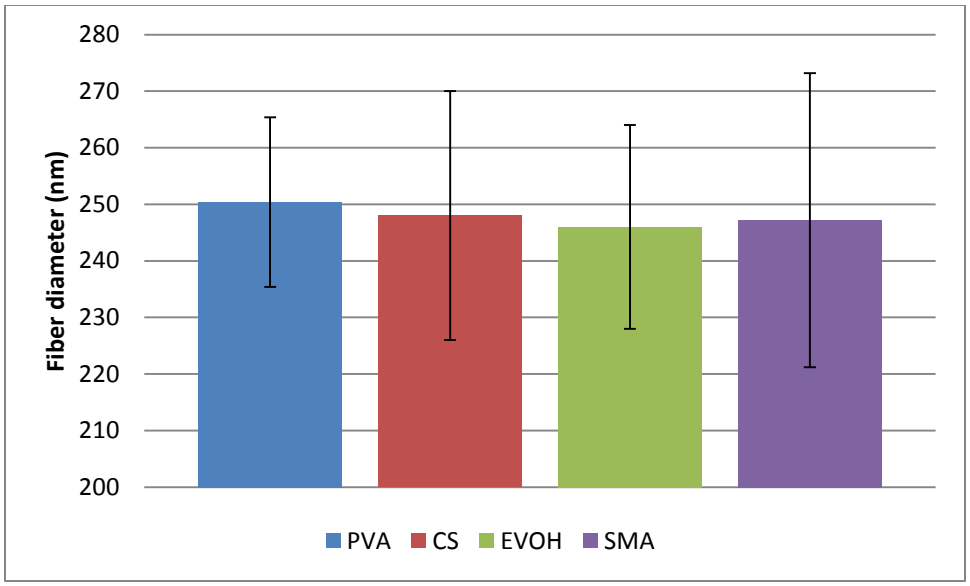

Figure 4.18: Comparison between average fiber diameters of polymers.

Table 4.1: Optimum conditions used for the electrospinning of the polymer solutions.

Polymer	**Concentration (wt%)**	**Applied voltage (kV)**	**Flow rate (ml/min)**	**Spinning distance (cm)**
PVA	12	+10/-10	0.01	10
Chitosan	4	+15/-15	0.02	15
EVOH	6	+10/-10	0.015	15
SMA	50	+10/-10	0.01	15

4.3 Incorporation of antimicrobial agent, 2,3-dihydroxybenzoic acid

The above electrospinning conditions were used for the fabrication of DHBA-loaded electrospun fibers. A fixed amount of DHBA (30 mg) was added to the solution before electrospinning. 3 ml of each polymer solution was electrospun and the resultant fibers were further used for analysis. SEM images and fiber distributions of PVA, chitosan, EVOH and SMA incorporated DHBA are shown in Figure 4.19.

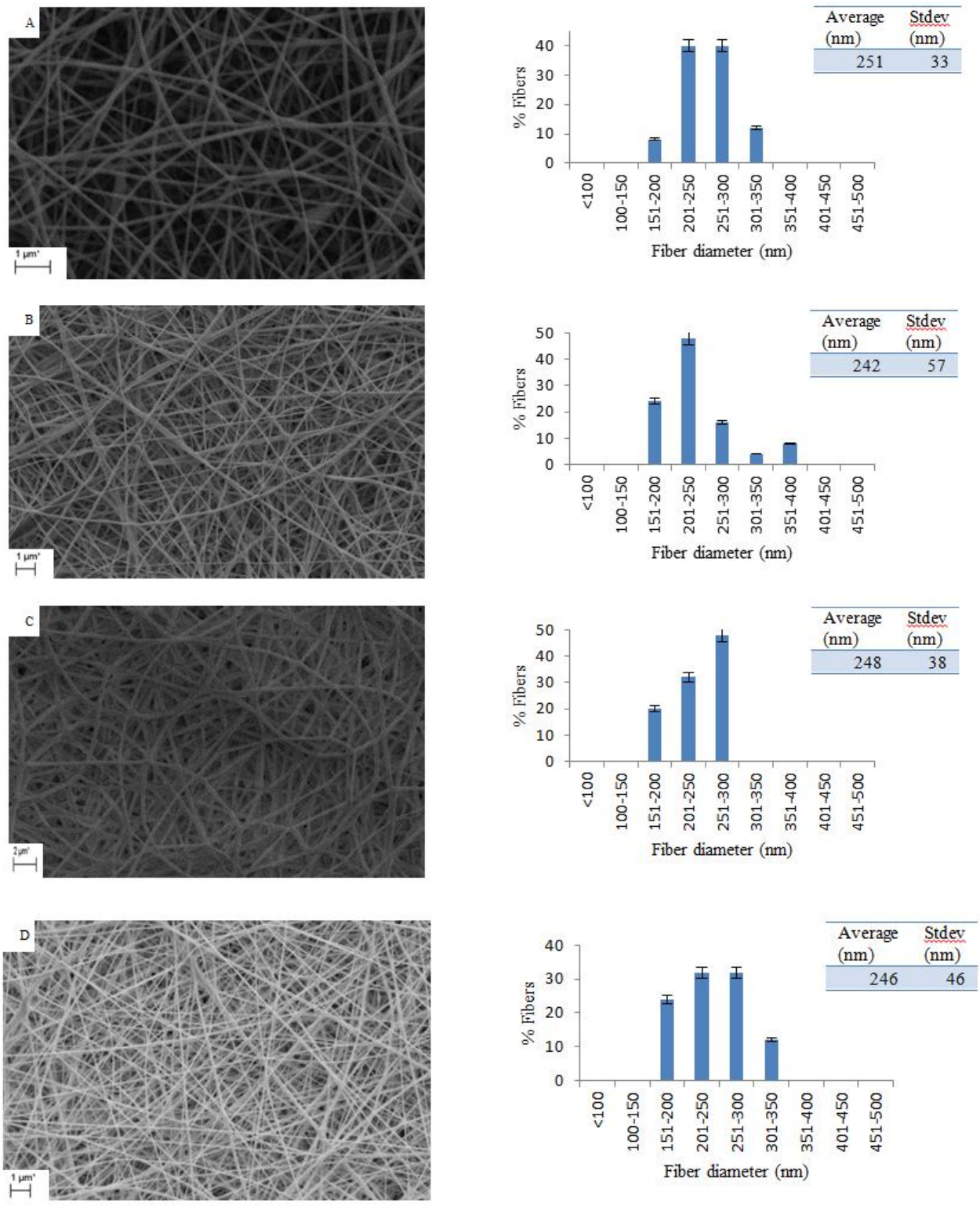

Figure 4.19: SEM images of A - DHBA-loaded PVA, B - DHBA-loaded chitosan, C - DHBA-loaded EVOH and D - DHBA-loaded SMA nanofibers.

The incorporation of DHBA did not have any effect on the average fiber diameter and smooth nanofibers were obtained. Based on these results, these nanofibers were used for further analysis.

4.4 Interaction and stability of DHBA-loaded electrospun mats

4.4.1 Attenuated total reflectance – Fourier transform infrared spectroscopy (ATR-FTIR)

The interaction of DHBA with the polymer matrix was studied using FTIR. The presence of DHBA was also confirmed using FTIR. FTIR is an easy way to identify the presence of certain functional groups in a molecule.

The FTIR spectrum of DHBA illustrated in Figure 4.20 shows the characteristic absorption bands used to identify the DHBA in the matrices as follows: the region 2800-3300 cm^{-1} (region A) is attributed to hydroxyl bond stretching, the peaks at 1650 and 1590 cm^{-1} (region B) reflects the relative position of the COOH group to the hydroxyl groups on the aromatic ring. The peak in the region of 1170 cm^{-1} (region C) is due to the stretching vibration of CO in COOH and has previously been used as the characteristic peak of DHBA in PEO and PDLLA[47]. In this study, the peaks at 1650, 1590 and 1170 cm^{-1} were used for identifying the presence of DHBA in the different polymer matrices.

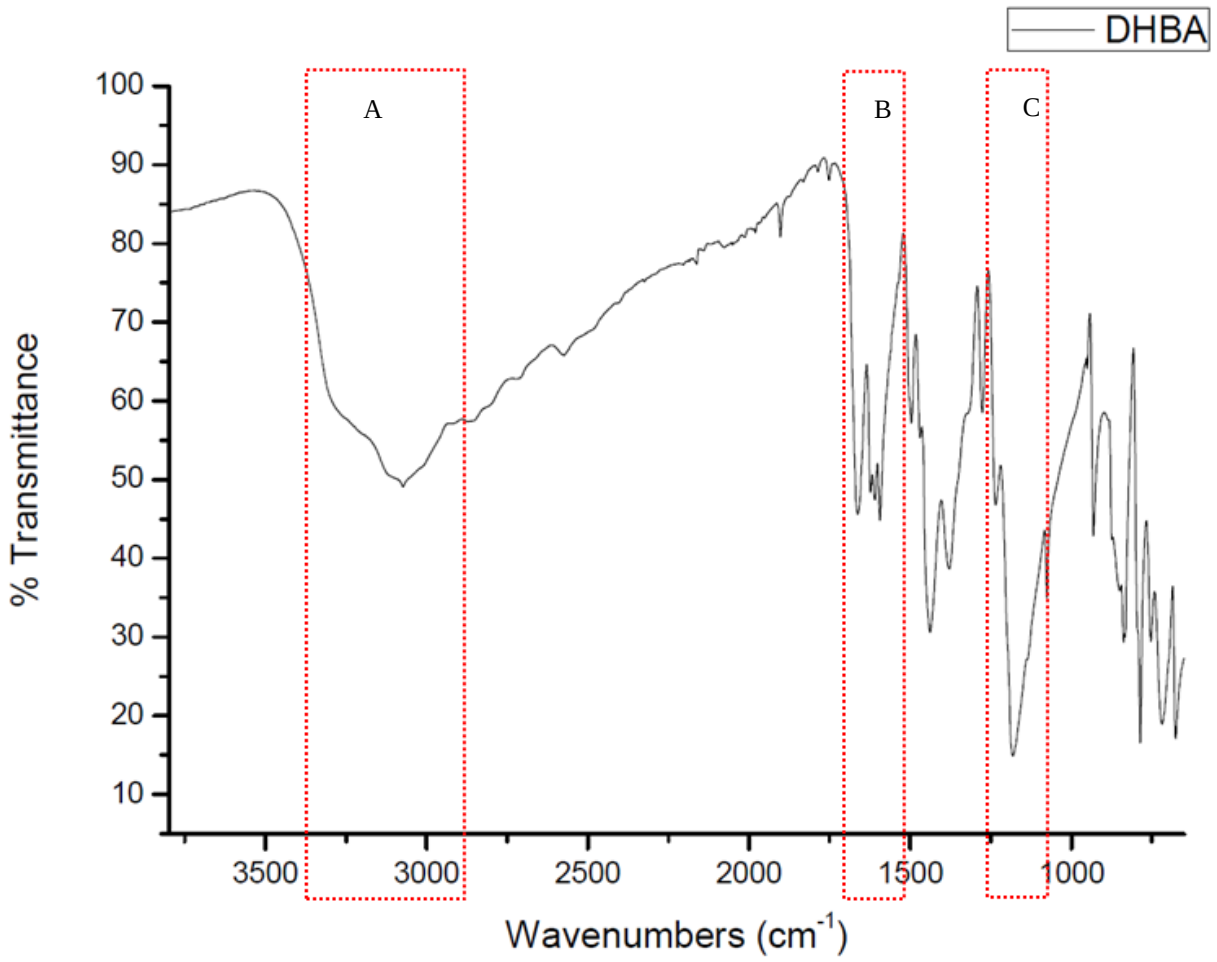

Figure 4.20: FTIR spectrum of DHBA showing characteristic absorption bands.

FTIR spectra of the control and DHBA-loaded electrospun mats are shown in Figure 4.21, where A represents PVA, B - Chitosan, C - EVOH and D - SMA.

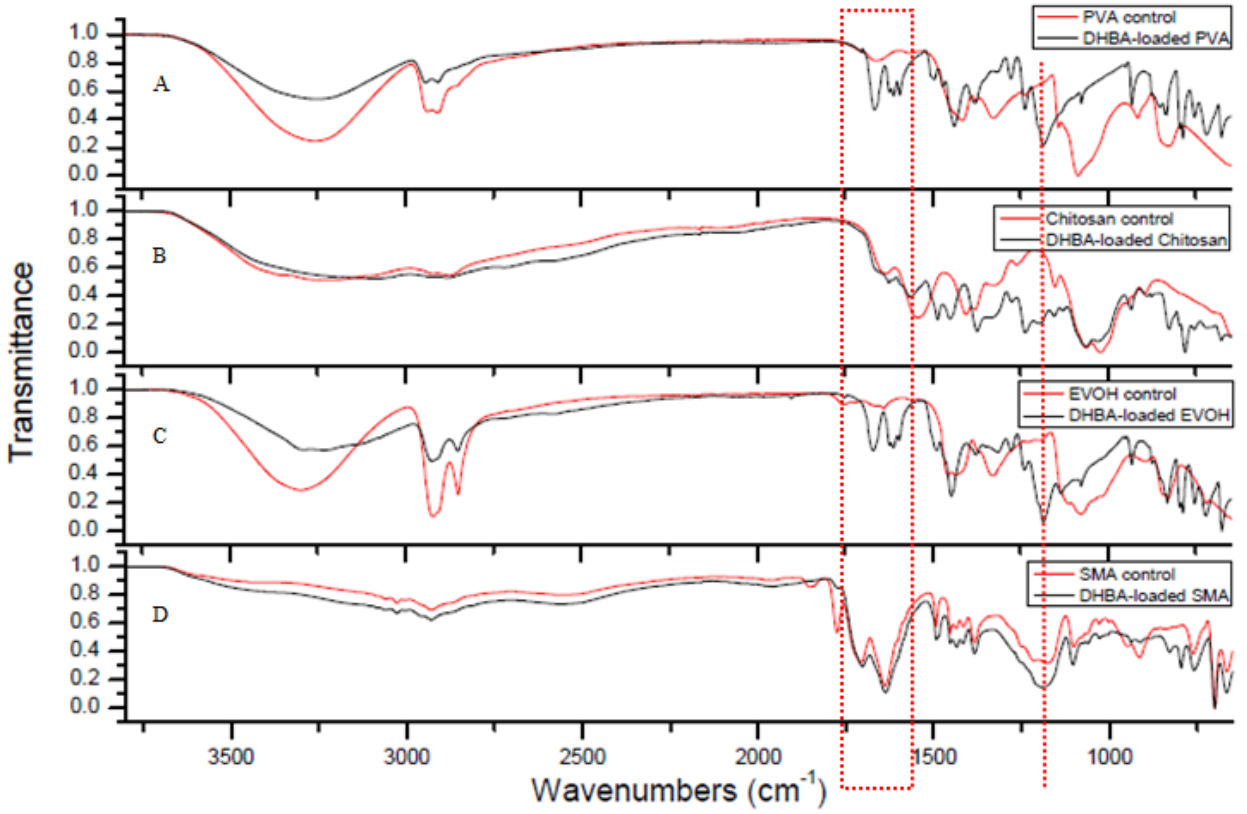

Figure 4.21: FTIR spectra of A - PVA, B - Chitosan, C - EVOH and D - SMA, each with and without DHBA.

In DHBA-loaded electrospun mats, the two peaks at 1650 and 1590 cm^{-1} represent the carbonyl group in DHBA. Just below 1250 cm^{-1}, a highly intensified peak is displayed in the DHBA-loaded electrospun mats. This is characteristic of the stretching vibrations of CO in COOH and also confirms the presence of DHBA.

A significant decrease in intensity in the region of 3000-3500 cm^{-1} is observed in DHBA-loaded PVA and EVOH, this may indicate that some of the hydroxyl groups participate in hydrogen bonding[48] with the carbonyl group of DHBA. PVA and EVOH are semi-crystalline polymers that exhibit a strong intermolecular interaction through hydrogen bonding[49]. However, in chitosan and SMA, some interaction might have taken place as noticed by a small decrease also in this region but interaction might be limited due to the steric hindrance effect[50].

4.4.2 Thermogravimetric Analysis (TGA)

Thermogravimetric analysis of the DHBA-loaded electrospun mats and control nanofibers was done to determine their stability as well as to establish the effect of DHBA on the stability of the fibers. Figure 4.22 presents the TGA curve of DHBA. Pure DHBA decomposed in two steps: the side functional groups (-OH and –COOH) in DHBA decomposed between 180 and 270 °C, and the aromatic rings decomposed between 270 and 350 °C[47].

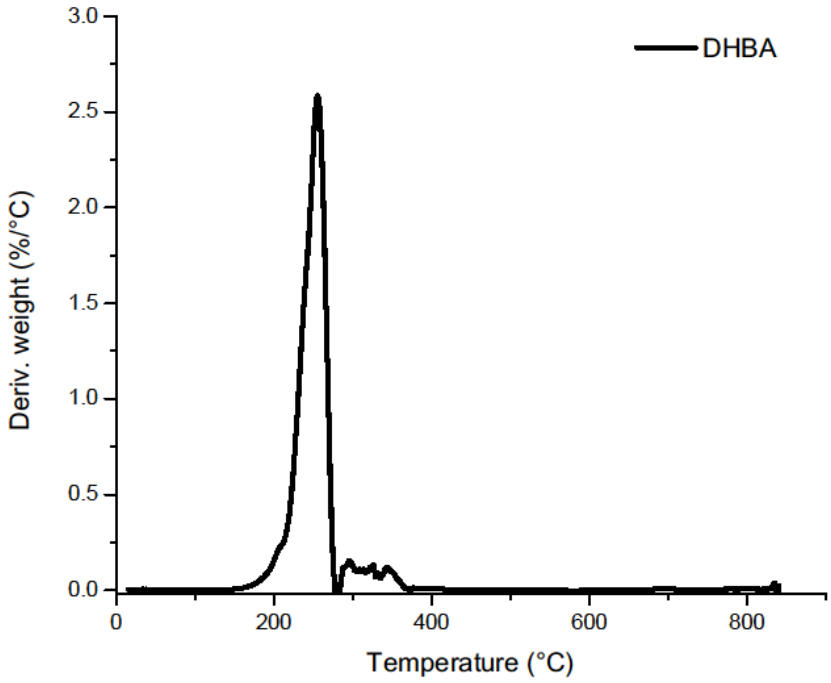

Figure 4.22: Derivative TGA curve of DHBA.

The derivative TGA curves of PVA, chitosan, EVOH, and SMA loaded with DHBA and control nanofibers are shown in Figure 4.23. PVA and chitosan experienced an immediate drop in the initial slope and can be seen as loss of moisture in the samples. Chitosan loses more water (5.57%) compared to PVA (3.30%) which can be attributed to the higher hydrophilicity of chitosan leading to more bound water as compared to PVA[51]. EVOH and SMA do not experience this initial peak which reflects the hydrophobic nature of these polymers.

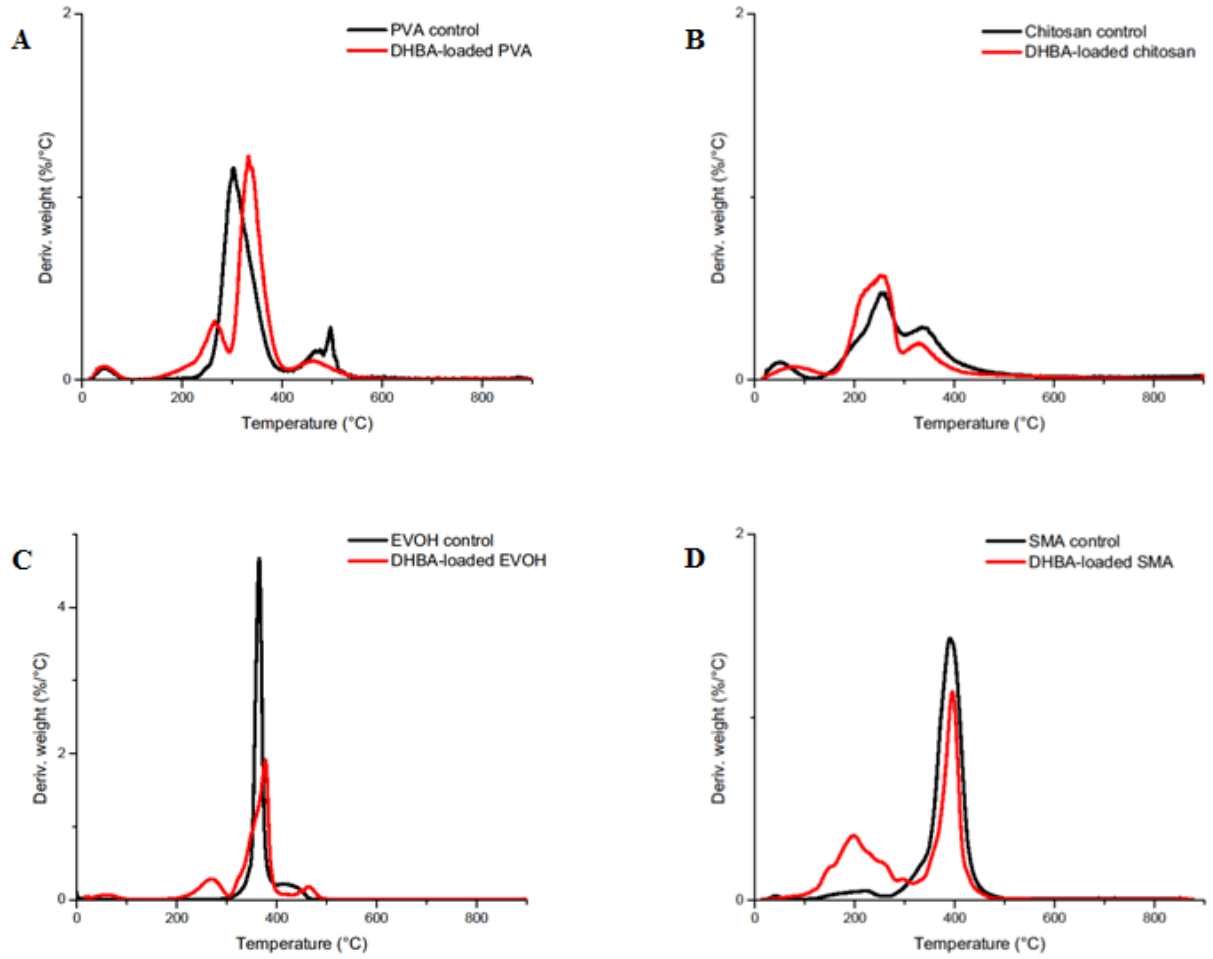

Figure 4.23: Derivative TGA curves of DHBA-loaded fibers and control fibers of A - PVA, B - Chitosan, C - EVOH and D - SMA.

The PVA control decomposed in three steps; the first step covered the temperature range of about 15 to 80 °C corresponding to the loss of moisture, while the second and third covered the temperature range of about 230 to 380 °C and 420 to 510 °C, corresponding to the thermal degradation of PVA which indicates the existence of a chemical degradation process resulting from bond scission (C-C bonds) in the polymer backbone[52]. For the DHBA-loaded PVA, four weight loss steps were observed. The weight loss between 180 to 280 °C represents the decomposition of the side functional groups of DHBA.

The decomposition of chitosan and the EVOH control occurs in 2 steps. The first weight loss peak in chitosan is attributed to the absorption of water and the weight loss between 180 and 420 °C is due to the decomposition of the glucosamine group. The peaks in the regions between 310 to 380 °C and 380 to 510 °C in EVOH correspond to the decomposition of the alcohol groups in the backbone of the structure and the chemical degradation process respectively[53]. With the incorporation of DHBA, weight loss peaks between 140 and 280 °C are observed in both polymers resembling the decomposition of the functional groups of DHBA.

SMA control and DHBA-loaded SMA exhibited a two-step degradation process. A weight loss peak between 110 to 200 °C and 80 to 280 °C in the SMA control and DHBA-loaded SMA are observed respectively. However, a larger weight loss peak was observed for DHBA-loaded SMA in this region which might be attributed to the incorporation of DHBA. The side functional groups of SMA and DHBA decomposed in this region while between 220 to 430 °C for the SMA control and 280 to 430°C for the DHBA-loaded SMA correspond to the degradation of the styrene functional groups.

Overall, the incorporation of DHBA seemed to delay the thermal degradation of PVA and EVOH while for chitosan and SMA, the temperature ranges stayed the same. The change in thermal degradation might be attributed to the interaction between PVA/EVOH with DHBA and resulted in an increase in the thermal stability of the matrices.

4.4.3 Differential Scanning Calorimetry (DSC)

Figure 4.24 displays the DSC curve for DHBA. A sharp endothermic peak was observed at 210 °C coupled with a wide endotherm peak (210 °C to 280 °C), which is well correlated with the thermal degradation observed in the TGA curve of DHBA.

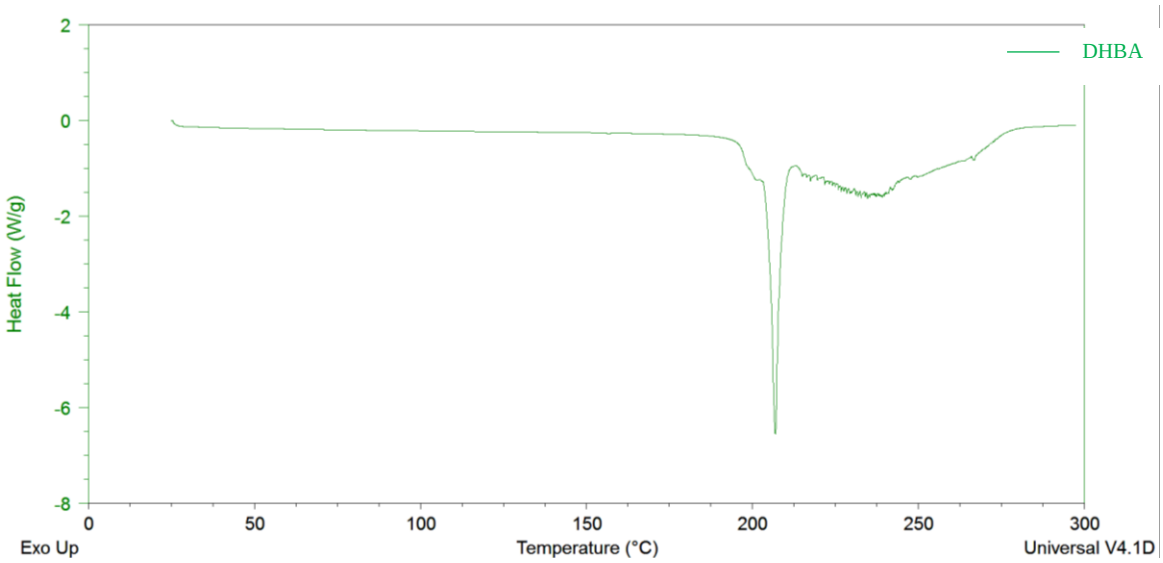

Figure 4.24: DSC thermogram for DHBA.

The DSC thermograms for the control and DHBA-loaded nanofibers are shown in Figure 4.25. A large endothermic peak is observed for PVA and chitosan with and without DHBA over a temperature range of about 50 to 80 °C due to the loss of moisture, coupled with a glass transition temperature. The incorporation of DHBA resulted in a decrease in the melting ranges of PVA and EVOH fibers compared to those of the control nanofibers. Specifically, the melting peak temperature decreased from that of the control fibers (230 °C for PVA and 187 °C for EVOH) to about 195 °C and 166 °C for PVA and EVOH respectively. The change in shape and area of the melting endotherm is also noticed and is attributed to a change in the crystalline structure which may result from polymer-DHBA interactions in the amorphous phase, therefore, disorder in the crystals is created, reducing the enthalpy of the phase change[54, 55]. Similar behavior was also observed for PEO incorporated with DHBA[47].

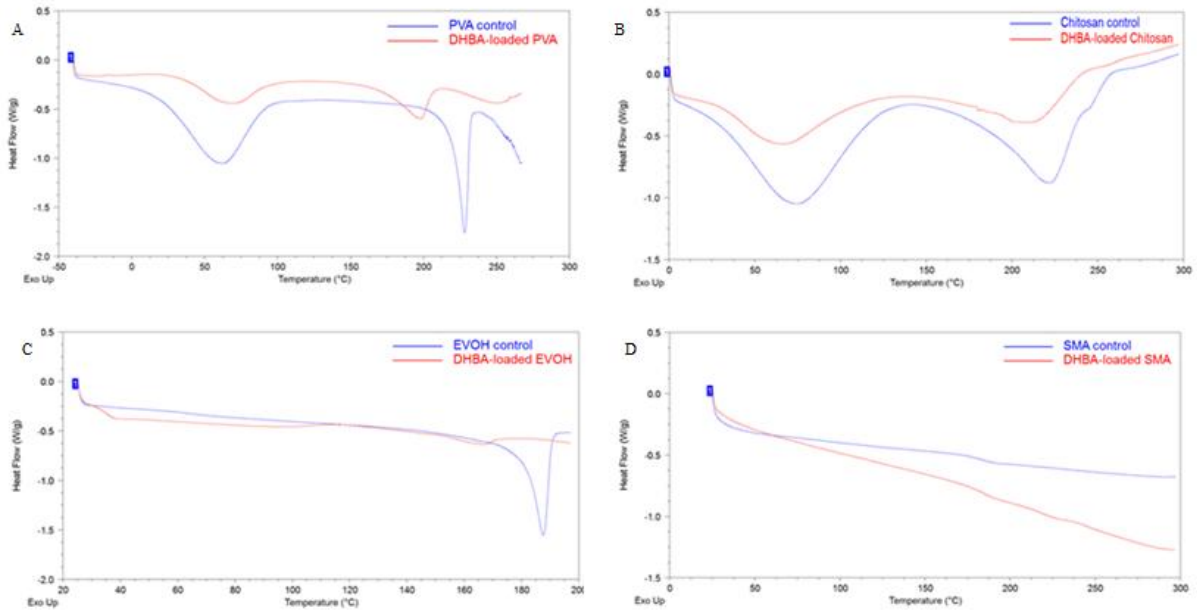

Figure 4.25: DSC thermograms of DHBA-loaded and control matrices: A - PVA, B - Chitosan, C - EVOH and D - SMA.

In the case of DHBA-loaded chitosan, the observed melting temperature is not significantly affected by the incorporation of DHBA, although a change in shape and area of the endotherm is observed. In DHBA-loaded SMA and control SMA, only a T_g is noticed at 180 °C. These observations imply that some interaction might have taken place between DHBA and the matrix.

The DSC results correlated well with the TGA results. With regards to the thermal degradation of DHBA-loaded matrices, the DSC results confirmed that these DHBA-loaded matrices also exhibited similar thermal degradation temperature ranges.

4.5 Conclusion

PVA, chitosan, EVOH and SMA nanofibers were successfully produced using the electrospinning technique. In all the polymer solutions, the morphology of the fibers was the most influenced by the concentration of the solutions. There was no linear relationship between the spinning distance and fiber diameter for chitosan, EVOH and SMA. The flow rate of the solutions showed a linear relationship with the fiber diameter. The morphologies of the different nanofibers can be controlled by manipulating the various parameters. The final fiber diameter for PVA, chitosan, EVOH and SMA nanofibers was around 250 nm.

Incorporation of the antimicrobial agent, DHBA, had no significant effect on the fiber diameter as well as the morphology of the fibers. The successful incorporation of DHBA was determined using FTIR. DHBA seemed to interact with PVA and EVOH but limited interaction with chitosan and SMA. The reason may be due to steric hindrance of the large molecules of chitosan and SMA compared to PVA and EVOH.

The thermal degradation of DHBA-loaded PVA and EVOH seemed to be delayed with the incorporation of DHBA while for chitosan and SMA, it stayed the same. This shows the influence DHBA has on the thermal stability of these matrices. These matrices show potential for use as wound dressings but need further investigation of how the interaction of DHBA with the polymer matrices as well as type of polymer, will be influencing the release behavior of DHBA.

References

1. Kim, B.; Kim, I. Recent nanofiber technologies. *Polym. Rev.* **2011,** *51,* 235-238.

2. Deitzel, J.; Kleinmeyer, J.; Harris, D.; Tan, N.B. The effect of processing variables on the morphology of electrospun nanofibers and textiles. *Polymer* **2001,** *42,* 261-272.

3. Park, J.; Ito, T.; Kim, K.; Kim, K.; Kim, B.; Khil, M.; Kim, H.; Kim, I. Electrospun poly (vinyl alcohol) nanofibers: effects of degree of hydrolysis and enhanced water stability. *Polym. J.* **2010,** *42,* 273-276.

4. Aljehani, A.K.; Hussaini, M.; Hussain, M.A.; Alothmany, N.S.; Aldhaheri, R.W. Effect of electrospinning parameters on nanofiber diameter made of poly (vinyl alcohol) as determined by Atomic Force Microscopy. *Biomed. Eng*. **2014,** 379-381.

5. Ohkawa, K.; Cha, D.; Kim, H.; Nishida, A.; Yamamoto, H. Electrospinning of chitosan. *Macromol. Rapid Commun.* **2004,** *25,* 1600-1605.

6. Ohkawa, K.; Minato, K.; Kumagai, G.; Hayashi, S.; Yamamoto, H. Chitosan nanofiber. *Biomacromolecules* **2006,** *7,* 3291-3294.

7. Kenawy, E.; Layman, J.M.; Watkins, J.R.; Bowlin, G.L.; Matthews, J.A.; Simpson, D.G.; Wnek, G.E. Electrospinning of poly (ethylene-co-vinyl alcohol) fibers. *Biomaterials* **2003,** *24,* 907-913.

8. Xu, C. Electro-spinning of poly (ethylene-co-vinyl alcohol) (EVOH) nanofibres for medical applications and its mechanical properties. PhD Thesis, Brunel University **2012,** 34-56.

9. Tang, C.; Ye, S.; Liu, H. Electrospinning of poly (styrene-co-maleic anhydride) (SMA) and water-swelling behavior of crosslinked/hydrolyzed SMA hydrogel nanofibers. *Polymer* **2007,** *48,* 4482-4491.

10. Cronje, L. Surface modification of styrene maleic anhydride nanofibers for efficient capture of Mycobacterium tuberculosis. PhD Thesis, Unversity of Stellenbosch **2012,** 49.

11. Kim, S.J.; Park, S.J.; An, K.H.; Kim, N.G.; Kim, S.I. Water behavior of poly (vinyl alcohol)/poly (vinylpyrrolidone) interpenetrating polymer network hydrogels. *J. Appl. Polym. Sci.* **2003,** *89,* 24-27.

12. Shenoy, S.L.; Bates, W.D.; Frisch, H.L.; Wnek, G.E. Role of chain entanglements on fiber formation during electrospinning of polymer solutions: good solvent, non-specific polymer–polymer interaction limit. *Polymer* **2005,** *46,* 3372-3384.

13. Eda, G.; Shivkumar, S. Bead structure variations during electrospinning of polystyrene. *J. Mater. Sci.* **2006,** *41,* 5704-5708.

14. Kriel, H. Polylactic acid core-shell fibers by coaxial electrospinning. MSc Thesis, University of Stellenbosch **2010,** 118.

15. Seeram, R.; Kazutoshi, F.; Wee-Eong, T.; Teik-Cheng, I,; Zuwei, M. An introduction to electrospinning and nanofibers. World Scientific Publishing Co. Pte. Ltd: Singapore, **2005.**

16. Demir, M.M.; Yilgor, I.; Yilgor, E.; Erman, B. Electrospinning of polyurethane fibers. *Polymer* **2002,** *43,* 3303-3309.

17. Zong, X.; Kim, K.; Fang, D.; Ran, S.; Hsiao, B.S.; Chu, B. Structure and process relationship of electrospun bioabsorbable nanofiber membranes. *Polymer* **2002,** *43,* 4403-4412.

18. Xu, J.; Zhang, J.; Gao, W.; Liang, H.; Wang, H.; Li, J. Preparation of chitosan/PLA blend micro/nanofibers by electrospinning. *Mater. Lett.* **2009,** *63,* 658-660.

19. Geng, X.; Kwon, O.; Jang, J. Electrospinning of chitosan dissolved in concentrated acetic acid solution. *Biomaterials* **2005,** *26,* 5427-5432.

20. Min, B.; Lee, S.W.; Lim, J.N.; You, Y.; Lee, T.S.; Kang, P.H.; Park, W.H. Chitin and chitosan nanofibers: electrospinning of chitin and deacetylation of chitin nanofibers. *Polymer* **2004,** *45,* 7137-7142.

21. De Vrieze, S.; Westbroek, P.; Van Camp, T.; Van Langenhove, L. Electrospinning of chitosan nanofibrous structures: feasibility study. *J. Mater. Sci.* **2007,** *42,* 8029-8034.

22. Hasegawa, M.; Isogai, A.; Onabe, F.; Usuda, M. Dissolving states of cellulose and chitosan in trifluoroacetic acid. *J. Appl. Polym. Sci.* **1992,** *45,* 1857-1863.

23. Venugopal, J.; Zhang, Y.; Ramakrishna, S. Electrospun nanofibres: biomedical applications. *Proc. Inst. Mech. Eng. N. J. Nanoeng. Nanosyst.* **2004,** *218,* 35-45.

24. Greiner, A.; Wendorff, J.H. Electrospinning: a fascinating method for the preparation of ultrathin fibers. *Angew. Chem. Int. Ed.* **2007,** *46,* 5670-5703.

25. Homayoni, H.; Ravandi, S.A.H.; Valizadeh, M. Electrospinning of chitosan nanofibers: Processing optimization. *Carbohydr. Polym.* **2009,** *77,* 656-661.

26. Ding, W.; Wei, S.; Zhu, J.; Chen, X.; Rutman, D.; Guo, Z. Manipulated electrospun PVA nanofibers with inexpensive salts. *Macromol. Mater. Eng.* **2010,** *295,* 958-965.

27. Garg, K.; Bowlin, G.L. Electrospinning jets and nanofibrous structures. *Biomicrofluidics* **2011,** *5,* 013403.

28. Ogata, N.; Lu, G.; Iwata, T.; Yamaguchi, S.; Nakane, K.; Ogihara, T. Effects of ethylene content of poly (ethylene-co-vinyl alcohol) on diameter of fibers produced by melt-electrospinning. *J. Appl. Polym. Sci.* **2007,** *104,* 1368-1375.

29. Baumgarten, P.K. Electrostatic spinning of acrylic microfibers. *J. Colloid Interface Sci.* **1971,** *36,* 71-79.

30. Fong, H.; Chun, I.; Reneker, D. Beaded nanofibers formed during electrospinning. *Polymer* **1999,** *40,* 4585-4592.

31. Martínez-Sanz, M.; Olsson, R.T.; Lopez-Rubio, A.; Lagaron, J.M. Development of electrospun EVOH fibres reinforced with bacterial cellulose nanowhiskers. Part I: Characterization and method optimization. *Cellulose* **2011,** *18,* 335-347.

32. Layman, J.; Wnek, G.; Kenawy, E. Electrospinning of vinyl alcohol polymer and copolymer fibers. Google patent: **2003**.

33. Buchko, C.J.; Chen, L.C.; Shen, Y.; Martin, D.C. Processing and microstructural characterization of porous biocompatible protein polymer thin films. *Polymer* **1999,** *40,* 7397-7407.

34. Lee, J.S.; Choi, K.H.; Ghim, H.D.; Kim, S.S.; Chun, D.H.; Kim, H.Y.; Lyoo, W.S. Role of molecular weight of atactic poly (vinyl alcohol) (PVA) in the structure and properties of PVA nanofabric prepared by electrospinning. *J. Appl. Polym. Sci.* **2004,** *93,* 1638-1646.

35. Megelski, S.; Stephens, J.S.; Chase, D.B.; Rabolt, J.F. Micro-and nanostructured surface morphology on electrospun polymer fibers. *Macromolecules* **2002,** *35,* 8456-8466.

36. Hsu, C.; Shivkumar, S. Nano-sized beads and porous fiber constructs of poly (ε-caprolactone) produced by electrospinning. *J. Mater. Sci.* **2004,** *39,* 3003-3013.

37. Baji, A.; Mai, Y.; Wong, S.; Abtahi, M.; Chen, P. Electrospinning of polymer nanofibers: effects on oriented morphology, structures and tensile properties. *Composites Sci. Technol.* **2010,** *70,* 703-718.

38. Bhardwaj, N.; Kundu, S.C. Electrospinning: a fascinating fiber fabrication technique. *Biotechnol. Adv.* **2010,** *28,* 325-347.

39. Lee, C.K.; Kim, S.I.; Kim, S.J. The influence of added ionic salt on nanofiber uniformity for electrospinning of electrolyte polymer. *Synth. Met.* **2005,** *154,* 209-212.

40. Lee, K.; Kim, H.; Khil, M.; Ra, Y.; Lee, D. Characterization of nano-structured poly (ε-caprolactone) nonwoven mats via electrospinning. *Polymer* **2003,** *44,* 1287-1294.

41. Liu, H.; Hsieh, Y. Ultrafine fibrous cellulose membranes from electrospinning of cellulose acetate. *J. Polym. Sci. Part B Polym. Phys.* **2002,** *40,* 2119-2129.

42. Lee, K.; Kim, H.; Bang, H.; Jung, Y.; Lee, S. The change of bead morphology formed on electrospun polystyrene fibers. *Polymer* **2003,** *44,* 4029-4034.

43. Zuo, W.; Zhu, M.; Yang, W.; Yu, H. Experimental study on relationship between jet instability and formation of beaded fibers during electrospinning. *Polym. Eng. Sci.* **2005,** *45,* 704.

44. Koombhongse, S.; Liu, W.; Reneker, D.H. Flat polymer ribbons and other shapes by electrospinning. *J. Polym. Sci. Part B Polym. Phys.* **2001,** *39,* 2598-2606.

45. Chen, S.; Huang, X.; Cai, X.; Lu, J.; Yuan, J.; Shen, J. The influence of fiber diameter of electrospun poly (lactic acid) on drug delivery. *Fibers and Polymers* **2012,** *13,* 1120-1125.

46. Moroni, L.; Licht, R.; de Boer, J.; de Wijn, J.R.; van Blitterswijk, C.A. Fiber diameter and texture of electrospun PEOT/PBT scaffolds influence human mesenchymal stem cell proliferation and morphology, and the release of incorporated compounds. *Biomaterials* **2006,** *27,* 4911-4922.

47. Ahire, J.J.; Neppalli, R.; Heunis, T.D.; van Reenen, A.J.; Dicks, L.M. 2, 3-dihydroxybenzoic acid electrospun into poly (d, l-lactide)(PDLLA)/poly (ethylene oxide) (PEO) nanofibers inhibited the growth of Gram-positive and Gram-negative bacteria. *Curr. Microbiol.* **2014,** *69,* 587-593.

48. Dai, L.; Ying, L. Infrared spectroscopic investigation of hydrogen bonding in EVOH containing PVA fibers. *Macromol. Mater. Eng.* **2002,** *287,* 509-514.

49. Hidalgo, M.; Reinecke, H.; Mijangos, C. PVC containing hydroxyl groups: II. Characterization and properties of crosslinked polymers. *Polymer* **1999,** *40,* 3535-3543.

50. Taepaiboon, P.; Rungsardthong, U.; Supaphol, P. Drug-loaded electrospun mats of poly (vinyl alcohol) fibres and their release characteristics of four model drugs. *Nanotechnology* **2006,** *17,* 2317.

51. Ujang, Z.; Diah, M.; Rashid, A.H.; Halim, A.S. The development, characterization and application of water soluble chitosan. *Biotechnology of Biopolymers* **2011,** 109-130.

52. Guirguis, O.W.; Moselhey, M.T. Thermal and structural studies of poly (vinyl alcohol) and hydroxypropyl cellulose blends. Nat. Sci. **2011,** 4 57-67.

53. Alexy, P.; Kachova, D.; Kršiak, M.; Bakoš, D.; Šimková, B. Poly (vinyl alcohol) stabilisation in thermoplastic processing. *Polym. Degrad. Stab.* **2002,** *78,* 413-421.

54. Wenig, W.; Karasz, F.; MacKnight, W. Structure and properties of the system: poly (2, 6-dimethylphenylene oxide) isotactic polystyrene. Small-angle x-ray studies. *J. Appl. Phys.* **1975,** *46,* 4194-4198.

55. Hammel, R.; MacKnight, W.; Karasz, F. Structure and properties of the system: poly (2, 6-dimethyl-phenylene oxide) isotactic polystyrene. Wide-angle x-ray studies. *J. Appl. Phys.* **1975,** *46,* 4199-4203.

Chapter 5

Release behavior of DHBA-loaded films and electrospun nanofibers

This chapter discusses the results obtained from the release behavior of DHBA from the various polymers and also how the release could be controlled.

5.1 Introduction

The antimicrobial agent, DHBA was incorporated into the polymer solutions as discussed in Chapter 3. The study of the release of DHBA from a polymeric material has only been discussed by Ahire *et al*[1]. They reported that DHBA was incorporated into PDLLA and PEO nanofibers and the release was efficient in inhibiting the growth of several bacteria. However, the release of DHBA was in the form of a burst release, releasing 100% in the first 2 hours. Controlling the release remains challenging and a matrix that can release an agent in a controlled manner for a period of time is highly in demand especially in the pharmaceutical and wound dressing fields[2-4].

A common way of controlling the release of an agent is by incorporating the drug into a polymer matrix. Drug dissolution and drug diffusion through the matrix are important phenomena in controlling the release characteristics of the matrix[4]. In this study, the release of DHBA from four different polymers is studied as well the ability to be able to control the release from these polymers. The following sections will discuss the release of DHBA from the films and the fibers separately.

5.2 Release behavior of DHBA

A standard curve of absorbance versus concentration of the free agent (DHBA) dissolved in distilled water was measured using a UV spectrophotometer (Figure 5.1). This calibration curve was used to determine the percentage DHBA released from the DHBA-loaded polymer matrices.

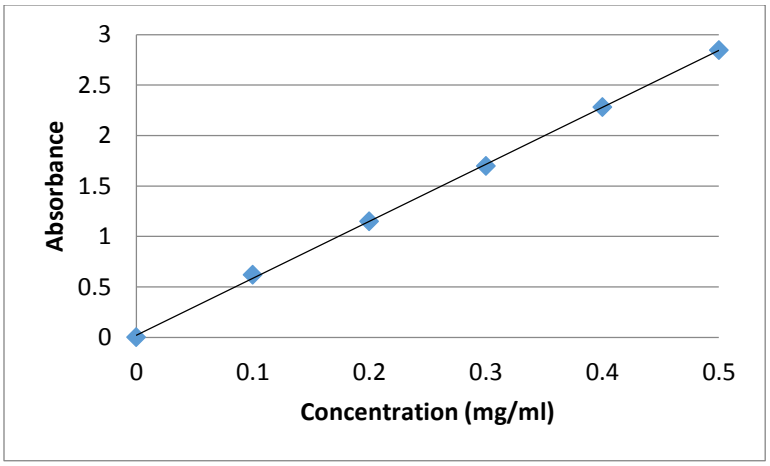

Figure 5.1: Calibration curve of DHBA.

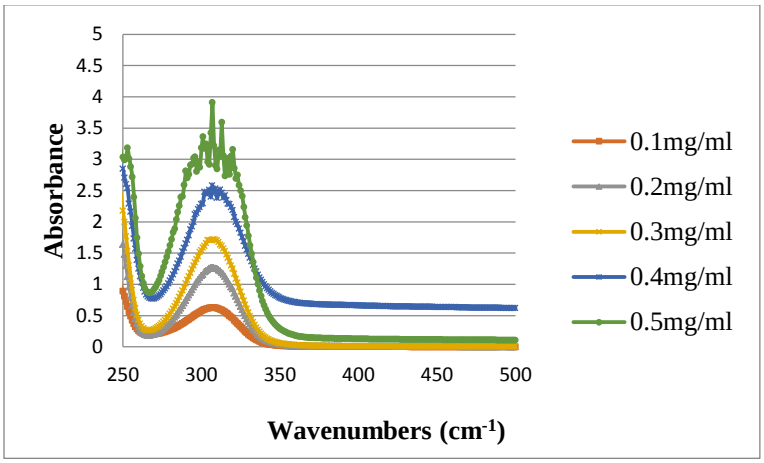

Figure 5.2: UV spectra of DHBA samples.

As shown in Figure 5.2, with increasing DHBA concentration, the absorbance at 310 nm also increases. At too high concentration, the absorbance spectra did not display a smooth curve and for this reason it was chosen to only add 30 mg DHBA into the films and electrospun mats.

5.3 Release behavior from films

Figure 5.3 shows the release behavior from PVA, chitosan, EVOH and SMA films. To be able to compare the release of DHBA from the different polymers, the same concentrations were used and 30 mg DHBA was added to the solutions before casting into a petri dish. Samples were taken in time intervals for up to a week, whereafter the percentage DHBA released with time was analysed using a UV spectrophotometer.

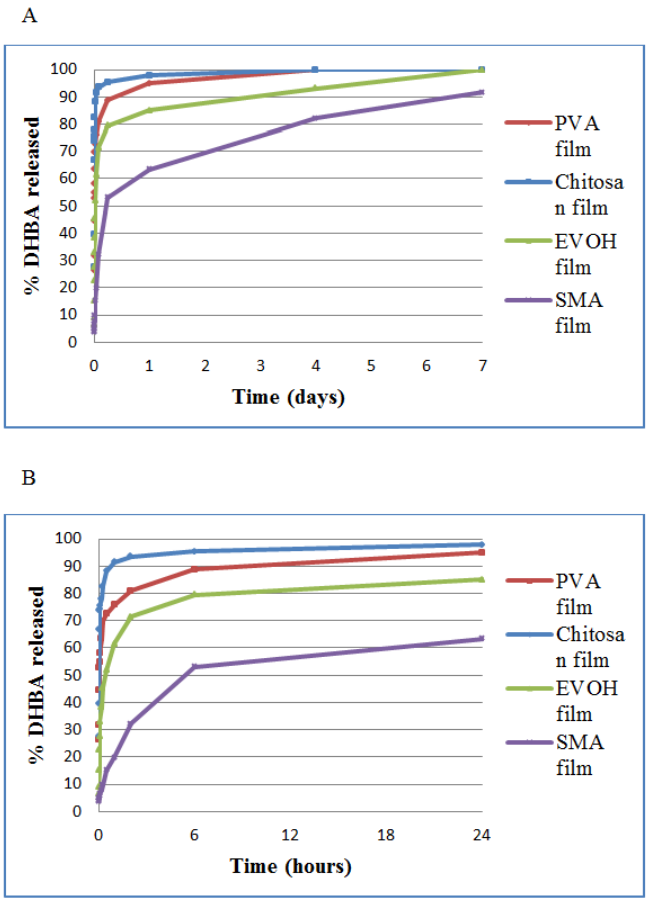

Figure 5.3: Release profiles of PVA, chitosan, EVOH and SMA films in A - 1 week and B - 24hours.

A burst release was observed from PVA and chitosan, releasing 95% and 98% respectively after 24 hours respectively (Figure 5.3 B). After 1 day all the DHBA was released from chitosan and after about 4 days the release from PVA was complete. The slower release from PVA compared

to chitosan may be attributed to the interaction between DHBA and PVA as discussed in Chapter 4. DHBA was released at a slower rate from EVOH and SMA films, releasing 85% and 63% respectively after 24 hours. The slower release from EVOH and SMA may be due to the hydrophobic nature of the polymers compared to PVA and chitosan which are hydrophilic polymers. For the carriers of a hydrophilic DHBA, the hydrophobic surface affects the release of DHBA in a very critical way, and generally higher hydrophobicity of the carrier surface will result in slower release rates of DHBA[5-7]. Xu *et al*[8] showed that with a hydrophobic film, there will be some residual air trapped within the complex structure, which will affect the wetting between the film and water. This residual air will reduce the direct contact area between the film and water, which will finally block the drug release[7]. Therefore, the hydrophilic drug loaded in the film became more difficult to release with the more hydrophobic polymers.

5.3.1 Swelling behavior

It is known that for the delivery of an agent from a matrix, one of the factors controlling the release of the agent is the swelling behavior of the matrix[9, 10]. To support the release behavior of DHBA from these films, the swelling behavior was done and is shown in Figure 5.4.

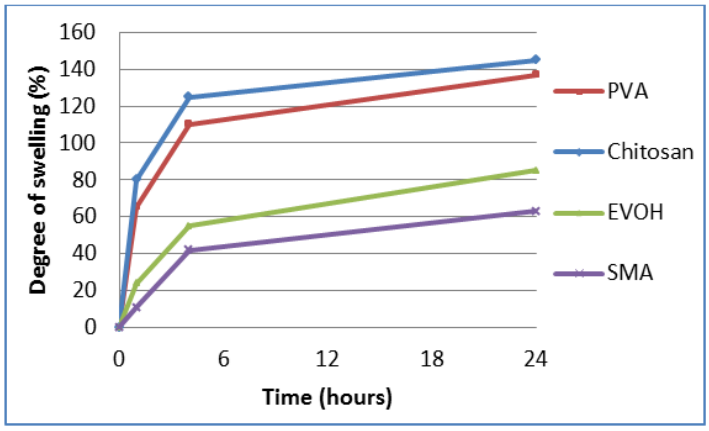

Figure 5.4: Swelling behavior of PVA, Chitosan, EVOH and SMA films after 24hours.

Chitosan and PVA experienced swelling quite significantly in 24 hours, absorbing water and increasing its initial weight with 145% and 137% respectively. This information reflects the release behavior of the films. The more hydrophilic polymers, PVA and chitosan are able to absorb water more, creating pores in the structure and releasing the DHBA at a faster rate[10]. This indicated that the mechanism for the burst release of DHBA included the swelling and the partial dissolution[11-13] of the PVA and chitosan films as well as the high solubility of DHBA within the test medium, i.e. water. EVOH and SMA consist of both hydrophilic and hydrophobic parts where the hydrophobic part of the polymer restricts the uptake of water but not the hydrophilic parts[14]. This allows DHBA still to be released but in a much slower manner.

5.3.2 Controlling the release from the films

The release behavior from the films shows a burst release which is expected but disadvantageous. The possibility of controlling the DHBA release rate from the films by coating the surface with another polymer was the next step. It is expected that the DHBA will have a longer diffusion path to travel to be released into the aqueous medium and resulting in more controlled release behavior[15]. Each polymer film was coated with the other polymer films, for example a PVA film were coated with a PVA, chitosan, EVOH, or a SMA film. DHBA was incorporated in the bottom film (see Section 3.4.3) and the release was monitored from this film. Figure 5.5 displays the release behavior from the coated-PVA, chitosan, EVOH and SMA films respectively.

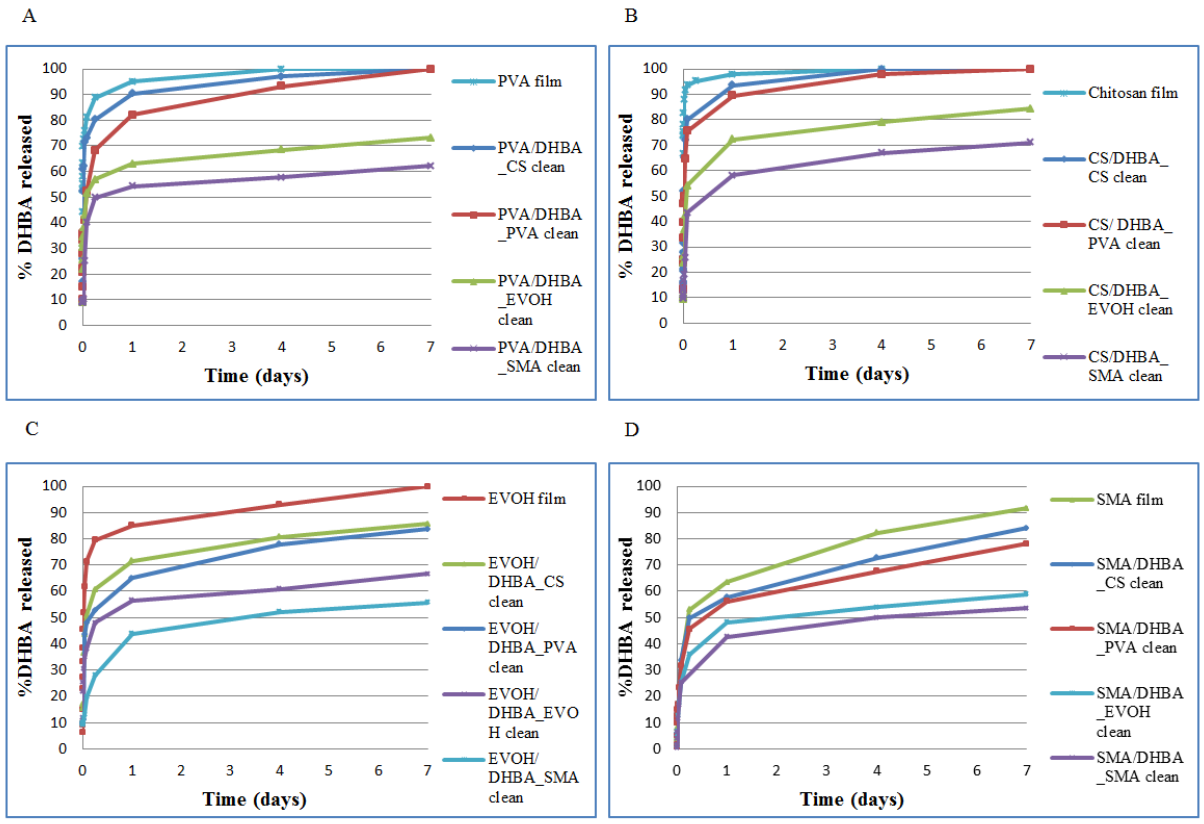

Figure 5.5: Release profiles of coated films of A – PVA, B - Chitosan, C - EVOH and D - SMA films.

PVA and chitosan-coated films experienced an initial burst release of DHBA but when coated with another film of PVA, chitosan, EVOH or SMA, the release was retarded. The release of DHBA from PVA films after 1 day shows an 82 and 90% release when coated with PVA and chitosan films, respectively. In the chitosan films, the release was retarded to 90 and 94% when coated with PVA and chitosan films. Coating the PVA and chitosan film with a hydrophobic film shows the most retardation of DHBA release, releasing only 63 and 72% when coated with EVOH and 54 and 58% when coated with SMA. PVA and chitosan swells significantly in water and when coated with a hydrophobic film, which does not swell readily, restricts the DHBA to be released in the release medium and resulted in slower release of DHBA.

For EVOH and SMA, the release of DHBA is slower compared to PVA and chitosan due to their hydrophobic nature. When these films are coated with another film, the release can even be further retarded. For EVOH films, the release was decreased from 85% in 1 day, to 64% coated

with PVA, 71% coated with chitosan, 56% with EVOH and 43% when coated with SMA. The release from the SMA films shows retardation from 63% released in 1 day to 44% when coated with SMA. From these results can be concluded that the release of DHBA from the coated films was depended on the hydrophilic-hydrophobic nature of the polymer[16, 17]. By coating the film with SMA, a hydrophobic polymer, the release of DHBA was the most effected. The PVA and chitosan-coated films release DHBA the fastest which is attributed to the high degree of swelling of these polymers. The release of DHBA was retarded by coating the films with another film which can be attributed to the fact that DHBA has a longer diffusion pathway to be released into the release medium.

5.4 Release behavior from electrospun nanofibers

Nanofibers produced by electrospinning have been proved to be efficient in controlling the release rate of an agent as compared to films[18]. The fibrous mesh possesses a three-dimensional structure with a high specific surface area, providing an ideal condition for controlled delivery[14, 19]. The polymer type is one of the conditions determining the release of the agent[10, 20].

Prior to investigating the release behavior of DHBA from the electrospun nanofibers, the actual amount of DHBA within the nonwoven mats needs to be measured as described in Section 3.4.4. Table 5.1 summarizes the actual amount of DHBA present in the electrospun mats, reported as percentage of the initial amount of 30 mg loaded in the spinning solutions. DHBA present in the DHBA-loaded electrospun mats ranged between 88 and 97%. Some DHBA may have been lost during the electrospinning process due to instability of the jet[21].

Table 5.1: Actual amount of DHBA in DHBA-loaded electrospun mats.

Type of polymer	**DHBA-loaded electrospun mats (%)**
PVA	97±0.89
Chitosan	88±1.15
EVOH	95±3.02
SMA	96±2.21

PVA, chitosan, EVOH and SMA were electrospun and incorporated with DHBA as discussed in Chapter 4. The release profiles are shown in Figure 5.6. SMA nanofibers show the smallest extent of burst release with a more sustained release pattern during a one week period, whereas PVA and chitosan nanofibers show a much higher extent of initial burst, releasing 87% and 93% in 24 hours respectively, and with less controlled release profiles during the same period. The release profiles of the electospun fibers are similar to the release profiles of the films, where the release rate of DHBA is determined by the dissolution of the matrix. The hydrophilic-hydrophobic nature is the determining factor in the release of DHBA from these matrices[22].

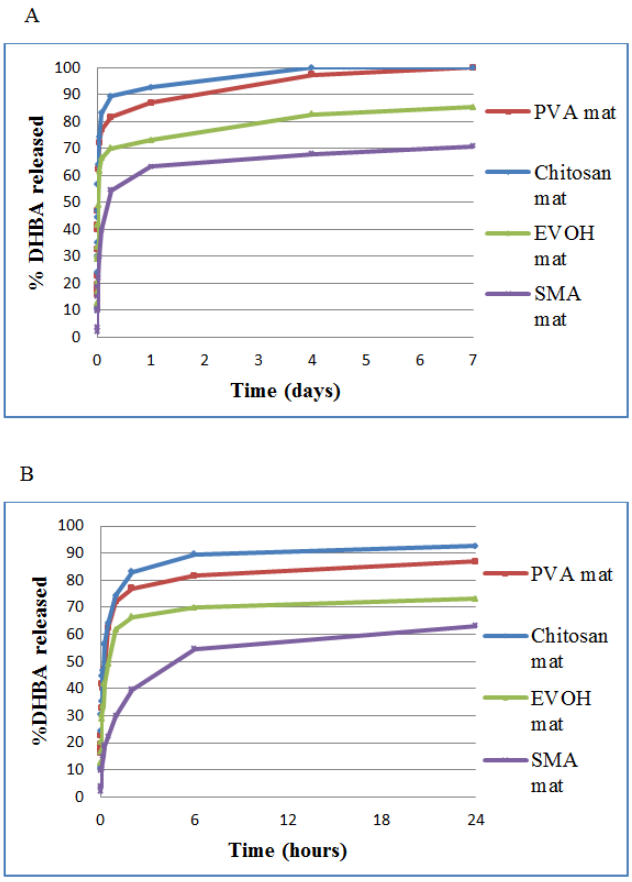

Figure 5.6: Release profiles of PVA, chitosan, EVOH and SMA electrospun mats in A - 1 week and B – 24 hours.

5.4.1 Fiber stability of electrospun mats

To fully understand the release of DHBA from these nanofibers, degradation of the electrospun mats were done. SEM images are shown in Figure 5.7 showing the morphology changes of PVA, chitosan, EVOH and SMA nanofibers in water for up to 24 hours. After 24 hours, the morphology of PVA and chitosan changed completely, the water molecules break the chemical bonds along the polymer chain, and the physical integrity of the polymer degrades and allows DHBA to be released[23].

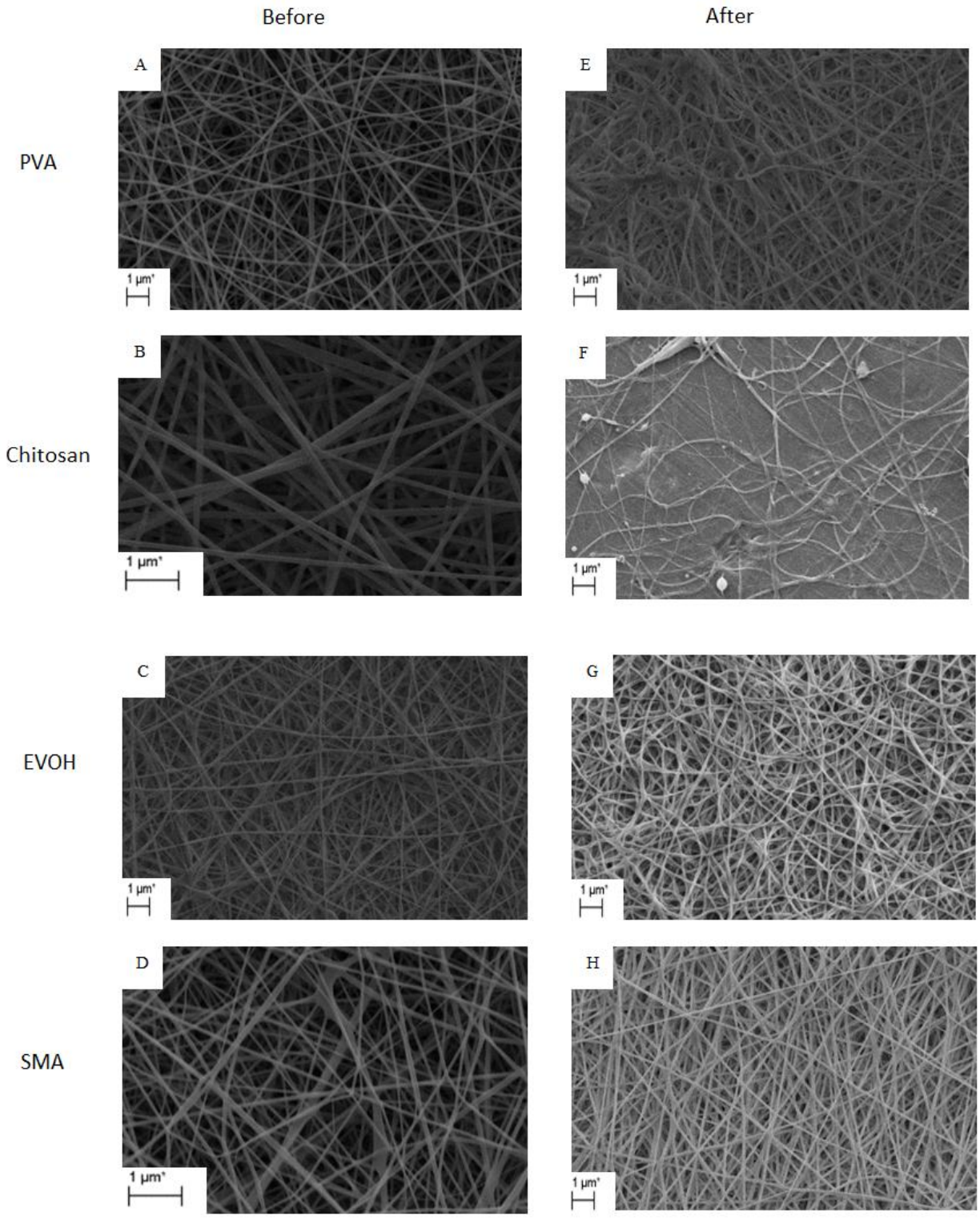

Figure 5.7: SEM images of control electrospun nanofibers before (Images A-D) and after immersion in water (Images E-H).

In the case of EVOH and SMA, the nanofiber morphology remained intact after immersion in water. This indicated the mechanism for the burst release of DHBA included the dissolution of PVA and chitosan matrices and the high solubility of DHBA within water. Zeng *et al*[24] studied the release of BSA from PVA nanofibers and found that the dissolution of PVA fibers was a contributing factor to the release characteristic of the fibers.

5.4.2 Effect of crosslinking

PVA and chitosan show poor stability in aqueous medium which drastically affects the release of DHBA, as reported previously[25]. A glutaraldehyde solution (GA) is commonly used to crosslink PVA[26, 27] and chitosan[28, 29], thereby retarding dissolution in aqueous medium. However, GA is highly toxic and therefore post-treatment of detoxification is required to prevent harmful effects of residual GA. Ramires and Milella[30] confirmed that crosslinking PVA using GA vapors produced membranes with no residual GA. This allows for a safer alternative in producing crosslinked PVA for biomedical applications without further detoxification[30]. For crosslinking to be successful the polymers have to possess an OH group. In this case PVA, chitosan and EVOH were crosslinked to study the effect it has on the release of DHBA.

5.4.2.1 Morphology of crosslinked nanofibers

The effect of crosslinking on the fiber morphology is shown in Figure 5.8. With an increase in the crosslinking time, a denser structure with closely packed nanofibers was produced. The change in the nanofiber structure may also contribute to delaying DHBA release due to the decrease in the surface area available for dissolution[26]. At the points of contact between neighboring nanofibers, crosslinking caused fibers to “fuse”, substantiating that crosslinking does not only occur within single nanofibers, but amongst the nanofibrous structure as well, as observed after 48 hours.

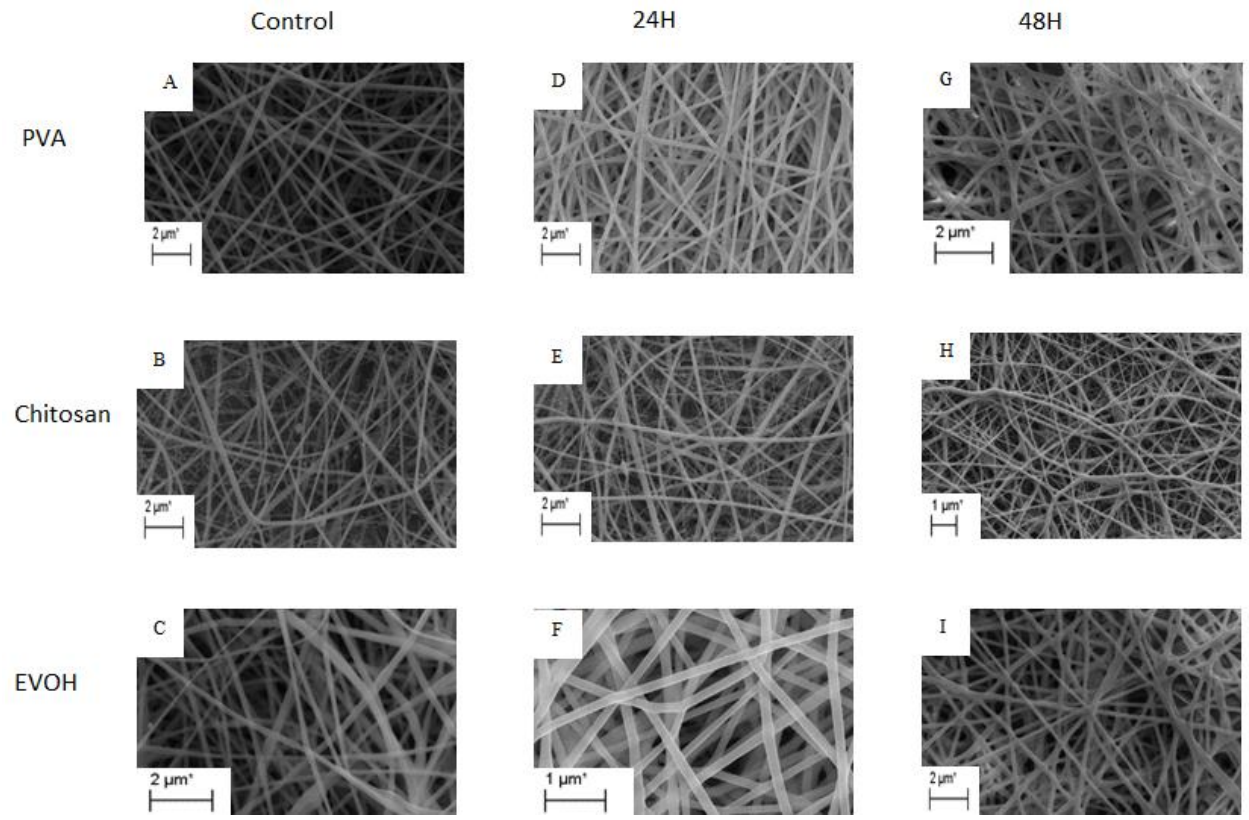

Figure 5.8: SEM images of control nanofibers (A-C), after 24 hours crosslinking (D-F) and after 48 hours crosslinking (G-I).

The electrospun nanofibers crosslinked for 24 hours were further used in this study. This is due to the morphology of the nanofibers that were relatively unchanged after crosslinking and directly influences the average fiber diameter which influences the release behavior of DHBA. For this reason it will still be possible for the various matrices to be compared.

5.4.2.2 Attenuated total reflectance – Fourier transform infrared spectroscopy (ATR-FTIR)

To confirm the successful crosslinking of the fibers, FTIR was done on the 24 hour crosslinked nanofibers. FTIR spectra of the PVA, chitosan and EVOH control before and after crosslinking are shown in Figure 5.9. Due to the similar chemical structures of PVA and EVOH, similar peaks in the FTIR spectra can be used to determine the successful crosslinking using GA.

Crosslinking had an impact on the establishment of inter- and intra-molecular crosslinks and is demonstrated by the variations in band intensities as observed in Figure 5.9. The crosslinking of PVA and EVOH generally occurs through the formation of a –C-O-C- bond between the –OH of a typical PVA and EVOH structure and the –C-C- of a GA molecule[30]. The transmittance bands at 1380 and 1030 cm^{-1}, indicative of C-OH bonding, and the transmittance band at 3300 cm^{-1}, indicative of an OH bond, decrease in intensity after crosslinking indicating that the OH was consumed in the reaction[31]. The disappearance of the shoulder peak at 1150 cm^{-1} is indicative of –C-O-C- bonds which are formed during the crosslinking reaction and the band at 1720 cm^{-1} which is characteristic of GA. These results indicate the decrement of C-OH bonds in the PVA and EVOH molecular structure allowing for the increment of C-H alkyl groups, thereby confirming that crosslinking between PVA/EVOH and GA did occur[26]. However, crosslinking of EVOH was not as significant as in PVA, this might be due to fewer hydroxyl groups being present in EVOH as compared to PVA.

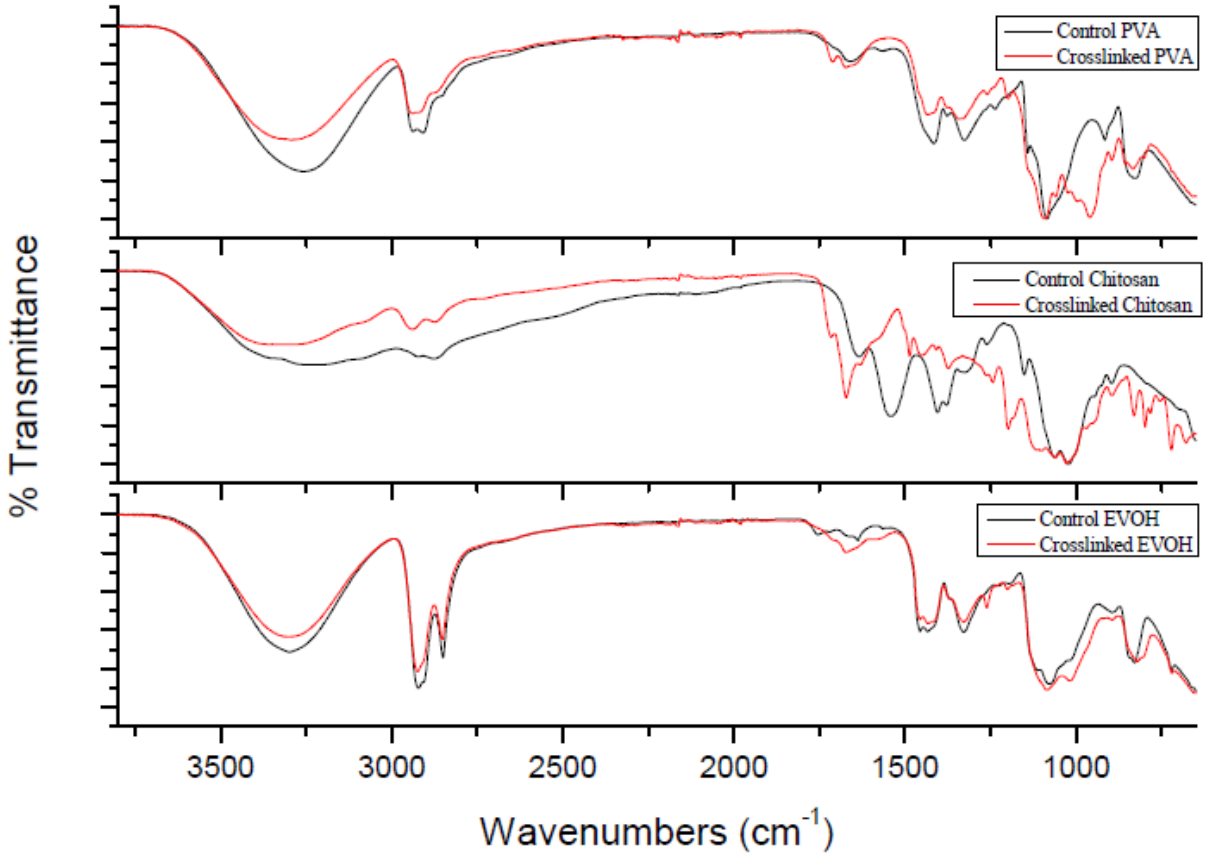

Figure 5.9: FTIR spectra of control nanofibers and crosslinked nanofibers of PVA, chitosan and EVOH.

For the crosslinking of chitosan, significant changes were observed in the FTIR spectra of the control versus the crosslinked chitosan nanofibers. The crosslinked fibers displayed a distinct change in the carbonyl-amide region. An increase in the absorption at 1655 cm^{-1} is seen due to imine bonds[32] and the shoulder next to the peak, corresponds to the ethylenic and free-aldehydic bonds, respectively[28]. The disappearance of the peak at 1560 cm^{-1} is due to the loss of the free amines. The same color change was also observed by Taul[33], namely, the mats became yellow upon crosslinking.

5.4.2.3 Release behavior of crosslinked fibers

The effect of crosslinking is known to delay the release of the agent[34, 35]. The release rate of DHBA from crosslinked PVA, chitosan and EVOH nanofibers slows down significantly as shown in Figure 5.10.

A

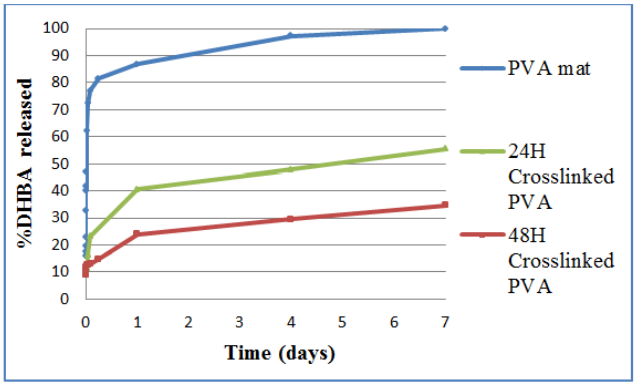

B

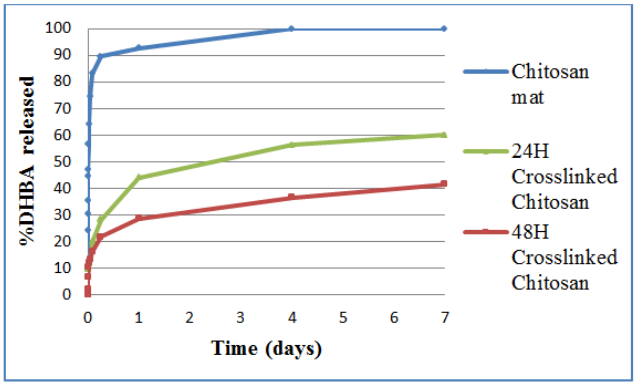

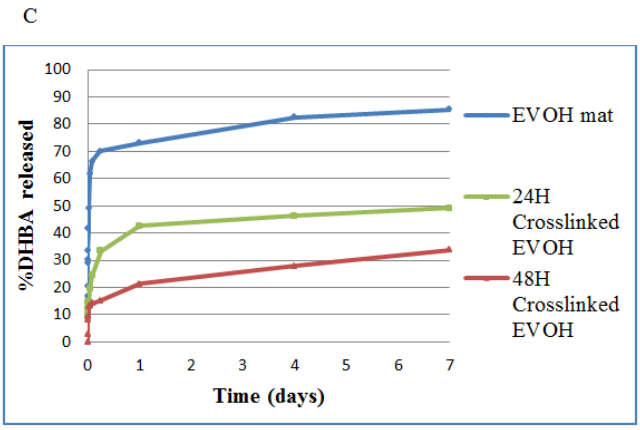

Figure 5.10: Release profiles of crosslinked A - PVA, B - Chitosan and C - EVOH nanofibers after 24 and 48hours.

PVA and chitosan experienced significant retardation of DHBA release when crosslinked with GA. Crosslinking stabilized the electrospun fibers and, thus, reduced the dissolution ability of the nanofibers that inevitably trapped the DHBA within the structure[29]. The crosslinking time also has an influence on the release behavior. Although EVOH was only crosslinked slightly as shown in the FTIR spectrum (Figure 5.9), the slower release of DHBA from crosslinked EVOH can be two-fold: firstly, EVOH is a hydrophobic polymer which can restrict the DHBA to be released and secondly, with crosslinking of the EVOH fibers, the hydrophobicity of these fibers are further enhanced and this resulted in a significant slower release of DHBA.

5.4.2.4 Stability of crosslinked fibers

The release rate of DHBA can be directly correlated with the degradation of the crosslinked nanofibers (Figure 5.11). After 24 hours immersion in water, the morphology change only slightly as compared to the control fibers. As shown in Figure 5.7, where the fibers disintegrated when immersed in water. However some swelling did occur in the crosslinked chitosan fibers after immersion in water and this may be attributed to uneven crosslinking of the nanofibers. GA may have agglomerated on some areas leaving other areas un-crosslinked and more susceptible to water uptake.

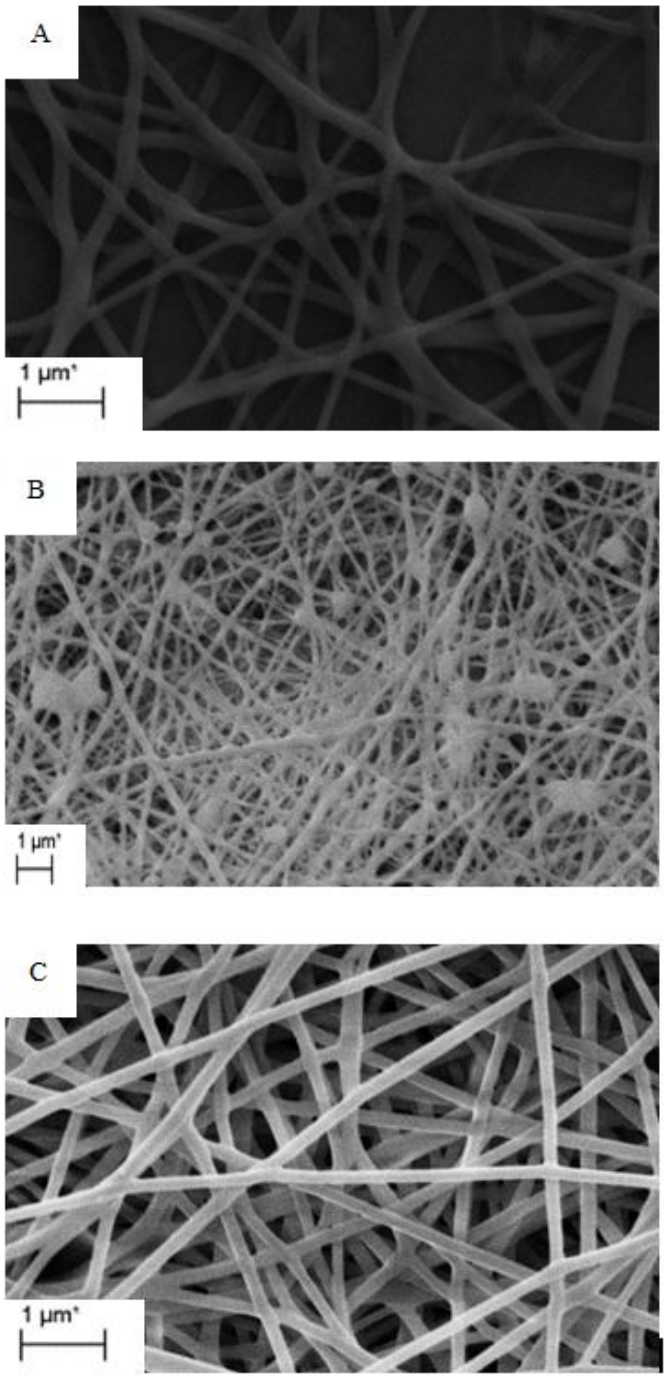

Figure 5.11: SEM images of crosslinked A - PVA, B - Chitosan and C - EVOH after immersion in water.

As the crosslinking time increases, the extent of crosslinking increases which resulted in the slowing down of the dissolution rate and the speed of DHBA released[36].

5.4.3 Controlling the release from electrospun mats

A fast release of DHBA from electrospun nanofibers were observed, especially for the PVA and chitosan nanofibers. It will be crucial for advanced applications to gain a better control over the release behavior of such DHBA-loaded nanofibers. This may be accomplished by modification of the shape of the polymer fibers, by changing of the molecular parameters (molecular weight, crystallinity) or by an additional coating on the DHBA-loaded electrospun nanofibers[24].

This section will focus on controlling the release of DHBA from the PVA and chitosan nanofibers because they exhibited the highest extent of burst release. The coating of EVOH and SMA and release of DHBA from these coated electrospun nanofibers have also been done (shown in Appendix A).

5.4.3.1 Morphology of coated electrospun nanofibers

The electrospun mats of each polymer were coated as discussed in Chapter 3. SEM images of the coated-electrospun mats of PVA and chitosan are shown in Figure 5.12 and the amount of polymer coated onto the electrospun fibers in table 5.2.

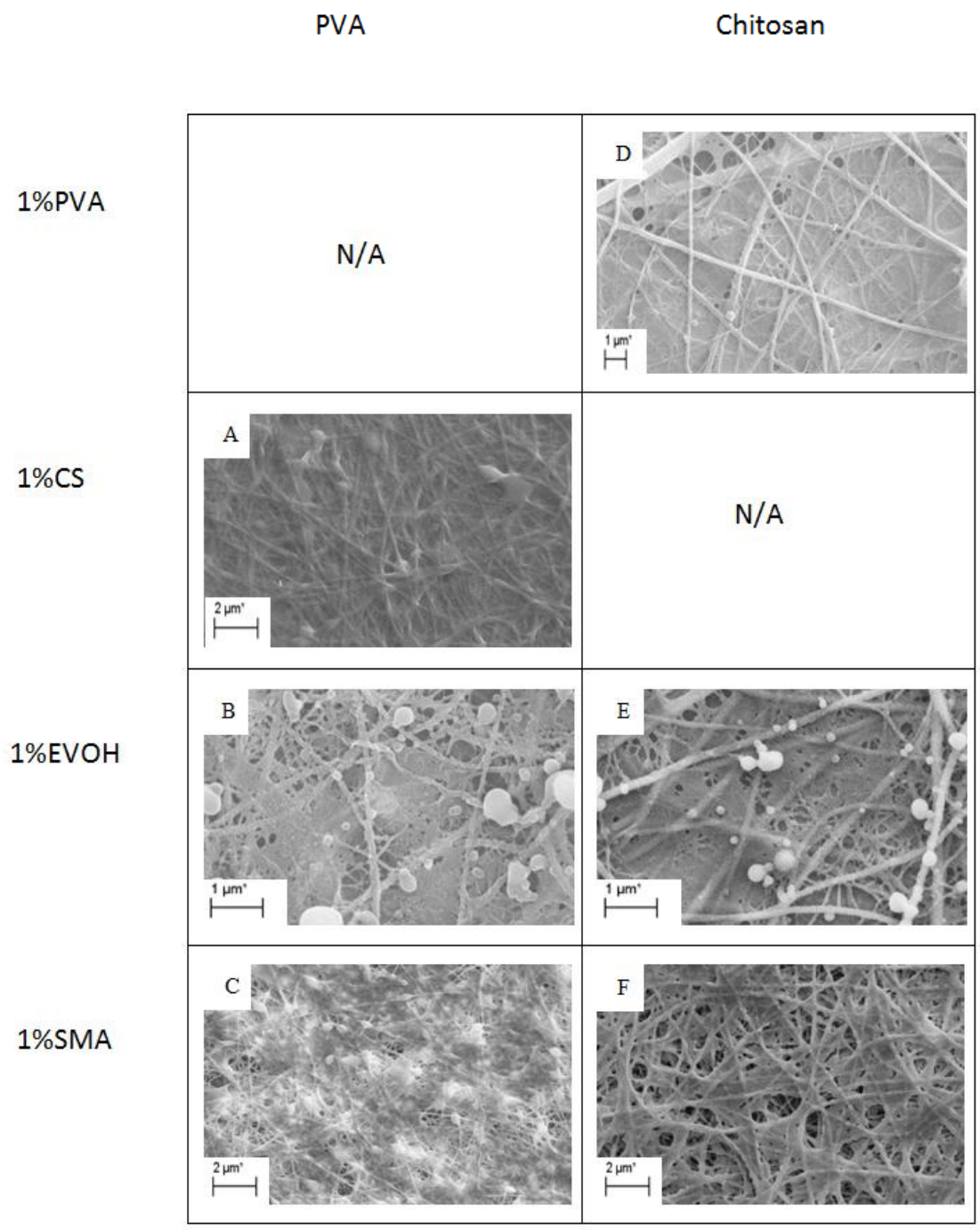

Figure 5.12: SEM images of coated PVA (Images A-C) and coated chitosan (D-F) nanofibers.

Table 5.2: Amount of polymer coated onto PVA and chitosan nanofibers.

	Amount coated on PVA (mg)	**Amount coated on chitosan (mg)**
1%PVA	-	6.7
1%CS	19	-
1%EVOH	6.8	7.1
1%SMA	11.1	11.5

PVA and chitosan nanofibers completely dissolved when immersed into the polymer solutions and for this reason, the crosslinked samples were used. The same was observed by Kang *et al*[37], when PVA nanofibers were coated with chitosan. As shown in Figure 5.12, coating of the nanofibers resulted in films forming in-between the fibers. PVA and EVOH had the tendency to form films in-between the fibers whereas chitosan and SMA were coated on the surface of the nanofibers. It was noticed that new joint welding of the fibers at their neighboring points and at their cross points was observed in the coated samples. Coating of the nanofibers with EVOH resulted in some particles forming on the fiber surface. EVOH is known to precipitate out of solution when cooled down which may explain the formation of the particles[38].

5.4.3.2 Attenuated total reflectance – Fourier transform infrared spectroscopy (ATR-FTIR)

To confirm the successful coating of these electrospun nanofibers, FTIR was done, shown in Figure 5.13 and Figure 5.14, representing the coated PVA and coated chitosan nanofibers, respectively.

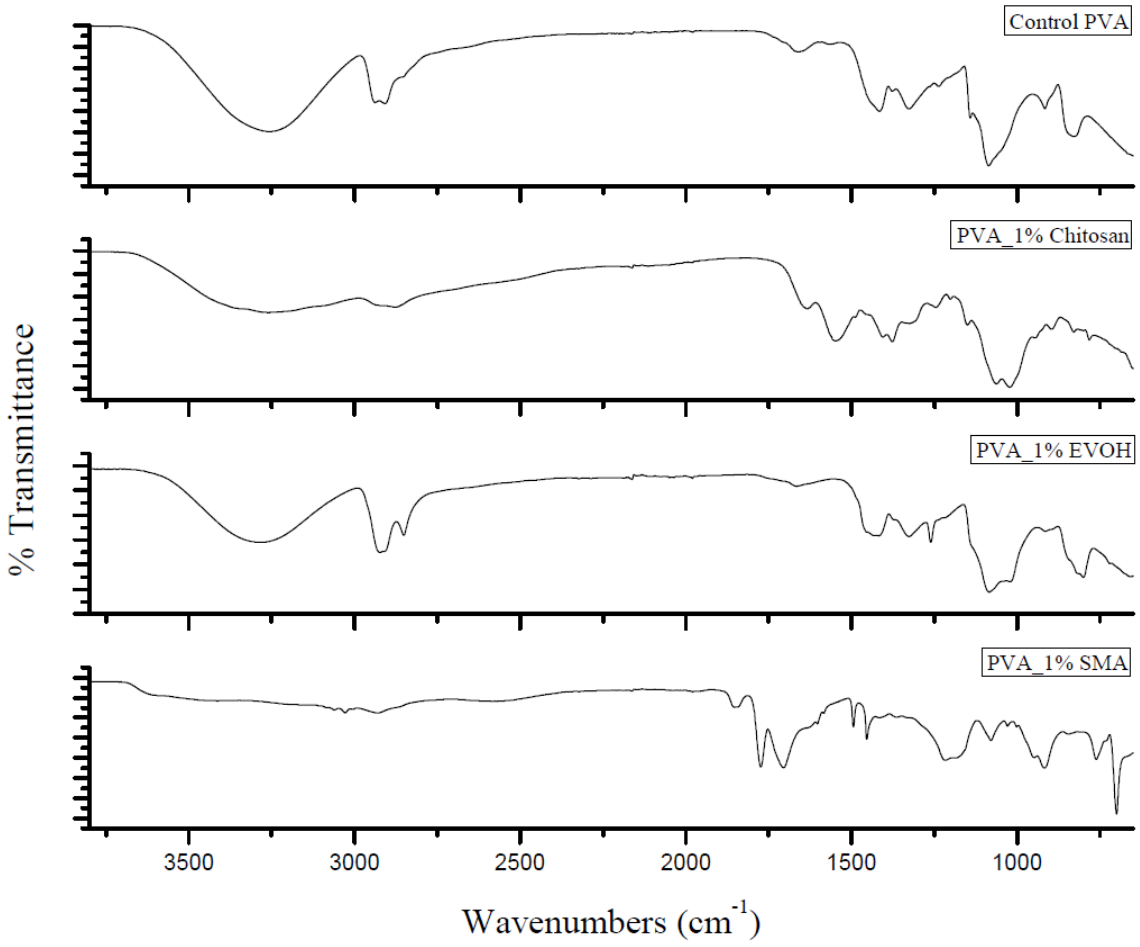

Figure 5.13: FTIR spectra of PVA coated nanofibers.

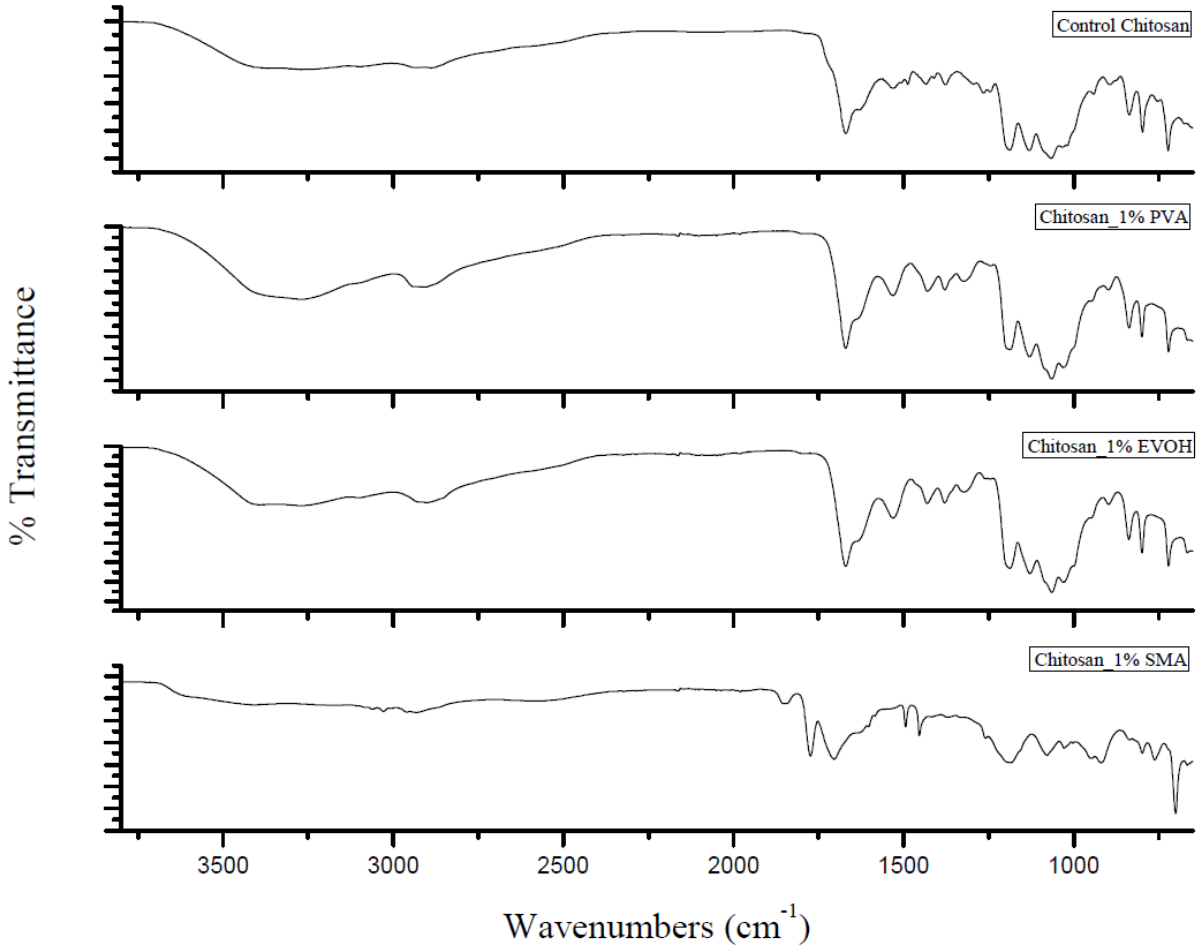

Figure 5.14: FTIR spectra of chitosan coated nanofibers.

Coating of PVA with EVOH was difficult to confirm due to similar functional groups in the molecular structure, however, it was confirmed with the coating of chitosan nanofibers. An increase in intensity at 2850 cm^{-1} was observed after coating with PVA or EVOH, resembling the C-H stretching; two new peaks formed at 1450 and 1380 cm^{-1}, which is indicative for the –C-H bending of PVA or EVOH. An increase in the OH peak intensity at 3300 cm^{-1} can be seen which is due to more OH groups present after coating with either PVA or EVOH[39]. The successful coating with chitosan is confirmed with the amine peaks at 1560 cm^{-1} and two small peaks at 1350 cm^{-1} resembling the N-H bending[40].

For PVA_1%SMA and Chitosan_1%SMA, a strong peak at 1770 cm^{-1} is indicative of the anhydride group in SMA[41]. In the region of 1500 cm^{-1}, two small peaks are characteristic of the styrene functional group present in the SMA molecular structure. From these results, it can be confirmed that the PVA and chitosan was successfully coated with the various polymer solutions.

5.4.2.3 Release behavior of coated electrospun nanofibers

The release of DHBA from these coated PVA and chitosan is shown in Figure 5.15. It is obvious that the release of DHBA from the coated electrospun nanofibers is retarded due to the coating. A significant release of DHBA was observed even after 7 days, especially when coated with the hydrophobic SMA. Quite obviously the release of DHBA from electrospun PVA and chitosan nanofibers was retarded significantly by coating the electrospun nanofibers by an additional layer of polymer, which does not readily dissolve in water. A release of DHBA was observed at prolonged time intervals as controlled by the water permeability of the coated polymer. Similar results were observed by Zeng *et al*[24], when PVA nanofibers were coated with a hydrophobic poly (p-xylylene) (PPX).

A

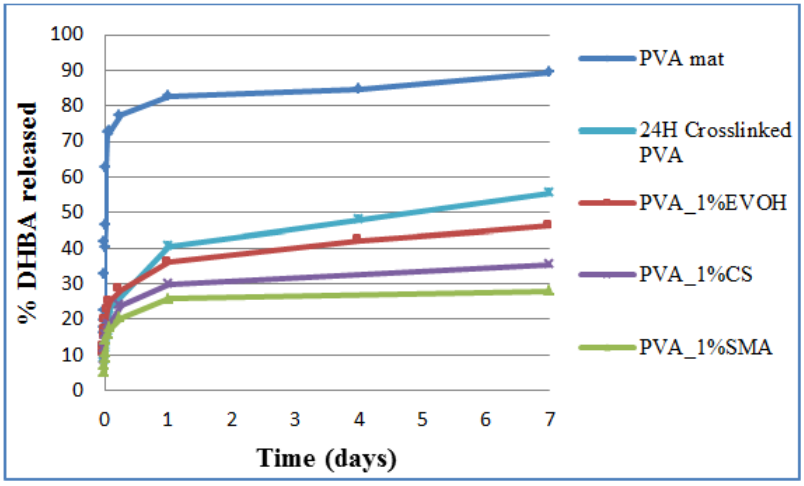

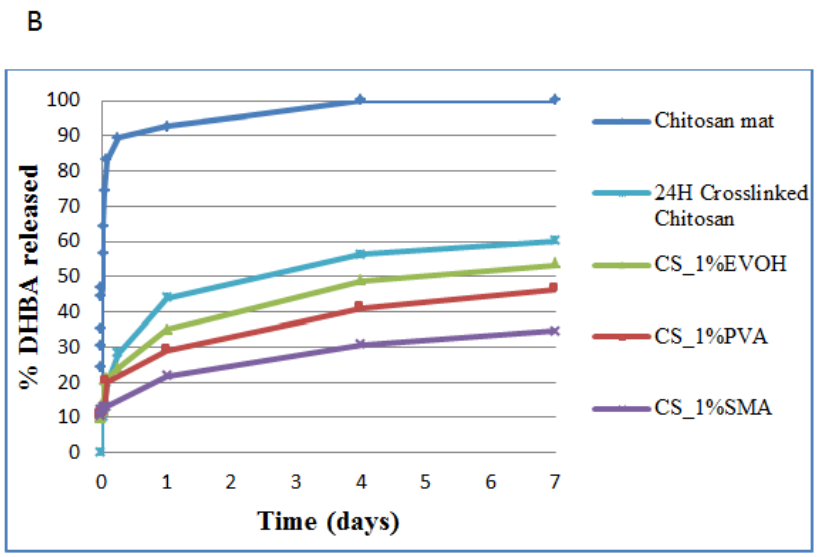

Figure 5.15: Release behavior of coated A - PVA and coated B - Chitosan nanofibers comparing with the uncoated nanofibers.

The release behavior was independent on the amount of polymer on the electrospun nanofibers but rather dependent on the type of polymer. PVA and chitosan nanofibers coated with EVOH experienced the fastest release of DHBA which might be due to the formation of particles of EVOH on the surfaces of the nanofibers. PVA electrospun nanofibers were coated with the most chitosan as shown in table 5.2 and the least with EVOH. Even though the same concentration of polymer solutions were used for the coating process, the chitosan solution seemed quite viscous compared to the other solutions, probably due to the higher molecular weight of the polymer.

The release of DHBA can be explained on how the nanofibers are coated. The PVA nanofibers coated with EVOH experienced the fastest release due to the EVOH solution forming films in-between the fibers, exposing the surface fibers to the aqueous medium. Chitosan and SMA formed a film layer on top of the nanofibers which can retard the release of DHBA. Chitosan nanofibers experienced similar results. In this case, PVA and EVOH formed films in-between the fibers whereas SMA formed a layer on the surface of the nanofibers. A possible reason for the slower release lies in the fact that the coating makes the diffusion passage more difficult for the DHBA to be released out of the nanofibers, which reduces the amount of DHBA release.

The release of DHBA from PVA and chitosan nanofibers can be controlled by an additional coating. The type of polymer and how the coating was done plays an important role in how DHBA is released. These coated-nanofibers show potential for use in biomedical applications, where a more controlled release is required.

5.5 Conclusion

Films that were produced via solvent casting and electrospun mats by using the electrospinning process were used to study the release of DHBA. Four polymers which differ in hydrophilic-hydrophobic nature were used to study the release behavior from these matrices. The type of polymer used imparts a conspicuous effect on the release behavior of DHBA. PVA and chitosan films showed an initial burst release of DHBA and this can be retarded by coating the films with another film. The release of DHBA from the hydrophilic films, which swell considerable in water medium, can be retarded by coating with a hydrophobic film. The results observed in this study, show that the release of DHBA from a hydrophobic matrix is less than from a hydrophilic matrix. The release of DHBA from the films shows a dissolution-controlled release where the coated films, have a more diffusion-controlled release.

Electrospun mats showed similar release behavior of DHBA as compared to the films. The release of DHBA from the electrospun mats was retarded with crosslinking of the fibers. The non-crosslinked nanofibers of PVA and chitosan completely changed morphology when immersed in water and resulted in a burst release of DHBA. With crosslinking, insolubility in water was achieved and this water-insoluble property would give these nanofibers a more sustained release of DHBA. The release of DHBA was further retarded by coating of the nanofibers. The amount of polymer coated onto the nanofibers and type of polymer used as the coating material, played a crucial role in the release of DHBA.

Dissolution and diffusion of DHBA from these matrices are the controlling parameters determining the release of DHBA. The controlled release of DHBA will significantly extend the possibilities for release-related applications for which a more sustained release is required, especially in the field of wound dressings.

References

1. Ahire, J.J.; Neppalli, R.; Heunis, T.D.; van Reenen, A.J.; Dicks, L.M. 2, 3-dihydroxybenzoic acid electrospun into poly (D, L-lactide) (PDLLA)/poly (ethylene oxide) (PEO) nanofibers inhibited the growth of Gram-positive and Gram-negative bacteria. *Curr. Microbiol.* **2014,** *69,* 587-593.

2. Shukla, A.; Fleming, K.E.; Chuang, H.F.; Chau, T.M.; Loose, C.R.; Stephanopoulos, G.N.; Hammond, P.T. Controlling the release of peptide antimicrobial agents from surfaces. *Biomaterials* **2010,** *31,* 2348-2357.

3. Szentivanyi, A.; Chakradeo, T.; Zernetsch, H.; Glasmacher, B. Electrospun cellular microenvironments: understanding controlled release and scaffold structure. *Adv. Drug Deliv. Rev.* **2011,** *63,* 209-220.

4. Huang, X.; Brazel, C.S. On the importance and mechanisms of burst release in matrix-controlled drug delivery systems. *J. Controlled Release* **2001,** *73,* 121-136.

5. Yohe, S.T.; Herrera, V.L.; Colson, Y.L.; Grinstaff, M.W. 3D superhydrophobic electrospun meshes as reinforcement materials for sustained local drug delivery against colorectal cancer cells. *J. Controlled Release* **2012,** *162,* 92-101.

6. Yohe, S.T.; Colson, Y.L.; Grinstaff, M.W. Superhydrophobic materials for tunable drug release: using displacement of air to control delivery rates. *J. Am. Chem. Soc.* **2012,** *134,* 2016-2019.

7. Zhang, X.; Bogdanowicz, D.; Erisken, C.; Lee, N.M.; Lu, H.H. Biomimetic scaffold design for functional and integrative tendon repair. *J. Shoulder Elbow Surg.* **2012,** *21,* 266-277.

8. Xu, H.; Li, H.; Chang, J. Controlled drug release from a polymer matrix by patterned electrospun nanofibers with controllable hydrophobicity. *J. Mater. Chem. B* **2013,** *1,* 4182-4188.

9. Borgquist, P.; Körner, A.; Piculell, L.; Larsson, A.; Axelsson, A. A model for the drug release from a polymer matrix tablet—effects of swelling and dissolution. *J. Controlled Release* **2006,** *113,* 216-225.

10. Reza, M.S.; Quadir, M.A.; Haider, S.S. Comparative evaluation of plastic, hydrophobic and hydrophilic polymers as matrices for controlled-release drug delivery. *J. Pharm. Pharm. Sci.* **2003,** *6,* 274-291.

11. Buonocore, G.; Del Nobile, M.; Panizza, A.; Corbo, M.; Nicolais, L. A general approach to describe the antimicrobial agent release from highly swellable films intended for food packaging applications. *J. Controlled Release* **2003,** *90,* 97-107.

12. Miller-Chou, B.A.; Koenig, J.L. A review of polymer dissolution. *Prog. Polym. Sci.* **2003,** *28,* 1223-1270.

13. Narasimhan, B.; Peppas, N.A. The physics of polymer dissolution: Modeling approaches and experimental behavior, In *Polymer Analysis Polymer Physics*, Anonymous ; Springer: **1997**, 157-207.

14. Maretschek, S.; Greiner, A.; Kissel, T. Electrospun biodegradable nanofiber nonwovens for controlled release of proteins. *J. Controlled Release* **2008,** *127,* 180-187.

15. Shukla, A.; Fuller, R.C.; Hammond, P.T. Design of multi-drug release coatings targeting infection and inflammation. *J. Controlled Release* **2011,** *155,* 159-166.

16. Hasimi, A.; Stavropoulou, A.; Papadokostaki, K.; Sanopoulou, M. Transport of water in polyvinyl alcohol films: effect of thermal treatment and chemical crosslinking. *Eur. Polym. J.* **2008,** *44,* 4098-4107.

17. Rohindra, D.R.; Nand, A.V.; Khurma, J.R. Swelling properties of chitosan hydrogels. *The South Pacific Journal of Natural and Applied Sciences* **2004,** *22,* 32-35.

18. Kenawy, E.; Bowlin, G.L.; Mansfield, K.; Layman, J.; Simpson, D.G.; Sanders, E.H.; Wnek, G.E. Release of tetracycline hydrochloride from electrospun poly (ethylene-co-vinylacetate), poly (lactic acid), and a blend. *J. Controlled Release* **2002,** *81,* 57-64.

19. Kim, T.G.; Lee, D.S.; Park, T.G. Controlled protein release from electrospun biodegradable fiber mesh composed of poly (ε -caprolactone) and poly (ethylene oxide). *Int. J. Pharm.* **2007,** *338,* 276-283.

20. Boza, A.; Caraballo, I.; Alvarez-Fuentes, J.; Rabasco, A. Evaluation of Eudragit® RS-PO and Ethocel® 100 matrices for the controlled release of lobenzarit disodium. *Drug Dev. Ind. Pharm.* **1999,** *25,* 229-233.

21. Taepaiboon, P.; Rungsardthong, U.; Supaphol, P. Drug-loaded electrospun mats of poly (vinyl alcohol) fibres and their release characteristics of four model drugs. *Nanotechnology* **2006,** *17,* 2317.

22. Karuppuswamy, P.; Venugopal, J.R.; Navaneethan, B.; Laiva, A.L.; Ramakrishna, S. Polycaprolactone nanofibers for the controlled release of tetracycline hydrochloride. *Mater. Lett.* **2015,** *141,* 180-186.

23. Rathinamoorthy, R. Nanofiber for drug delivery system–principle and application. *Pak. Text. J* **2012,** *61,* 45-48.

24. Zeng, J.; Aigner, A.; Czubayko, F.; Kissel, T.; Wendorff, J.H.; Greiner, A. Poly (vinyl alcohol) nanofibers by electrospinning as a protein delivery system and the retardation of enzyme release by additional polymer coatings. *Biomacromolecules* **2005,** *6,* 1484-1488.

25. Korsmeyer, R.W.; Gurny, R.; Doelker, E.; Buri, P.; Peppas, N.A. Mechanisms of solute release from porous hydrophilic polymers. *Int. J. Pharm.* **1983,** *15,* 25-35.

26. Shaikh, R.P.; Kumar, P.; Choonara, Y.E.; Du Toit, L.C.; Pillay, V. Crosslinked electrospun PVA nanofibrous membranes: elucidation of their physicochemical, physicomechanical and molecular disposition. *Biofabrication* **2012,** *4,* 025002.

27. Tang, C.; Saquing, C.D.; Harding, J.R.; Khan, S.A. In situ cross-linking of electrospun poly (vinyl alcohol) nanofibers. *Macromolecules* **2009,** *43,* 630-637.

28. Beppu, M.; Vieira, R.; Aimoli, C.; Santana, C. Crosslinking of chitosan membranes using glutaraldehyde: Effect on ion permeability and water absorption. *J. Membr. Sci.* **2007,** *301,* 126-130.

29. Schiffman, J.D.; Schauer, C.L. Cross-linking chitosan nanofibers. *Biomacromolecules* **2007,** *8,* 594-601.

30. Ramires, P.; Milella, E. Biocompatibility of poly (vinyl alcohol)-hyaluronic acid and poly (vinyl alcohol)-gellan membranes crosslinked by glutaraldehyde vapors. *J. Mater. Sci. Mater. Med.* **2002,** *13,* 119-123.

31. Figueiredo, K.; Alves, T.L.; Borges, C.P. Poly (vinyl alcohol) films crosslinked by glutaraldehyde under mild conditions. *J. Appl. Polym. Sci.* **2009,** *111,* 3074-3080.

32. Berger, J.; Reist, M.; Mayer, J.M.; Felt, O.; Peppas, N.; Gurny, R. Structure and interactions in covalently and ionically crosslinked chitosan hydrogels for biomedical applications. *Eur. J. Pharm. Biopharm.* **2004,** *57,* 19-34.

33. Tual, C.; Espuche, E.; Escoubes, M.; Domard, A. Transport properties of chitosan membranes: influence of crosslinking. *J. Polym. Sci. Part B Polym. Phys.* **2000,** *38,* 1521-1529.

34. Thacharodi, D.; Rao, K.P. Propranolol hydrochloride release behaviour of crosslinked chitosan membranes. *J. Chem. Technol. Biotechnol.* **1993,** *58,* 177-181.

35. Korsmeyer, R.W.; Peppas, N.A. Effect of the morphology of hydrophilic polymeric matrices on the diffusion and release of water soluble drugs. *J. Membr. Sci.* **1981,** *9,* 211-227.

36. Yang, D.; Li, Y.; Nie, J. Preparation of gelatin/PVA nanofibers and their potential application in controlled release of drugs. *Carbohydr. Polym.* **2007,** *69,* 538-543.

37. Kang, Y.O.; Yoon, I.; Lee, S.Y.; Kim, D.; Lee, S.J.; Park, W.H.; Hudson, S.M. Chitosan-coated poly (vinyl alcohol) nanofibers for wound dressings. *J. Biomed. Mater. Res. Part B Appl. Biomater.* **2010,** *92*, 568-576.

38. Du Toit, M.L. Incorporation of polysaccharide nanowhiskers into a poly (ethylene-co-vinyl alcohol) matrix. MSc Thesis, Stellenbosch University **2013,** 1.

39. Dai, L.; Ying, L. Infrared spectroscopic investigation of hydrogen bonding in EVOH containing PVA fibers. *Macromol. Mater. Eng.* **2002,** *287*, 509-514.

40. Brugnerotto, J.; Lizardi, J.; Goycoolea, F.; Argüelles-Monal, W.; Desbrieres, J.; Rinaudo, M. An infrared investigation in relation with chitin and chitosan characterization. *Polymer* **2001,** *42*, 3569-3580.

41. Wang, K.; Huang, W.; Xia, P.; Gao, C.; Yan, D. Fluorescent polymer made from chemical modification of poly (styrene-co-maleic anhydride). *React. Funct. Polym.* **2002,** *52*, 143-148.

Chapter 6

Conclusions and Recommendations

This chapter gives summarized conclusions on the various sections discussed in this study as well as recommendations for future work

6.1 Conclusions

6.1.1 Electrospinning of PVA, chitosan, EVOH and SMA

The main goal of this study was to incorporate an antimicrobial agent, 2,3-Dihydroxybenzoic acid into nanofibers through the electrospinning technique. To study the release of DHBA from these nanofibers it was necessary to obtain nanofibers with similar average fiber diameters. This was done by optimization of the electrospinning setup and different parameters namely, concentration of the polymer solution, applied voltage, flow rate of the spinning solution and the spinning distance were investigated. The optimum spinning conditions were established for the different polymer solutions to achieve smooth bead-free fibers. The influence of the different parameters on the fiber diameter was also investigated. This was done by keeping three parameters constant and varying the fourth parameter. The influence of the different parameters varied for the different polymers. However, similar trends were observed. The final average fiber diameters for the nanofibers were quite similar being at around 250 nm. The incorporation of DHBA into the different polymer solutions did not have a significant effect on the average fiber diameter or the morphology of the nanofibers. This confirms that the incorporation of DHBA did not influence the electrospinning of the polymer solutions and altering the different parameters was not necessary. The successful production of nanofibers with similar fiber diameters has been achieved.

6.1.2 Characterization of DHBA-loaded matrices

Successful incorporation of DHBA into the matrices was confirmed by FTIR showing the functional characteristic groups of DHBA. Any interactions such as hydrogen bonding with the polymers were also confirmed with FTIR. Interaction of DHBA with the polymer will have an effect on the release behavior of DHBA from the matrices. The chemical structure of the polymers influenced any interactions taking place, with the smaller molecules such as PVA and EVOH, interaction did take place but with the larger molecules, chitosan and SMA, interaction with DHBA was limited due to the steric hindrance effect.

The presence of DHBA was also confirmed with TGA. DHBA had an influence on the thermal stability as shown by TGA and DSC. The DHBA-loaded PVA and EVOH showed a delay in the

thermal stability while DHBA-loaded chitosan and SMA, no change in the thermal stability was observed. These findings can be attributed to the interactions between DHBA and the matrix.

6.1.3 Release study

The present study involved the comparative evaluation among four polymers which differ in hydrophilic-hydrophobic nature and to assess the effect it has on the release behavior of DHBA. The release of DHBA was studied from the films and nanofibers produced with the solvent casting and electrospinning techniques, respectively. The release of DHBA from the films and nanofibers was analysed using UV spectroscopy. Similar trends were observed for both the films and nanofibers. The type of polymer used imparts a conspicuous effect on the release behavior. The data generated in this study also showed that DHBA released from the hydrophobic matrix was less than from the hydrophilic matrix. The degradation of the nanofibers dictates the rate and duration of DHBA released; the slower degradation of EVOH and SMA, the slower was the release of DHBA. The burst release of DHBA from PVA and chitosan was dissolution-controlled release behavior. The hydrophobic polymers did not experience such a significant burst release and more sustained release behavior was observed, releasing DHBA in a diffusion-controlled manner.

Stability of PVA, chitosan and EVOH in water was improved by crosslinking with a glutaraldehyde solution. Successful crosslinking was confirmed using FTIR and degradation studies. The increase in degradation of these nanofibers showed a significant retardation of DHBA. The water-insoluble property of these nanofibers gives a more prolonged release of DHBA. Thus the rate of DHBA release can be modulated by the choice of polymer used.

6.1.4 Controlling the release of DHBA

The burst release from hydrophilic polymers aroused the interest to study the effect of coated films and nanofibers on the release behavior. These were done by coating the films and nanofibers with different polymer solutions and study the release of DHBA. The release of DHBA was controlled by coating of the films and nanofibers. The nature of the coating material played a vital role in the release behavior of DHBA. The release depended on the hydrophilic-

hydrophobic nature of the coated material. The successful coating of the nanofibers was confirmed using SEM and FTIR. The results showed that the release of DHBA from hydrophilic matrices can be controlled by coating with a hydrophobic material. The nature of the polymer and the amount that is coated onto the nanofibers determine the release profile. The release of DHBA from the coated films and nanofibers are diffusion-controlled where the DHBA has a longer path to travel to be released into the release medium. It can be concluded that the release of DHBA can be significantly retarded with the type of polymer used to coat the films and nanofibers and shows great potential for use as controlled release systems in the wound dressing field.

6.2 Recommendations

Recommendations for further studies include:

- The effect of different fiber diameter on the release of DHBA.
- Attachment of a fluorescent dye on DHBA to study the dispersion of DHBA inside the nanofibers.
- Blending of the hydrophilic and hydrophobic polymers and study of the release of DHBA from the different ratio blends.
- Coaxial electrospinning is another option that can be explored where the nanofibers consists of a shell and core, the effect of different polymers used as either the shell or core on the release behavior can be studied.

Appendix A

Controlling the release from electrospun mats

EVOH and SMA nanofibers were coated with different polymer solutions as discussed in Chapter 3. SEM was used to investigate how the morphology changed. The successful coating of the nanofibers with the polymers was confirmed using FTIR. The release of DHBA from these coated nanofibers was analysed using UV spectroscopy. The results obtained are shown below.

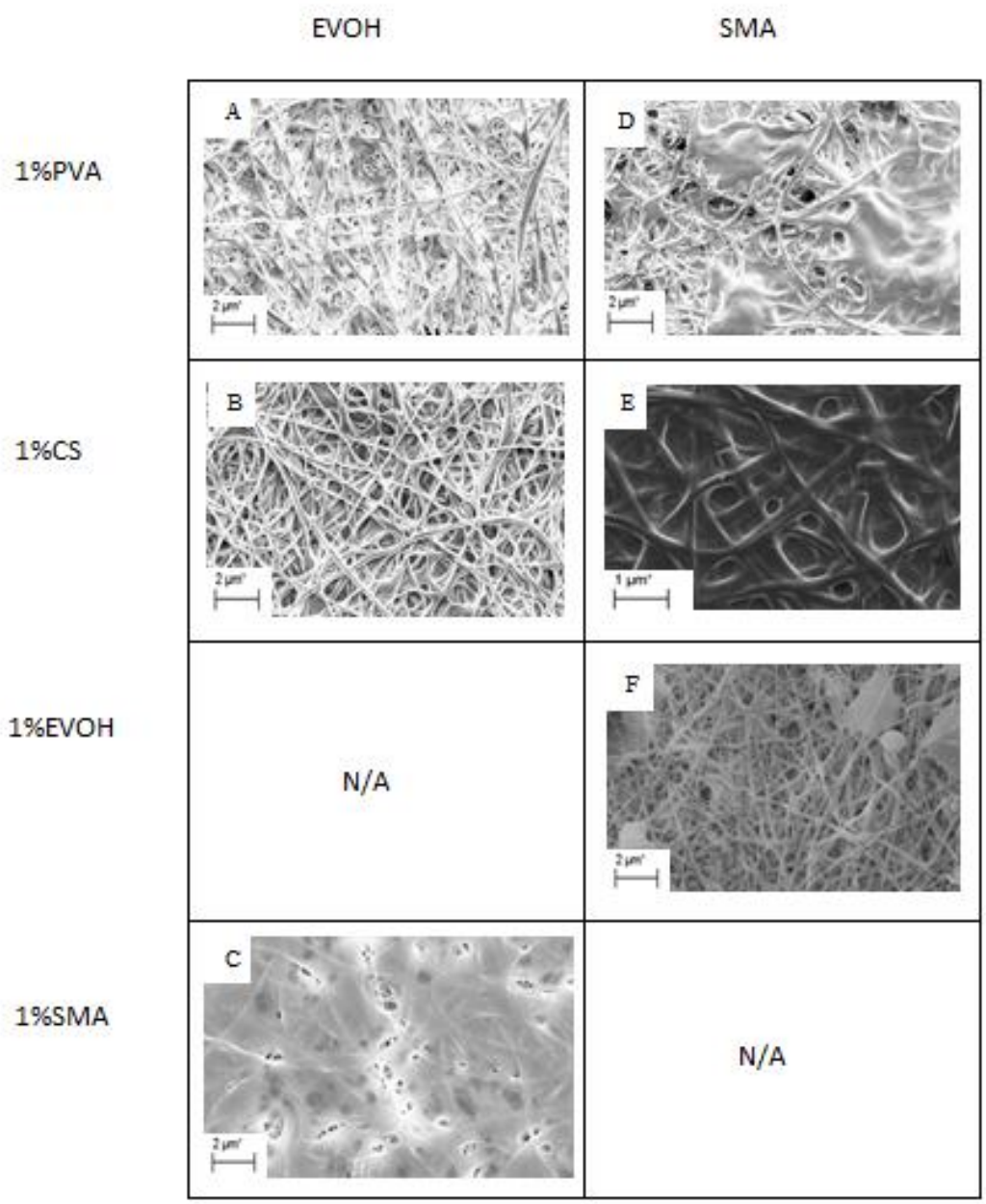

Figure A1: SEM images of coated EVOH (images A-C) and coated SMA (images D-F) nanofibers.

Table A1: Amount of polymer coated onto EVOH and SMA nanofibers.

	Amount coated on EVOH (mg)	**Amount coated on SMA (mg)**
1%PVA	5.2	6.4
1%CS	18.1	19.3
1%EVOH	-	7.3
1%SMA	10.6	-

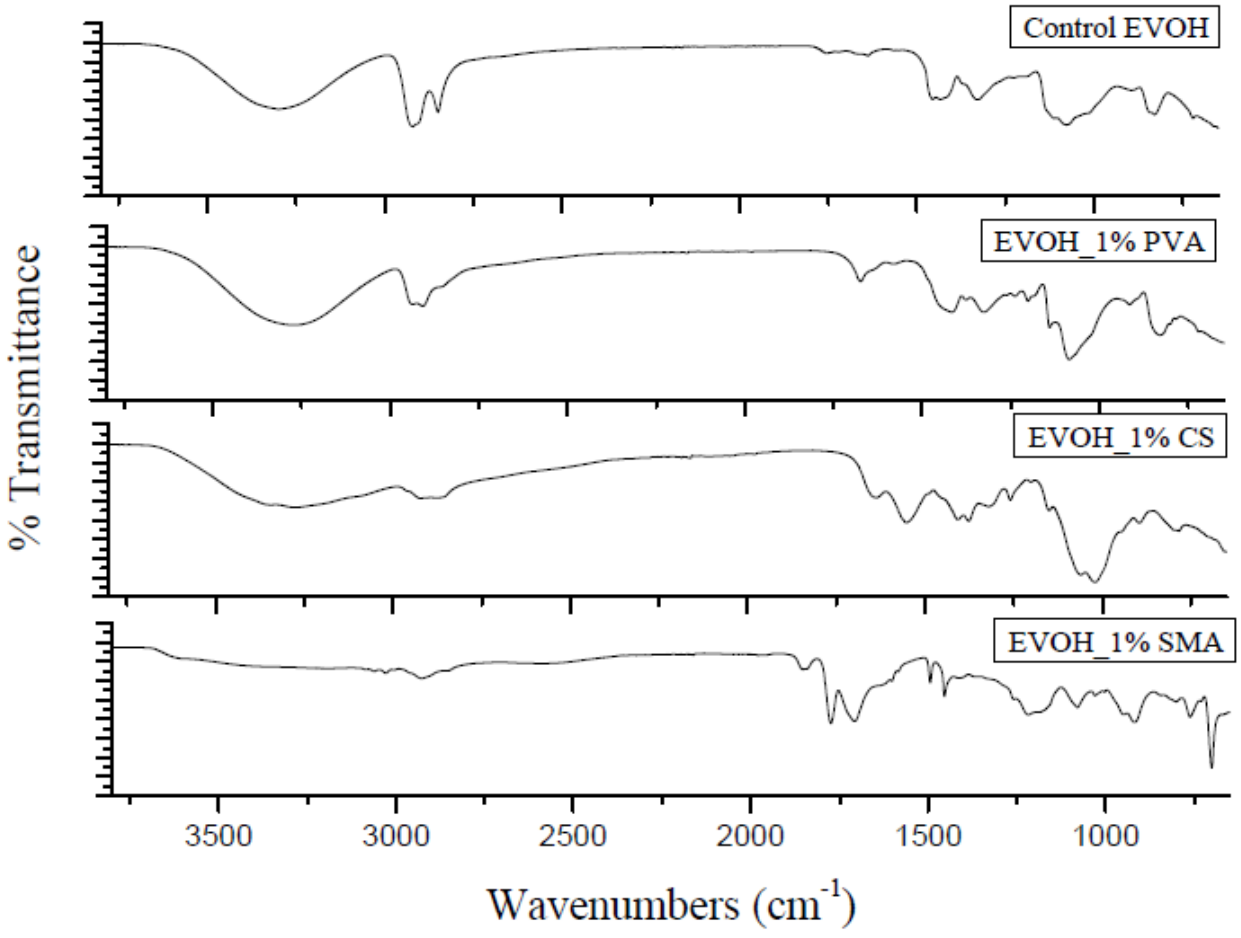

Figure A2: FTIR spectra of EVOH coated nanofibers.

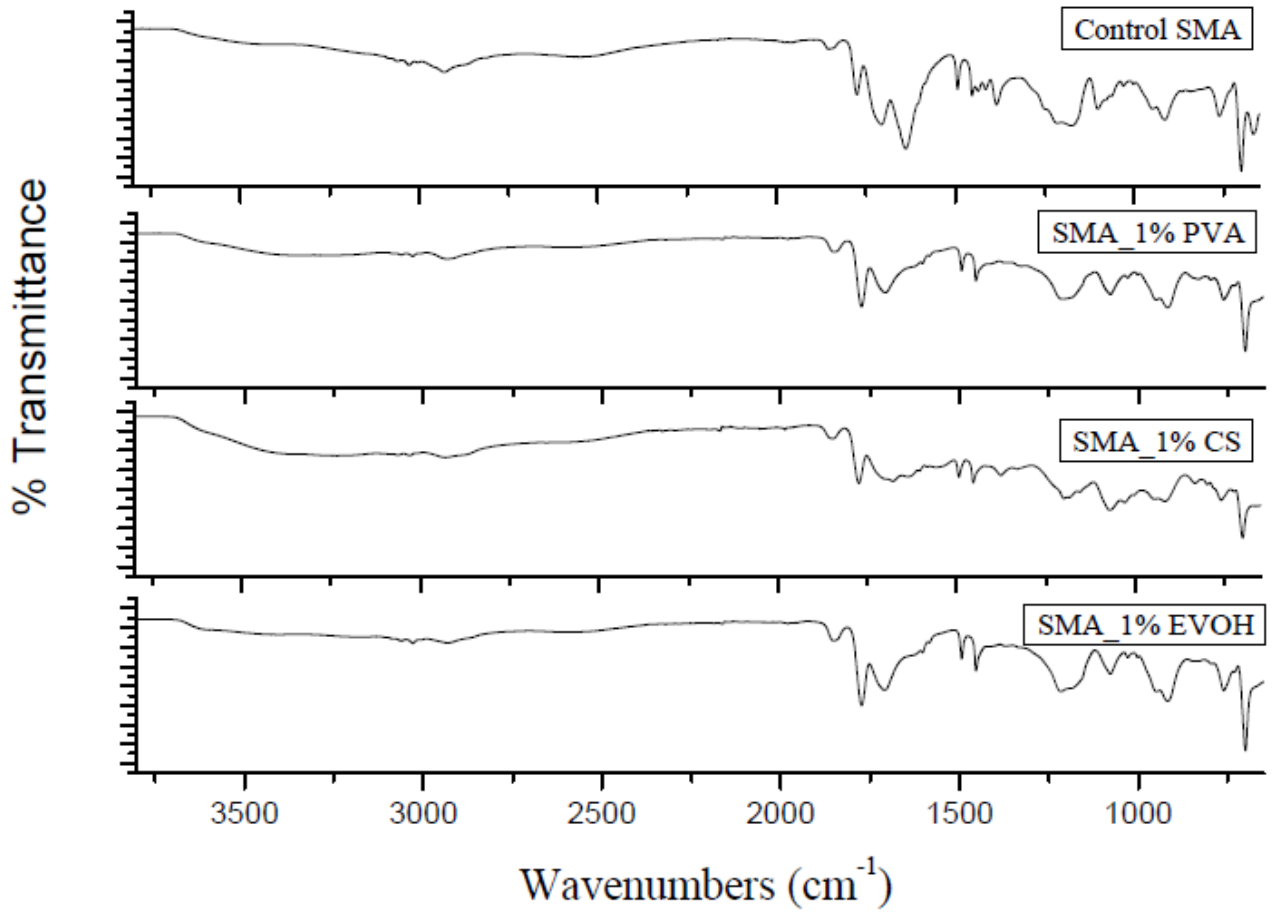

Figure A3: FTIR spectra of SMA coated nanofibers.

A

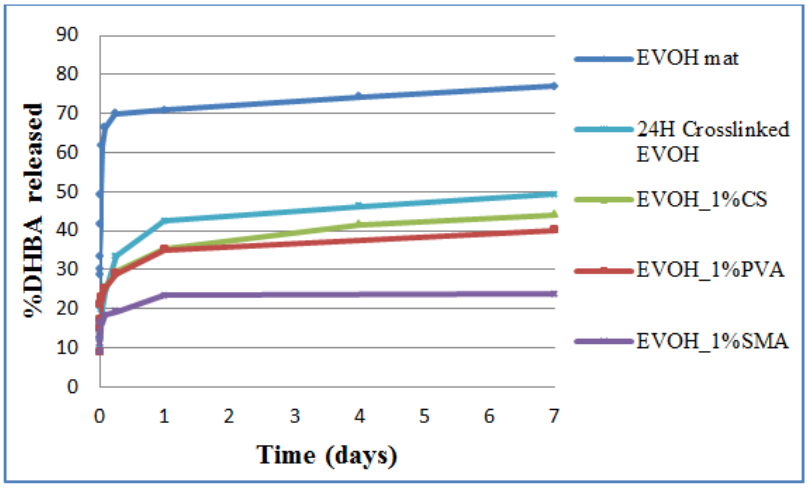

B

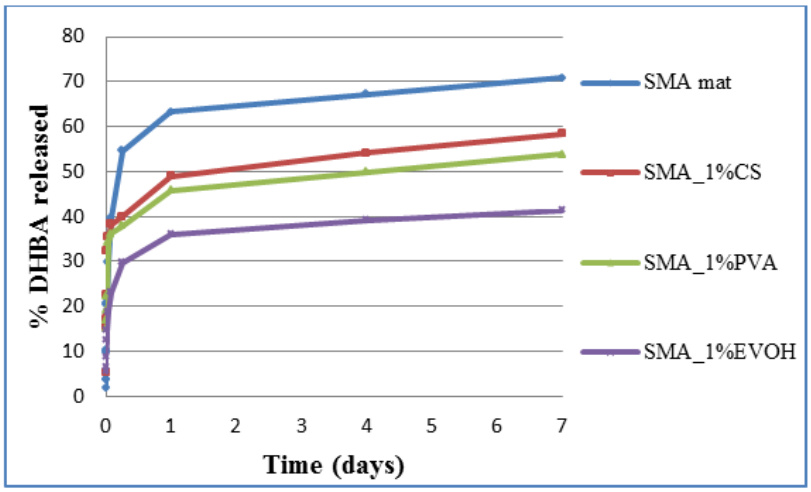

Figure A4: Release behavior of coated A - EVOH and coated B - SMA nanofibers comparing with the uncoated nanofibers.